SEASON

Self-Managed Sustainable High-Capacity Optical Networks

This project is supported by the SNS Joint Undertaken through the European Union's Horizon RIA research and innovation programme under grant agreement No. 101096120

Deliverable D3.1

End-to-end design of next generation smart optical networks

Editor A. Napoli (INF-G)

Contributors All partners

Version 2.0

Date 03-06-2024

Distribution PUBLIC (PU)

REVISION HISTORY

Revision	Date	Responsible	Comment
1.0	July, 27, 2023	Antonio Napoli [INF-G]	First version
1.1	Aug, 23, 2023	Antonio Napoli [INF-G]	Extending the 1st version
1.2	Dec, 15, 2023	Antonio Napoli [INF-G]	Complete list of missing sections in view of the D3.1
2.0	Mar, 06, 2024	Antonio Napoli [INF-G]	Finalized version.

LIST OF AUTHORS

Partner	Name Surname
ADTRAN	Lutz Rapp, Florian Azendorf
CNIT	Filippo Cugini, Margita Radovic, Nicola Sambo
CTTC	Laia Nadal, Ramon Casellas, Josep Maria Fàbrega, Francisco Javier Vílchez, Ricardo Martínez, Michela Svaluto Moreolo, Luca Vettori, Carlos Hernández
INF-G	Antonio Napoli, Carlos Castro, Mohammad Hosseini
INF-P	Cátia Pinho, João Pedro, André Souza
HHI	Caio Santos, Johannes K. Fischer, Behnam Shariati, Abdelrahmane Moawad
SSSA	Nicola Sambo
TIM	Marco Quagliotti, Emilio Riccardi, Anna Chiadò Piat, Annachiara Pagano, Roberto Mercinelli
TID	Antonio Melgar Gonzalez, José Manuel Rivas Moscoso
UC3M	José Alberto Hernández, David Larrabeiti, Fernando Díaz de María
WEST	Stefano Tennina, Andrea Marotta, Cristian Antonelli
ERI	Gianluca Gambari, Roberto Magri

EXECUTIVE SUMMARY

This document reports the work carried out within the first 13 months of the project SEASON.

It starts by mentioning the network topologies and architectures as they have been defined in the WP2. In particular, it reports the segments of access, metro aggregation, and metro. Here, thanks to the contribution of the network operators, we discussed in detail the state of the art, the current limitations, and the envisioned SEASON network architecture. In this context, network and physical layer requirements are reported and the possible solutions that will be discussed within the project.

Next, the transmission models for multi-band over single core fiber and multi-core ones that have been developed over the last decade are discussed and, when needed, modified, or extended in SEASON. This refers mainly to the generalized Gaussian noise model that have been simplified to achieve faster computational speed. These models are fundamental to estimate, plan and manage modern optical networks. In fact, as split step Fourier method is time consuming, in particular when considering transmission over multi band, then an accurate and fast transmission model is highly valuable. In SEASON, we do not only use existing models, but we improved them to target studies to support the requirements discussed withing WP2.

Data plane is also a fundamental topic in an optical communication project. In SEASON, we investigate it in terms of: (i) transmission, (ii) transceivers, (iii) node architecture, and (iv) monitoring.

i) In the transmission part, we consider multi-band and multi-core, and relative components and system level optimization carried out with simplified but fast transmission models.
ii) For what concern transceivers, we proposed flexible solutions, using direct or coherent detection, and being them point-to-point or point-to-multipoint. These could either be low-cost solutions (with direct detection) or could enable network simplification (coherent with point-to-multipoint capabilities).
iii) The node architecture is investigated based on assumptions defined within the WP2. In this context, solutions for multi-band and multi-core are individually proposed. As SEASON aims at proposing solution also for the access part of the network, a novel node architecture approach is proposed for the edge segment.
iv) Data monitoring is fundamental for sensing natural event or identifying soft-failure, and thus being capable of providing early detection and thus improving maintenance. In SEASON, both optical and digital monitoring are discussed and investigated.

All the studies carried out in terms of data plane are finally mapped in four large comprehensive use cases, whose studies are carried out under certain requirements and with certain capabilities and levels of accuracy.

We identified the follow four use cases, which will be widely covered during the next two years of the project: (i) front- and mid-haul, and access; (ii) ultra-high-capacity access network also using multi-core-based passive optical networks; (iii) optical bypass, and (iv) metro-aggregation.

TABLE OF CONTENTS

Dissemination Level	SEN (Sensitive - limited under the conditions of the Grant Agreement)

1 INTRODUCTION

Next generation optical networks will need a mix of characteristics to realize the future telecommunication infrastructures, so that it will be capable of supporting the advances in terms of Internet of Things, augmented / virtual reality, 4k/8k streaming, beyond 5G and 6G mobile transport, etc.

In this context, numerous aspects must be considered: (i) high-capacity transmission, (ii) flexible high-efficiency transceivers, (iii) low-power devices, (iv) high-resilient and robust network architectures, (v) optical fibers capable of enabling wideband transmission, (vi) multi-core fibers, etc. Clearly, this list of needs – to realize future networks – is longer than the one above. For example, in the case of the transmission medium, the hollow-core fibers are seen as an option for next generation mobile transport, as they intrinsically reduce the latency or help to extend the length of mobile networks. On the other hand, that list is already quite comprehensive of the needs and even more relevant, all those topics are parts of the Self-Managed Sustainable High-Capacity Optical Networks (SEASON) project.

In this first deliverable of the WP3, entitled "End-to-end design of next generation smart optical networks", we report on the first results and studies that have been carried out within the first thirteen months of the project.

This deliverable is organized as follows. In Section 2, a comprehensive description of the requirements in terms of physical layer, network, and use cases is reported. This is based on the work carried out within the WP2 and provides the state of the art of the existing networks of the two operators participating to SEASON (Telecom Italia Mobile and Telefonica). Here, the limitations of the existing optical fiber infrastructure are discussed for all architectures of the different segments of the network and the physical layer which is required to fulfil the beyond state-of-the-art SEASON goals. Stemming from this description, the envisioned topologies for access-metro and metro-core are reported, together with the requirements. These are listed and mapped into the key-performance indicators (KPIs) and objectives of the project. Finally, we discuss, the solutions to achieve high-capacity flexible transmission, to lower the costs and the power-consumption, to reduce the number of elements deployed in the network, and to enable spatial aggregation in passive optical network (PON) thank to multi-core fibers.

Section 3 presents a series of mathematical modelling of propagation over fiber, both single- or multi-core. These models are needed to rapidly, but accurately, assess the optical performance of different proposed solutions. In fact, one of the main objectives of SEASON is to design an optical system so that it can achieve a significant increase in terms of fiber throughput. This can be obtained in different ways, and all of them are not mutually exclusive.

The first approach (the simplest) is to use dark fibers or to deploy more fibers. This solution is mature and already widely used. Nevertheless, in case of lack of fibers, it could be highly expensive. The second, is multi-band transmission. Here, the idea is to transmit also in the additional bands beyond C, or C+L. Among them, we could consider the O-band, the E-band, the

S-band, up to the U-band to extend the fiber throughput. In this investigation, several solutions have been proposed. In SEASON, besides using the existing models, we also extend them to reduce the computational time and to investigate approaches where Raman amplification can help to equalize the optical performance in other bands. The main (pragmatic) idea of our investigation has been on the next steps, in terms of bands to be enable, after C+L. Finally, multi-core fiber is also considered. The models are presented, and the use case provided for higher-capacity in PON, with the target to achieve lower power consumption. In all three scenarios, a proper node architecture must be studied.

Section 4 is entirely dedicated to data plane technologies and is divided into four parts: literature review, transmission, node architecture, and monitoring for optical communication.

Following the comprehensive literature review, we describe the functionality of the sliceable bandwidth variable transmitter and how it can enable multi-band and multi-core transmission. Several studies covering these two approaches are investigated. Multi-core fibers, in particular, have been extensively researched with respect to cross-talk, reach, and component performance, among other factors. Subsequently, we conducted a series of system-level design investigations to compare the efficacy of solutions after C+L and superC + superL saturation. In this context, we considered S+C+L versus E+C+L, both with and without the incorporation of distributed Raman amplifiers. We then propose a technology and network architecture aimed at reducing the number of opto-electronic-opto conversions, or more generally, the number of network elements or components. This is achieved by implementing coherent point-to-point or point-to-multipoint transceivers. Finally, we describe the use of super channel transmission to realize elastic optical networks and propose a solution for ultra-high-efficient transmission through an advanced software-defined network controller.

The third part of section 4 is dedicated to the different node architectures. As a solution which would fit all possible use cases is neither not doable nor cost effective, we decided to optimize the node architecture for the different segments of the network. Multi-band and/or multi-core node architectures are considered for the metro and metro-core segments of the network. While a filterless approach will be proposed for the metro-access segment. Finally, also a possible architecture and simplification obtained with coherent point-to-point and point-to-multipoint transceivers in edge-node is discussed.

The last subsection of section 4 is dedicated to monitoring and sensing, both as optical monitoring (optical time-domain reflectometer (OTDR), interrogator, and fiber sensing) and as digital signal processing, where the information is extracted within the chain of digital signal processing modules. In this context, we also investigated computer science techniques that enable to reduce data imbalance, in order to detected a wider range of events.

The final segment of the deliverable, section 5, is divided into two distinct parts. The first one is devoted to the methodology employed for network design, along with an exploration of the requirements and necessities of the various segments. The second one discusses the most relevant use cases, namely front-haul, access, optical bypass, and metro-aggregation.

2 NETWORK AND PHYSICAL LAYER REQUIREMENTS

2.1 PROGRESS BEYOND STATE-OF-THE-ART

2.1.1 State of the art

The following sections summarize the network topologies provided by TID and TIM within SEASON, and those aspects of the network that are relevant for WP3. Further details can be found directly in D2.1 of WP2.

2.1.1.1 Telefónica networks and systems state of the art

Telefónica's data plane architecture is divided into three layers: the IP layer, the Optical Transport Network (OTN) or electrical switching layer, and the optical layer, which mainly consists of rings, horseshoes, and photonic meshes. According to the IP layer structure, the network is arranged following a typical hierarchical structure comprising five levels (HL1 - HL5):

- The HL5 level comprises OLTs that aggregate Fiber-to-the-x (FTTx) households, radio access points, and mobile base stations connected to cell site gateways (CSG), where traffic is encapsulated in L3 Virtual Private Networks (VPNs) to reach the packet core.
- The HL4 level is composed of routers that handle traffic classification, subscriber credentials authentication, validation of users' access policies, routing data to their destination, and aggregation of traffic from different locations of the metro network, as well as from OLTs and radio access points.
- The HL3 level gathers traffic from HL4 and HL5 nodes and performs IP grooming towards the next level.
- The HL2 level hosts critical services like TV and Content Delivery Network (CDN) caching.
- The HL1 level is the top level of the national backbone network and interfaces the IP network to the Internet as well as to other ISP providers.

The Telefónica's network comprises of around 9,000 HL5 nodes (horseshoe structures dual hubbed to two HL4 nodes), 700 HL4 nodes (horseshoe structures dual hubbed to two HL3 nodes), 100 HL3 nodes, 20 HL2 nodes, and <10 HL1 nodes forming a photonic mesh.

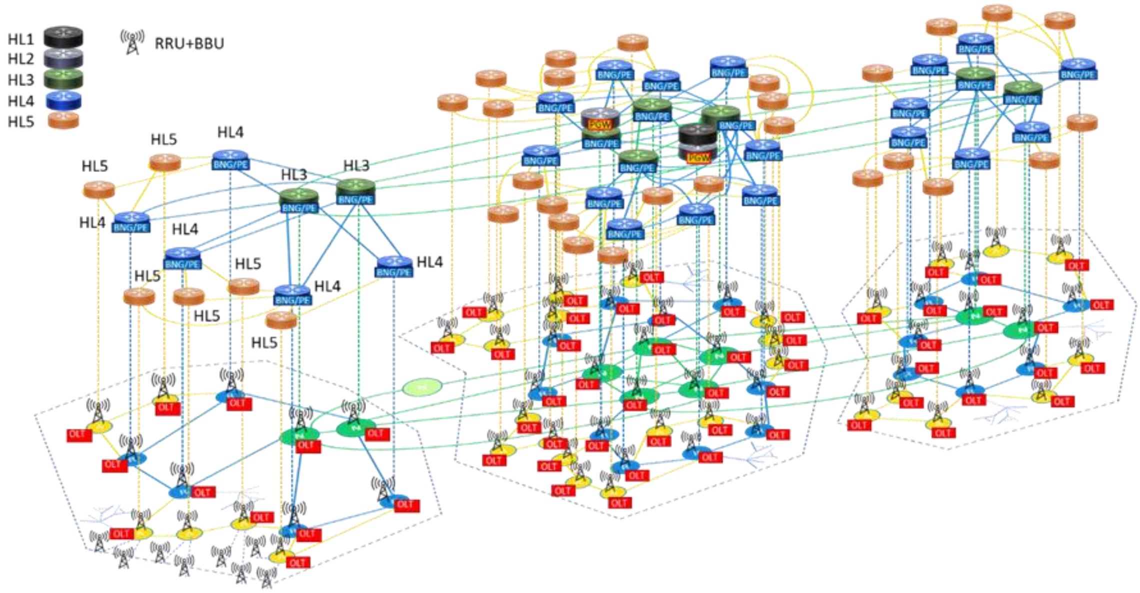

Figure 2-1 – Telefónica's simplified packet-optical network topology.

Figure 2-1 shows the current Telefónica's simplified IP and optical layer architecture, as well as the different segments in which the optical layer is structured and the associated IP hierarchical levels (HLx) at which the data from each of the network segments is aggregated and statistically multiplexed. Shown are three encircled geographical areas (left -L-, middle -M- and right -R-), which represent two medium-sized regions (L and R), consisting of HL5-HL4-HL3 nodes, and a large metropolitan area (M), where the HL2 and HL1 nodes are located.

Logical connectivity between HL3-HL2-HL1 nodes is shown for all three geographical areas. The physical topology comprises the access, metro-regional, and national networks represented by orange, blue, and green structures, respectively. The light-green node between the L and M regions denotes a national-network pass-through node without traffic add/drop, consequently, without an associated router in the IP layer. PON networks are depicted branching out from a few selected sites just for reference, but all sites with the red OLT tag are the termination point of a PON network. Radio station placement is indicated with the antenna icon.

As depicted in the L region only for a few HL5 sites, antennas not co-located with an HL5 site are linked to the nearest HL5 site through microwave (MW) or dark-fiber connections. The placement of telco functions, such as BNG, PE and PGW, are indicated in the IP layer. The national network is divided into 50 regions (with Figure 2-1 only showing three of them) which are connected through a meshed topology based on Colorless Directionless (CD) and Colorless Directionless Contentionless (CDC) ROADMs and coherent transmission of >100G channels (no dispersion compensation modules). Two HL3 nodes in each region serve as termination points for HL4 horseshoe structures, which are based on colourless ROADM nodes and 100G coherent transmission (no dispersion compensation modules).

Finally, the HL5 nodes, implemented with FOADM in the optical layer, form horseshoe structures dual hubbed to two HL4 nodes, based on mixed 10G/100G transmission. The HL5/HL4 sites function as terminating points for fixed and mobile access network deployments. FTTH is deployed through PON networks (with OLTs installed at the HL5 or HL4 nodes –hosting up to 3 racks with 2 chassis/rack-, and the ONTs deployed at the customer premises) using passive splitters daisy-chained to provide a 1:64 splitting factor implementing GPON and XG(S)-PON technologies, with maximum distance in the range of 10-20 km. When it comes to mobile access, there are generally less than 12 base stations per HL4 site and less than 4 base stations per HL5 site.

Finally, regarding the placement of telco functions in Telefónica's network architecture, BNG/PE are distributed to the far edge nodes (HL4 sites), but the PGW are centralized in about 5 locations nationwide (usually at the HL2 level).

2.1.1.2 TIM networks and systems state of the art

TIM network is articulated in three main segments: access, metro-regional (organized in two sub-segments, aggregation end core) and backbone. Hereafter the main characteristics of the three network segments are reported with an overview of the topology and technologies used in each of them. Some in-depth information is given below on the WDM layer as shown in Figure 2-2. For architectural details on the packet layer and cloud functions (both telco and service) please refer to the project deliverable D2.1, Figure 2-2.

The primary Access network is physically composed by cables hosting a multifiber infrastructure (G.652 conventional fiber) connecting the Access COs (about 3500 all over Italy) either to cabinets, curb or home. While the secondary access network is limited to copper pairs connecting cabinets to the access termination point, i.e., to the customer site. The most evolved access services are mainly based on FTTH (with maximum distance of about 20 km and average distance of about 3 km), including Point-to-Point (P2P) fiber connectivity for business customers (Gigabit Ethernet - GE services) and mobile antenna sites with connections at 10/40/100GE, as well as Point-to-Multi-point (P2MP) connectivity for residential customers based on GPON and XG(S)-PON technologies (with optical line terminals – OLTs, installed at Access COs). That, through passive splitters with a 1:64 splitting factor, respectively provide a total bandwidth of 1 Gb/s and 10 Gb/s, allocating over each single fiber the upstream traffic flows in the O band and the downstream traffic flows respectively in S and short-L bands.

The Metropolitan Area Network (MAN) over Photonic Metro-Regional and the Packet Core (OPC) over Photonic National Backbone both consist of IP/MPLS networks supported by Dense Wavelength Division Multiplexing (DWDM) networks on a fiber infrastructure mainly realized by G.652 fibers in Metro-Regional and G.655 in National Backbone.

Each MAN (30 all over Italy) is composed by routers installed at Access, Regional and National COs (routers numbers range from 50 to more than 200 in each MAN). The router at Access CO (Aggregator) is dual homed to two routers (Feeder) in two different Regional COs (where maximum distance is about 200 km). While the router located at Regional CO (whose number amounts to about 600 all over the Country) is dual homed to two routers installed in the same National CO (Metro 1 and Metro 2 in Figure 2-2), with a maximum physical distance between routers in Regional CO and National CO of about 300 km. MAN exploits the photonic connections of the underlaying DWDM Metro-Regional network (each Metro-Regional DWDM network provides circuits for one, two or more IP MANs, depending on the geographical extension of the WDM Metro-Regional network).

The Packet National Backbone is based on high-performance routers interconnecting 33 National COs with circuits at 100G and 400G. Of the total of 33 National POPs, 25 are Secondary COs double-hubbed to 8 Primary COs. Primary COs are interconnected together with a mesh. A subset consisting of 4 Primary COs represents the Core Hubs, interconnected to peers and Internet through the Seabone, an infrastructure devoted to interconnecting networks from different Countries and Operators.

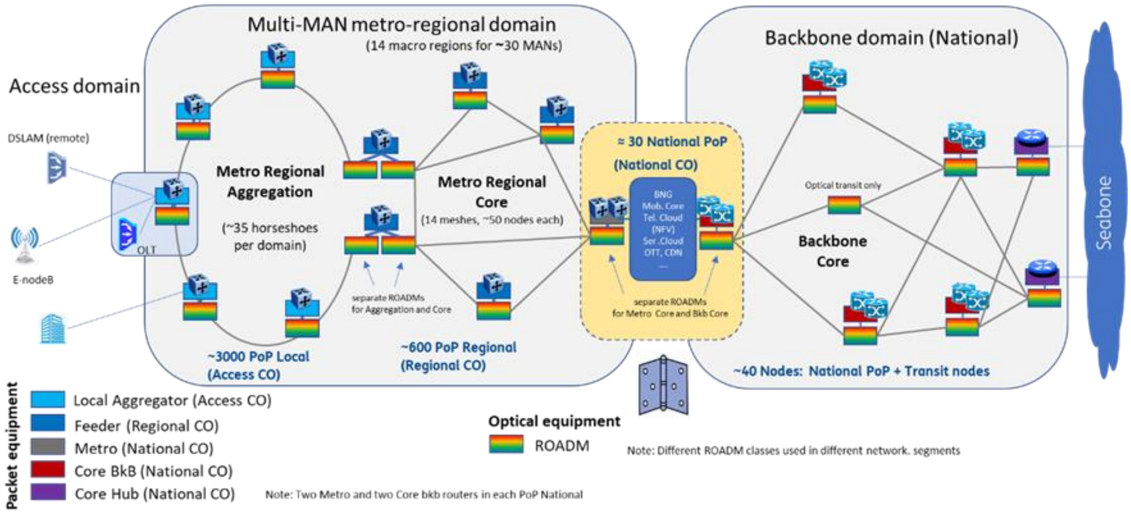

Figure 2-2 – TIM optical network level architecture.

Figure 2-2 shows the architecture of the Wavelength Division Multiplexing (WDM) transport network used to transport flows between routers; the WDM network is segmented in Metro-Regional Aggregation, Metro-Regional Core and Backbone, with different topologies and classes of WDM equipment (for both switching and transmission) in each segment. The first network level (the Aggregation level, between Access COs and Regional COs) is realized with ROADMs and direct detection transponders at 10 Gb/s line rate mainly (100G is also present on some limited cases), connected in horseshoe topologies (2 to 7 Access COs, acting as “leaves”, ended by two Regional COs with the role of “hubs”, line systems have dispersion compensation modules (DCM)), while the second network level (the Metro-Core level, between Regional COs and National COs) is realized by ROADMs and 100 Gb/s coherent transponders (in many cases with 2×100G on tributary side and 200 Gb/s on line side), connected with a mesh topology.

The backbone is a mesh network with around 50 nodes and 80 links (Figure 2-10). Fifty nodes include all the National CO plus some Regional CO and also additional transit/regeneration only sites. The devices used in the optical layer are CDC ROADM made with Flexgrid WSS1×20 and 8×16 MultiCast Switch (MCS) add/drop modules. Concerning transponder and muxponder in use client rate is mainly 100G (lower rates, e.g., 1G and 10G, groomed by the OTN layer or through muxponders) while line rates range from 100G to 400G (used for N x 100G clients) and trials with higher line rates are already successfully performed (e.g., 600 Gb/s in 100 GHz over 1000 km reach has been demonstrated in 2022).

2.1.2 Limitations with the existing network architecture

Network operators face significant challenges in scaling optical systems to meet the ever-growing traffic demands. One limitation lies in the capacity constraints of existing optical fibers limited by the commercial availability of C-band only systems (C+L band systems exist, but costs currently place restrictions on their introduction), which can only carry a finite amount of data before reaching their limits. Additionally, as more devices connect to the network and bandwidth-intensive applications will proliferate (such as AR/VR glasses, things, and connected cars), the need for higher data rates strains the capabilities of current optical equipment.

In addition to capacity constraints, the scarcity of fiber optic cables presents a significant hurdle to scalability for network operators. Deploying new fiber infrastructure involves substantial investment and often faces logistical challenges, particularly in densely populated urban areas where space is limited. Moreover, the cost of implementing solutions that parallelize lines, such as node architecture, can be prohibitively expensive. Thus, while parallelization can potentially increase network capacity, the high upfront and ongoing costs associated with these solutions may pose additional barriers to scalability for network operators, highlighting the complex economic considerations inherent in expanding optical systems.

In the context of the metro aggregation network, there is a pressing need to surpass the limitations of the existing 10 Gb/s data rate infrastructure. To meet the escalating demands of modern communication, it is imperative to swiftly transition towards providing data rates of 100G and even 200G or 400G in certain dense-urban specific scenarios. By adopting higher data rates, network operators can effectively future-proof their infrastructure, ensuring it remains robust and capable of handling the exponential growth in data transmission requirements expected in the coming years. This strategic move not only enhances the network's scalability but also fosters improved efficiency and responsiveness, ultimately enriching the user experience and enabling seamless connectivity across diverse applications and services.

For the metro core and backbone network today at 100G and 400G, tributaries at 800G and 1.6T will be necessary, and the C band only does not have enough spectrum resources for multiple lambdas operating at multi-Tb/s. Thus, newer bands beyond C will be necessary, including mainly C + L and optionally the S for long-range transmission.

2.1.3 Physical layer SEASON network architecture beyond state-of-the-art

The goal of the SEASON project, from a physical layer network architecture perspective, is to overcome the aforementioned limitations affecting current operators' data plane infrastructures by designing and validating an innovative transport network able to:

- Support beyond 5G and new emerging services with a physical layer infrastructure spanning the access, aggregation, and metro/long-haul segments.
- Exploit Multi-Band and Space Division Multiplexing (SDM) in a cost-effective way.
- Integrate packet, optical and computing layers.
- Target network efficiency in terms of capacity and energy efficiency.

In particular, the target SEASON architecture considers joint MB and SDM (MBoSDM) and SDM-PON networking, in terms of transmission and switching, while addressing innovation in terms of sliceable Bandwidth Variable Transceivers (S-BVTs) enabling P2MP along with the integration of (coherent) pluggable optical modules on open packet/optical white boxes (open devices with hardware and software - referred to as the Network Operating System, or NOS – decoupling and providing open control and management interfaces), smart Network Interface Cards (NICs) or the latest generation Data Processing Units (DPU). A critical objective of such architecture is to ensure energy efficiency, relying on advanced Digital Signal Processing (DSP) applied also to SDM/Multicore fibers, and MBoSDM optical switching and P2MP S-BVTs allowing traffic aggregation/router bypassing, thus reducing the number of Optical to Electrical to Optical (O/E/O) conversions.

2.2 Reference Network Topologies

The reference architecture for the SEASON project (details in Deliverable in D2.1) includes both Access-Metro and Backbone topologies. These reference networks can be used, together with considerations on use cases and related generated traffic and on enabling technologies, for dimensioning studies and techno-economic evaluations in SEASON project.

2.2.1 Topology for Access-Metro domain

In the Access-Metro domain of SEASON architecture solution proposed in WP2, transport solutions (access and metro) would integrate with each other, and with network and service functions as well, to allow the satisfaction of all requirements, i.e., bandwidth, latency, computational and storage capacity and energy savings.

Conversely, in operator networks, network segmentation today includes at least three clearly demarcated segments: access segment (fixed fiber component (e.g., FTTH) and mobile radio (4G/LTE and 5G/NR), metro or metro-regional segment (depending on case to case, but typically divided into two sub-segments, aggregation and metro core), and a backbone for long-distance connections on a national scale.

According to SEASON's target architecture for the long term, the clear demarcation of the access and metro segments would like to be removed by seeking, as far as possible, optimized solutions throughout the entire part of the network from the access termination (of any type) up to the first national backbone node.

Starting from the operators' networks as they are today and to use them consistently with the SEASON target architecture, an adaptation must be made. What is proposed is to consider the regional metro networks as they are today, with central offices as possible candidate points to host switching and cloud equipment. Furthermore, current fiber topology will be assumed as the baseline for the new optical network and the extension of this typology towards the access areas is carried out through a categorization of the access areas using regular models based on realistic statistics. Operators, for confidentiality reasons, cannot provide details about their access networks, but they can provide average typical values for modelling the areas in terms of size (covered area in km^2) and amount of collected households and gathered mobile sites. The proposed model involves the categorization of access areas into four geotypes: dense urban, urban, suburban and rural. Each central office (of any level) included in the current network topologies is associated with one of the above geotypes.

Traffic collection and aggregation points today are central offices (of any type: local, regional or national) and in SEASON architecture this point is a possible candidate to become a Far Edge or Edge point. In addition, Far Edge points under specific needs can be placed also in other more distributed points that today are places hosting cabinets or mobile sites. These additional more peripheral points are provided through regular typical models for the geotypes mentioned above, i.e., dense urban, urban, suburban, or rural areas. As the market is under evolution, model parameters or the model itself can be changed to consider the evolution in time in the access architecture, especially on potential deployment of small cells in some areas which require to collect very high amount of traffic per square kilometer. Fixed technologies are expected to evolve for instance in terms of PON technologies with higher capacity than they have today (e.g., from 10 Gb/s PON of today standard deployment to 25/50 Gb/s PON of next deployment, in short term, to 200/400 Gb/s coherent PON or even SDM PON in the long term).

In line with the segmentation of the current networks in the field (and not with the SEASON architectural model which sees access and metro combined together) below we will first present a general model for the access part and then some physical topologies for the metro and backbone segments.

2.2.1.1 Regular models for the access part

To extend the networks toward the access for a complete coverage of the access metro domain defined in SEASON, regular structures as the ones shown in Figure 2-3 can be considered. In Figure 2-3 the typical distribution of mobile sites and cabinets is depicted. Today mobile sites with macro cell equipment (Radio Unit and Baseband Unit) are present, in future there will be also mobile sites with small cells. Cabinets today host PON splitters, in future they will be potentially candidate to become Far Edge points hosting active equipment. The average urban area (urban geotype) shown in Figure 2-3 is a square of 1.6 km side (2.56 km^2) and it is served by a topological node (blue circle in the center, in current deployment can be host a central office at metro aggregation, metro core or national level, in SEASON architecture the blue circle can be a Far Edge, an Edge or a Cloud CO). The distribution of both cabinets, the green circles covering squares of 200 m each, and mobile radio sites, yellow triangles for small cell sites and violet diamonds for small cell sites, are regular or almost regular. Obviously, this applies to the abstract model based on real statistical data, but it does not correspond exactly to any real case.

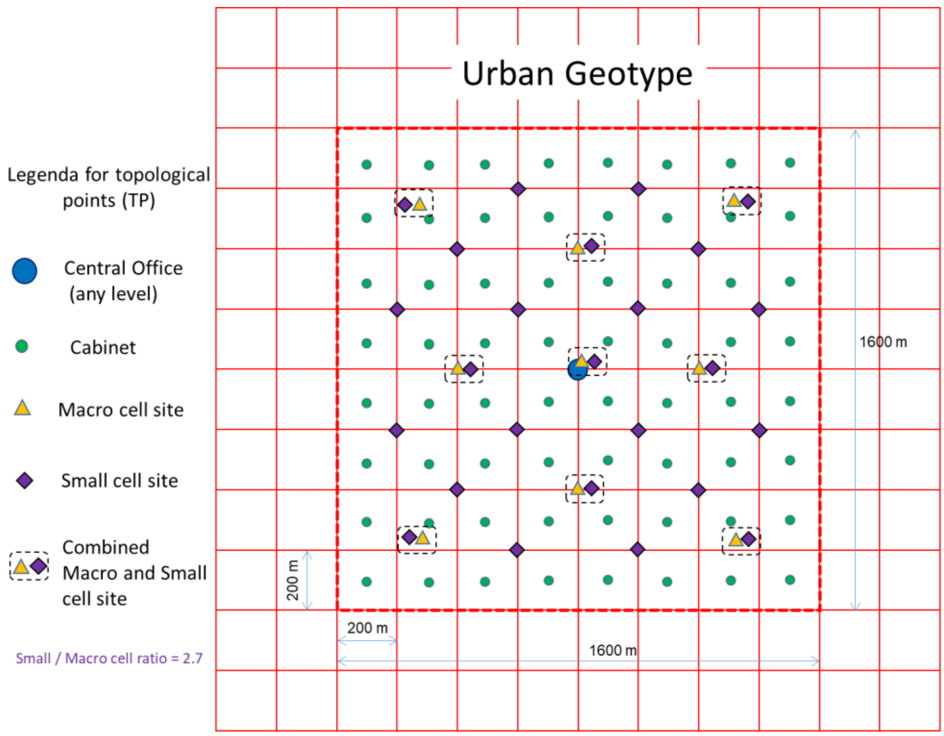

Figure 2-3 – Example of a regular model for the access Urban area geotype collected by a central office based on statistical data from a big city in Italy. (small cell mobile sites is a projection not based on operator's plan, in the picture their distribution is not homogeneous within the squared area, but it is denser in the central part and more spread out near the borders: other types of distribution are possible).

As each topological node collects access basins of different type (in terms of amount and sort of access points as well as socioeconomical environment and geographical size) and, potentially, all different from each other, the modelling choice as already mentioned assumes four categories of areas covered by each topological node, where nodes are those of the metro segment represented in Figure 2-5 and Figure 2-6. The four geotypes proposed are the Urban (shown in Figure 2-3) the Dense Urban, the Suburban and the Rural. Although this modelling does not allow us to accurately represent the reality in the field, it does however allow us to make realistic assessments given that different areas have different customer and traffic densities. By attributing a geotype to each topological node, it is possible to make evaluations based on the traffic (mobile and fixed) generated by that node. Furthermore, based on traffic distribution and other criteria, it will be possible to decide which nodes will perform the Far Edge role (it could be a spartan and cheaper CO) and which will perform the Edge role (as current Telco grade central offices) in the SEASON architecture while the Cloud role is constrained by the national level central office locations in current networks by assumption.

Typical values characterizing each geotype is given in Table 2-1. We want to underline that numbers for small cell mobile sites are projections based on alleged suitable rates between number of macro cells radio site and small cell radio sites (compared to the one of Urban geotype the density of small cell mobile suites is higher in Dense Urban, lower in Suburban, and zero - no small cell mobile radio sites- in the Rural geotype).

Table 2-1: Values of parameters for the four-access area Geotypes.

Geotype	Size* [km]	Area [km^2]	Population	Households	Cabinets	Macro Cell sites	Small Cell sites density**
Dense urban	0.8	0.64	10000	6000	36	5	Very high
Urban	1.6	2.56	27500	12500	64	9	high
Suburban	3.2	10.24	13750	6250	36	9	spotted
Rural	12.8	163.48	5500	2500	16	6	Nil or rare spots

Dense Urban, Urban and Suburban access areas can be placed close together to compose a scenario as it is exemplified in Figure 2-4 where the central part is made of four areas of Dense Urban type (it could be the downtown of a big city), surrounded by urban-type areas and then fading into suburban-type area. This is only an example but other patchworks of geotypes can be composed to create scenarios to be analysed and taken for dimensioning and techno economic studies.

Figure 2-4 – Example of an extended area of a city and its surroundings modeled as a chessboard of Dense Urban, Urban and Suburban geotypes. (small cell mobile site not represented).

Furter details on geotype like draws of Dense Urban, Suburban and Rural geotypes and the fiber physical topology that can be built in the geotype grid can be found in deliverable D2.1 of the project.

2.2.1.2 Topologies for Metro domain

Two reference network topologies for the metro segment are proposed for SEASON, one resembles the properties and structure of MANs in TIM, the other one does so for TID.

TIM MAN topology

One of the network topologies proposed as a reference for SEASON network study is presented hereafter and it is inspired by Metro-Regional networks of TIM. The network has a metro core level made of metro core nodes connected by a mesh of fiber links plus several aggregation horseshoes made of a chain of aggregation nodes (leaves of horseshoe structure) and attached to the core in two metro core nodes (hubs of the horseshoe, they can be at Regional or National level). The typical hierarchical structure is depicted in Figure 2-5.

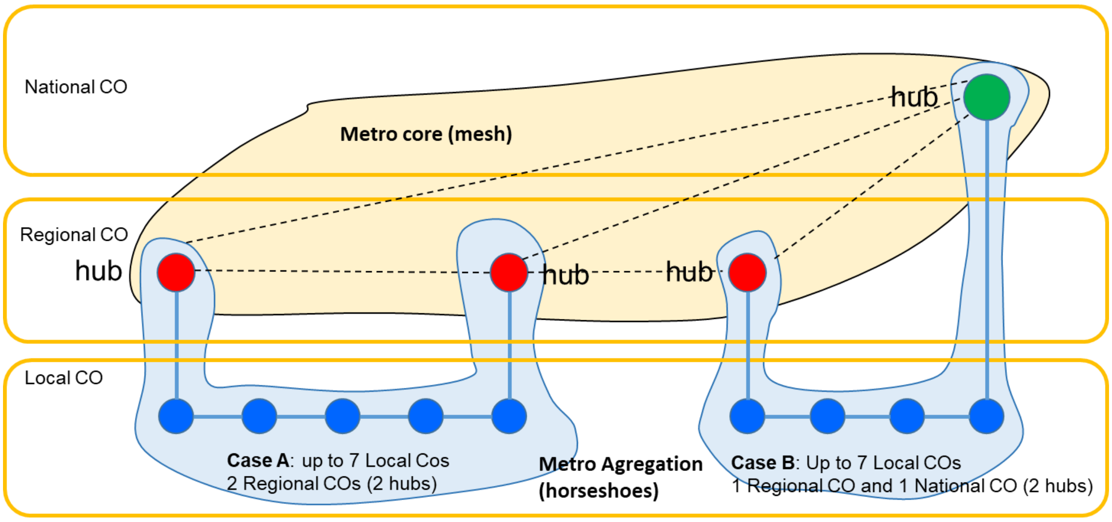

Figure 2-5 – Hierarchical structure of Metro-Regional network of TIM. Metro core mesh is within hubs (a hub can be in a Regional CO or in a National CO): Metro aggregation horseshoes end on hubs that can be both at Regional level (Case A) or one at Regional CO and the other at National level (Case B). The upper limit of Local COs leaves on horseshoes is 7 making 9 the maximum number of nodes in a horseshoe.

The fiber topology of the metro core reference network selected for the project is shown in Figure 2-6, where red nodes (MC01 to MC21) are the nodes that currently take part of the Regional level, while green nodes (BB01 and BB02) are the nodes that are located in National level central offices. In total there are 23 nodes, two of which are National, and 29 links. These nodes can be hubs for aggregation horseshoes.

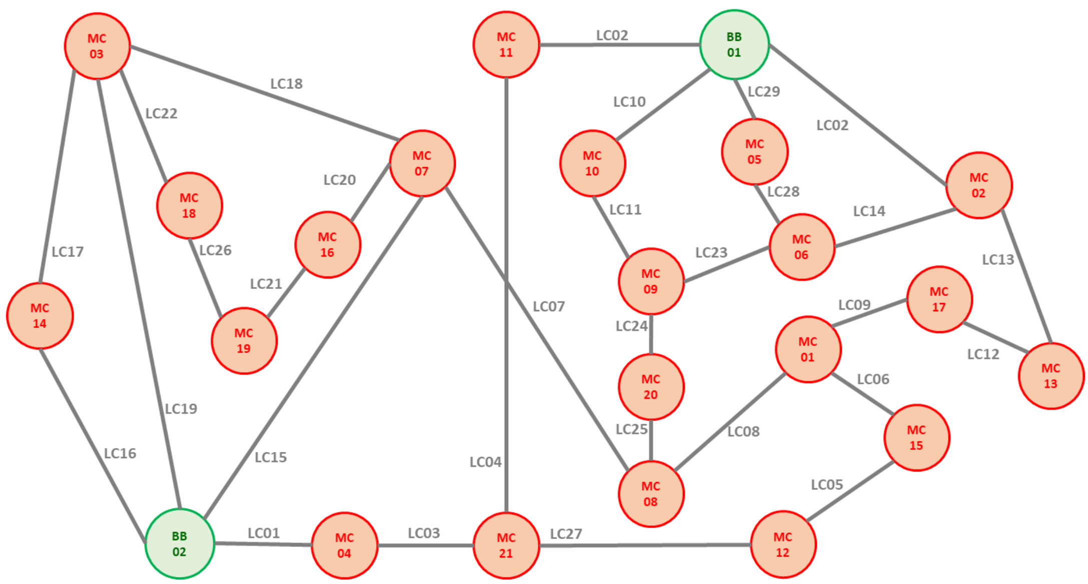

Figure 2-6 – Metro core mesh of the Metro-Access segment proposed as reference topology.

In fact, pairs of nodes of the metro core network collect one or more horseshoes and Figure 2-7 shows the example of the BB02 and MC04 nodes which act as hubs for three aggregation horseshoes, two of them collect four metro aggregation nodes (in blue) each and two metro aggregation nodes.

Dissemination Level	SEN (Sensitive - limited under the conditions of the Grant Agreement)

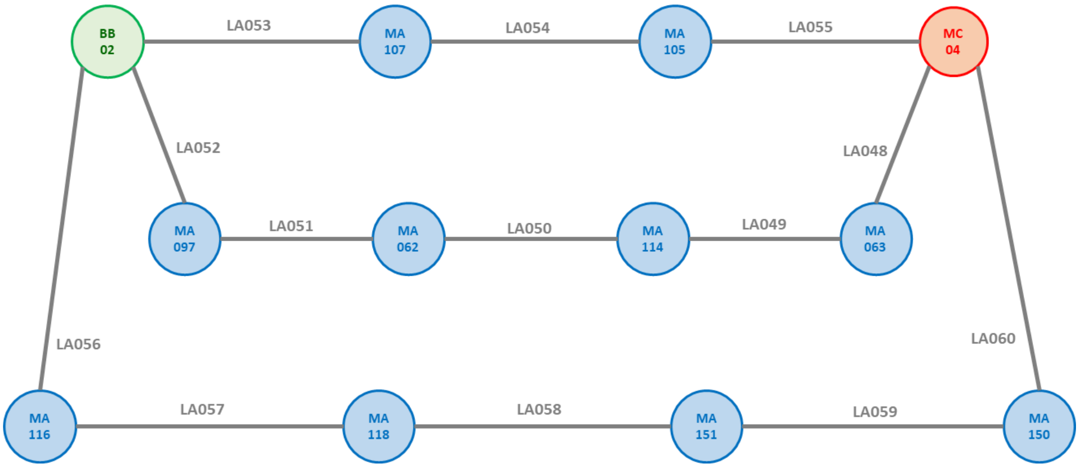

Figure 2-7 – Example of horseshoes collected by a twin of hubs in the Metro-Access segment.

The entire topology (metro core mesh plus all horseshoe structures) is provided in an excel file and made available to project partners for network studies within. In the file in addition to link lengths some characterization parameters are provided for each node, i.e., the number of households covered, the number of mobile radio site hosting macro cells and the number of mobile radio sites that, in future, could potentially host a small cell mobile radio site. The macro cell mobile site counts provided in the file are possible educated guesses but do not constitute a TIM deployment plan.

TID MAN topology

The second network topology proposed as a reference for SEASON network study is inspired by metro-access and metro-regional networks of Telefónica, which includes HL4 nodes and is composed of IP routers at metro-aggregation sites that handle traffic classification, subscriber credentials authentication, validation of users' access policies, routing data to their destination, and aggregation of traffic from different locations of the metro network, as well as from OLTs and radio access points (in densely populated areas). At the HL4 nodes terminate HL5 nodes, which are the nodes that aggregate the data from radio access points and mobile base stations, as well as OLT, which collect the traffic from/to FTTH households.

The metro-regional networks consist of a few HL4 rings multi-homed to two HL3 aggregation nodes belonging to the national network, as is explained in the next section. Depending on the region’s size and population, five different ring configurations can be observed, which can be illustrated in the five representative models presented in Figure 2-8.

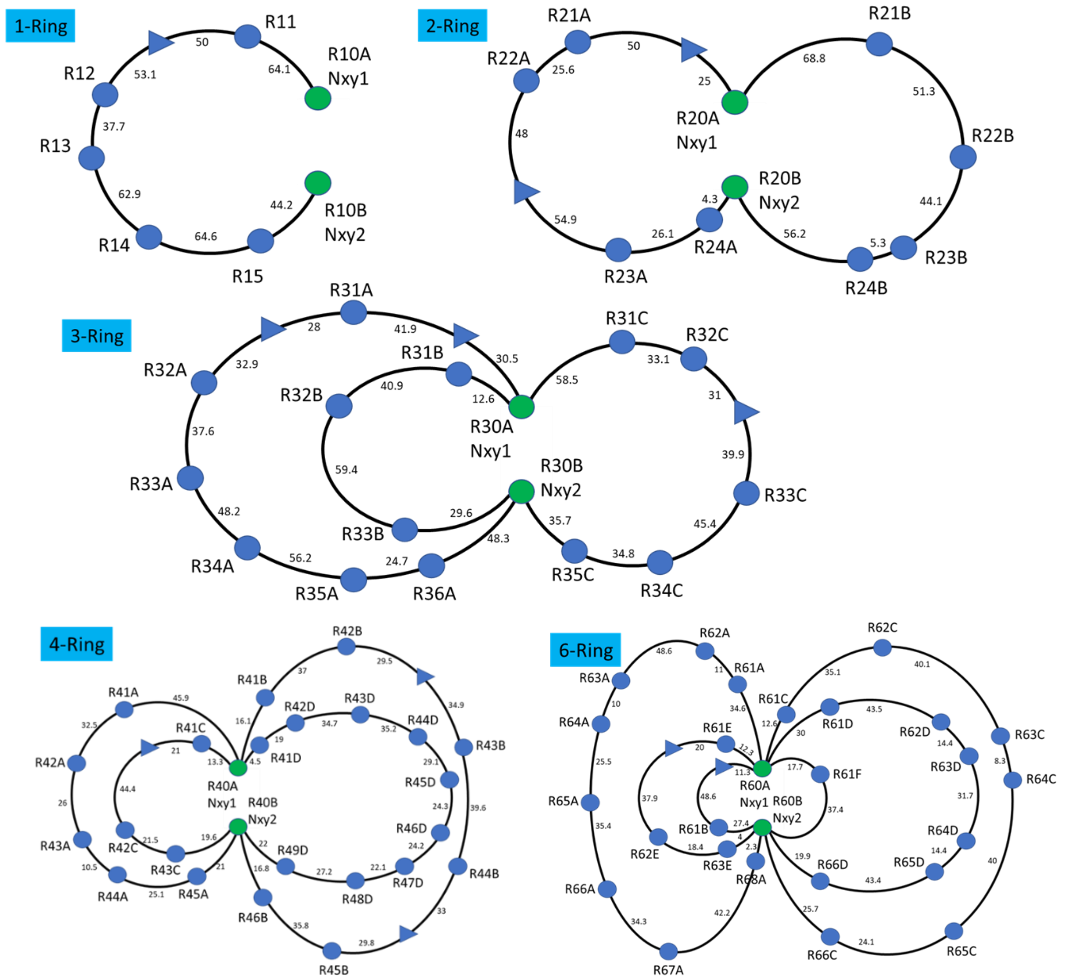

Figure 2-8 – SEASON metro-regional reference network topologies: topologies composed of 1, 2, 3, 4 and 6 rings. The triangle indicates an amplification site.

In Table 2-2 we present the fiber parameters for the metro-regional networks.

Table 2-2: SEASON reference national network fiber specifications.

	Metro-regional Rings	
Fiber type	G.652.D	G.652.B
Attenuation @ 1310 nm	0.34 dB/km	0.4 dB/km
Attenuation @ 1550 nm	0.20 dB/km	0.3 dB/km
Attenuation @ 1625 nm	0.22 dB/km	0.35 dB/km
CD @ 1550 nm	18 ps/(nm·km)	20 ps/(nm·km)
PMD	0.1 ps/sqrt(km)	0.2 ps/sqrt(km)

On the other hand, the metro-access networks consist of semi-rings composed of HL5 nodes (remote nodes) that are connected to two HL4 nodes (aggregation nodes) belonging to either a common metro-regional ring or different rings. As shown in Figure 2-8, four semi-ring models can be defined in terms of their number of nodes, ranging from three to six nodes. In this case, nodes are named following a code consisting of A (for Access) followed by two digits, the first one representing the number of nodes in the semi-ring and the second one serving as the node identifier. For the aggregation nodes, an alternative code is provided, following the naming convention in Figure 2-9, as these nodes also belong to the metro-regional rings.

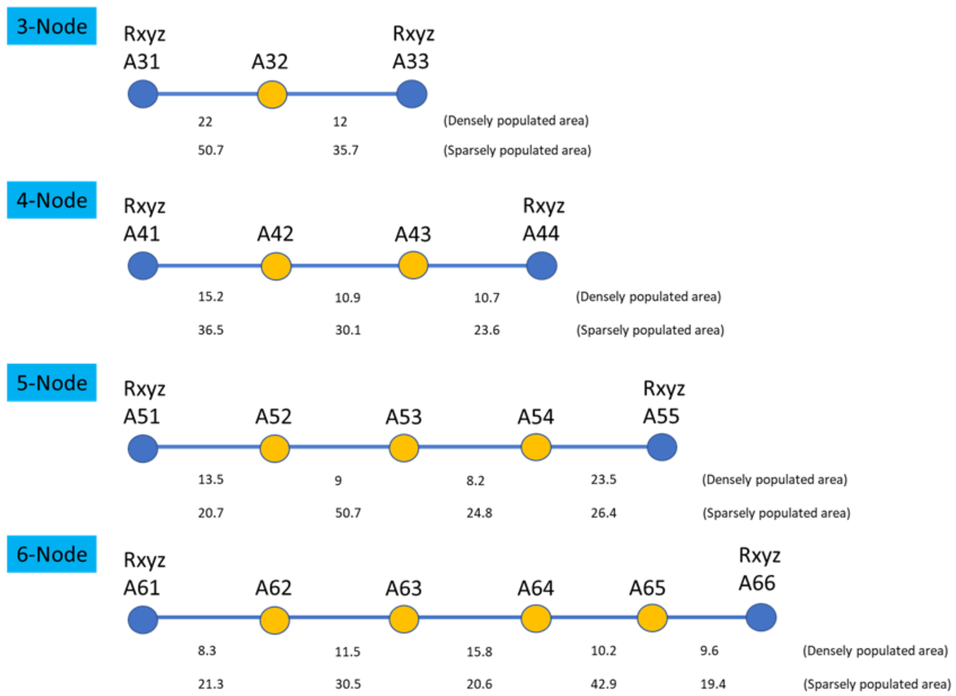

Figure 2-9 – SEASON metro-access reference semi-ring models, formed by a number of nodes ranging from 3 to 6, with link lengths provided for densely and sparsely populated areas. It must be understood that the variable combinations xyz for the aggregation nodes on both ends of each semi-ring model are different.

2.2.2 Topology for Backbone domain

Again, for backbone networks, two reference topologies are proposed, one based on TIM's Italy network topology and another one for TID's Spain network topology.

TIM backbone topology

As a backbone network, a model inspired by the TIM backbone network is proposed. The TIM photonic network is evolving and includes today a number of nodes equal to approximately 50 and a number of links of about 80. A topological representation of the network is given in Figure 2-10 where some statistics on nodal degree and link length are also reported.

Of the 50 national topological nodes equipped with ROADMs all are National COs, some are Regional COs, and some are pure transit site only (i.e., there are no add and drop features on them). Links are the topology edge between ROADMs.

Concerning the type of fiber used on links, fiber: G.655 is prevalent (≈65%) and G.652 takes the remaining part of the share (≈35%). There are residual quantities of G.653 (a few %).

OLA are placed at 80 km on average with distances from 40 to 100 km, but there are exceptions for submarine links (in that case distances between OLAs are greater or significantly greater than 100 km).

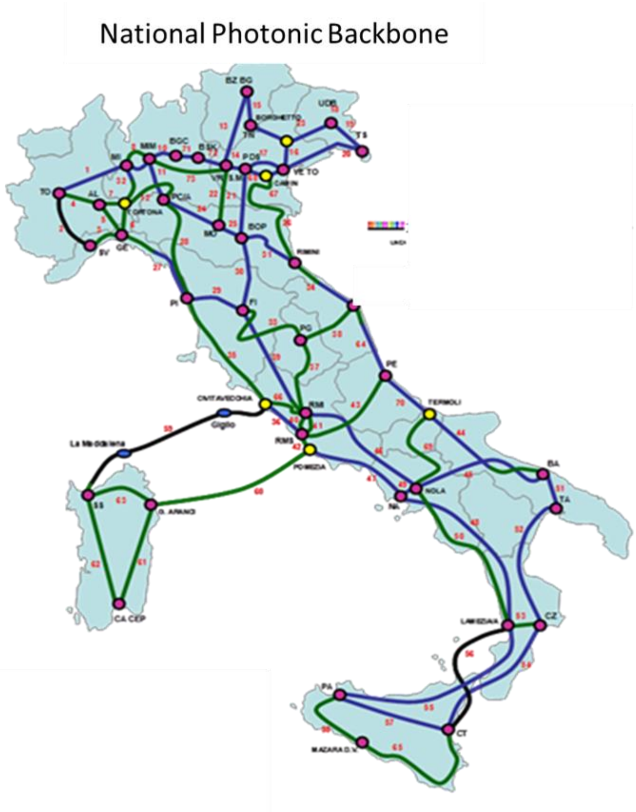

Topological degree	Occurence
1	0
2	10
3	18
4	12
5	4
6	0

Link length L	% of links
0 < L <= 50 km	15.5%
50 < L <= 100 km	16.9%
100 < L <= 200 km	33.8%
200 < L <= 400 km	25.4%
400 < L <= 600 km	8.5%

Figure 2-10 – Topology of the Italian Backbone of TIM proposed as reference network with some node and link statistics. Network are in evolution (number of nodes and links are growing) and the topology depicted above does not correspond to the updated version.

Also in this case, an excel file with the data of the backbone topology appropriately anonymized is made available to project partners to carry out network studies.

<u>TID backbone topology</u>

The other backbone network model presented is based on Telefónica national network. The proposed backbone network is mapped to the HL3-HL2-HL1 IP levels and connects the different regional networks, providing connectivity to data centres, the Internet and other ISP providers. The reference topology considered for SEASON is shown in Figure 2-11, where the nodes are denoted using the following naming convention: N (for National) + two digits (representing a city) + 0, 1, 2… (0 meaning that only one HL3 exists in that city, and 1, 2… differentiate between multiple nodes within the same city). When there is only one HL3 node available in a city (e.g., N050), the metro-regional rings (described in the next section) will be hubbed to two HL3 nodes located in different cities (in this example, to N050 and N060).

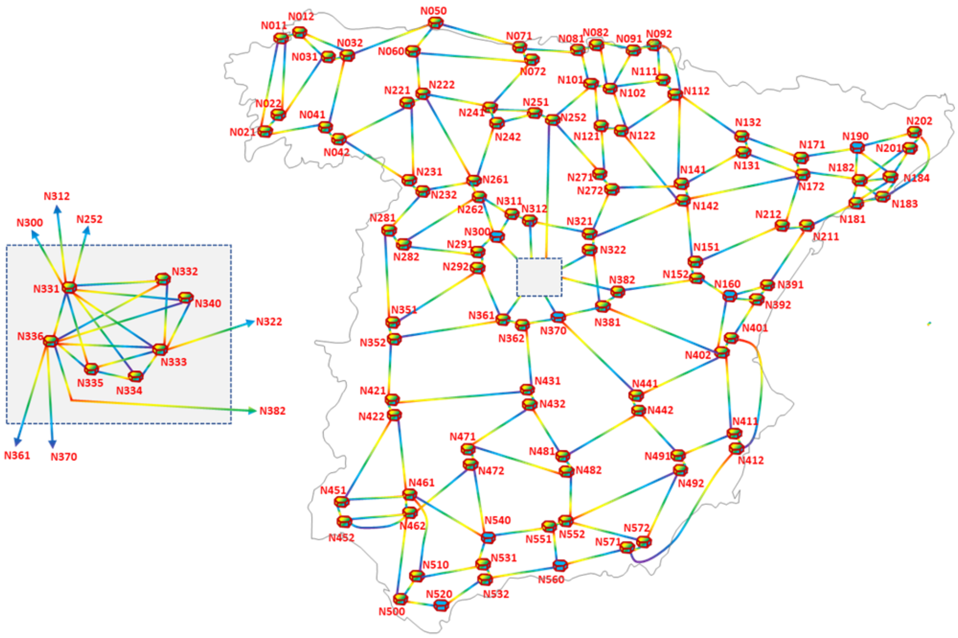

Figure 2-11 SEASON national reference topology. Blue switches indicate nodes without traffic add/drop. The inset shows the optical fiber connections in the Madrid region.

The backbone network is composed of 190 links with an average link length of 104.9 km and an average number of amplification spans per link of 2. The average span length is 53.1 km. Other parameters related to the number of nodes and nodal degree are provided in Table 2-3 and the fiber parameters are indicated in Table 2-4.

Table 2-3: Some statistics regarding the nodes and links classified according to the Telefónica IP hierarchy.

Node Level	Nodal Degree Avg. [Min, Max]	Number of Sites
HL1	6.0 [3, 9]	5
HL2	4.8 [3, 9]	16 (5 also HL1)
HL3	3.4 [3, 9]	98 (13 also HL2; 3 also HL1)
Ø (No A/D)	3.6 [2, 4]	7

Table 2-4: SEASON reference backbone network fiber specifications.

Fiber Type:	ITU-T G652.D
Chromatic Dispersion at 1550nm	18 ps/(nm·km)
Attenuation Coefficient:	
1310 nm	0.34 dB/km
1550 nm	0.20 dB/km
1625 nm	0.22 dB/km
PMD coefficient	0.1 ps/km$^{1/2}$

2.3 Requirements and solutions

2.3.1 Requirements

2.3.1.1 Architectural and general level (network) requirements

WP2 analysed a first set of requirements derived from the project objectives and KPIs of a general scope, such as those relating to the data and control plane architectures and to the monitoring system. The details can be found in Deliverable D2.1.

Other specific requirements are under analysis within the relevant WPs; in particular, for WP3, these requirements are expressed in the following subparagraph 2.3.1.2.

The project objectives considered relevant at general level are the one included in Table 2-5. Obj. 2, Obj. 5 and Obj. 6 are related to WP2 while Obj. 4 was added because of its general relevance and high importance for the project, as it concerns the access architecture and in particular the RAN which places particularly challenging requirements on the transport network.

Table 2-5: Project objectives relevant for architectural and general level in SEASON project.

Objective	Description
Obj. 2	*Design and validate a scalable ultra-high capacity, and power efficient MBoSDM network infrastructure from access to cloud.*
Obj. 4	*Develop an innovative access and front/mid-haul transport solution supporting power-efficient functional split implementations as well as cost-effective small/free cells solutions.*
Obj. 5	*Develop a pervasive monitoring infrastructure for secure and truly self-managed networking.*
Obj. 6	*Provide and validate smart edge nodes for packet/optical integration with computing resources.*

The list below includes the requirements that can be derived from objectives reported above and from their specific KPIs and the actions, activities, and solutions that the project is developing to meet them.

Requirement 1: increase in the optical bandwidth of systems by a factor ×120

This requirement is directly connected to project KPI 2.1 "*Increase the available bandwidth of the fiber from actual C-band (~35 nm) to O, E, S, L, U bands (~415 nm) that, together with the usage of SDM, e.g., with >10 fibers / cores, will make the available bandwidth to grow by a factor ×120 compared to current C-band capacity".*

Drivers: new service use cases for 5G-Advanced and 6G era (in particular Metaverse environment) which require increasingly high bandwidth (data rate) in highly pervasive context.

Considerations: operators' plans pose specific needs and constraints, such as the exploitation of assets already owned before new investments.

Identified actions and enabling technologies to satisfy Requirement 1:

- use of type of fibers for high-capacity transmission;
- use MB and/or SDM transmission.

Requirement 2: 50% of CAPEX reduction

This requirement is directly connected to project KPI 2.2 "*50% CAPEX reduction by (1) designing an architecture that jointly leverages on parallel fibers (where fiber resources are abundant), multiple bands (where fiber resources are scares), and multi-core fibers (where fibers are not present, e.g., for cell densification); (2) limiting intermediate aggregation in routers thanks to the ultra-high capacity of MBoSDM and by exploiting smart coherent pluggable to remove aggregation layers and unnecessary O/E/O conversions".*

Drivers: generic economic saving objective, essential for the sustainability of investments and to make SEASON solutions preferable to alternatives.

Considerations: operators express some actions that aim to achieve the objective. These actions are in mostly part of ongoing processes and must be accelerated and completed.

Identified actions and enabling technologies to satisfy the requirement:

- operators' view on innovative architectural solutions for achieving CAPEX reduction includes introduction or enhancement of: i. network softwarization, ii. intelligent control-plane and network automation, iii. efficient data-plane hardware, iv. multi-band and SDM;
- CAPEX reduction by the use of P2MP in combination with DSCM;
- coordination of radio access and optical transport.

Requirement 3: end-to-end service creation time < 3 min

This requirement is directly connected to project KPI 2.3 "*Network connectivity service with creation time < 3 min combining control and data planes. In [Sha21], 3 mins were needed for network connectivity in the metro segment only, mainly due to laser configuration. In SEASON, connectivity will be extended to cover end-to-end, including front-haul, PON and metro/core.*

Driver: generic and synthetic objective on service time creation as a whole and end-to-end with the aim of improving the performance of current manually assisted or semi-automatic systems.

Considerations: very complex to model and treat as it involves the whole architecture of the control plane and its interaction with the data plane. It can also depend on the size of the network (number of objects under control and coordination involved).

Identified actions and enabling technologies to satisfy the requirement:

- high-level definition of the overall control and orchestration architecture;
- list of relevant use cases;
- effect of control management and orchestration architecture, control protocol stack and AI/ML;
- telemetry role;
- workflows and control plane functions;
- hardware configuration;
- overall assumptions for KPI service provisioning.

Requirement 4: mobile user latency reduction from >5ms to <1ms

This requirement is directly connected to project KPI 4.1 "*<1ms mobile user latency via coordinated resource allocation at optical access and mobile network for SDM-PON mid-hauled RU/DU as a result of SEASON's target integration against >5ms delay in non-integrated approach [Li18]".*

Driver: some service use cases (like the ones of pervasive Metaverse) can require sub-millisecond latency.

Considerations: involves the radio access network (RAN) architecture.

Identified actions and enabling technologies to satisfy the requirement:

- definition of the reference disaggregated sliced open RAN architecture to be adopted;
- introduction of a set of additional features enabling sub-ms latency for the xURLLC service class;

Requirement 5: target of >50% of energy saving via dynamic transmission management

This requirement is directly connected to project KPI 4.2 "*>50% contribution in energy saving via dynamic spatial channels aggregation and deactivation of unused transceivers or spectrum at the OLT side basing on traffic conditions over total 70% energy saving targeted by [SRIA20]".*

Driver: Energy saving is a must in network innovations. 50% saving compared to legacy solutions is considered a satisfactory target.

Considerations: involves the fixed part of radio access network (RAN) architecture and the fiber optics infrastructure.

Identified actions and enabling technologies to satisfy the requirement:

- introduction of a mechanisms that allow to turn on/off wavelengths to follow the traffic fluctuations in a SDM PON architecture;

- use of pluggable modules instead of traditional OLT cards to achieve further energy savings.

Requirement 6: 400Gb/s RAN fronthaul ports capacity

This requirement is directly connected to project KPI 4.3.

Driver: radio systems with carrier width of 100 MHz and above, possibly at multi-carrier sites, may require aggregate front haul bandwidths greater than 100 Gb/s.

Considerations: involves the fixed access network architecture.

Identified actions and enabling technologies to satisfy the requirement:

- the use of low-cost coherent technology for x-haul applications in the RAN;
- assessment of WDM ring architecture for 400G ports capacity fronthaul.

Requirement 7: develop a pervasive monitoring infrastructure for secure and truly self-managed networking

This macro-requirement is directly connected to project Obj. 5 and includes the following specific KPIs that will be addressed in WP4 mainly.

- KPI 5.1: Achieve sub-km (<500 m) and sub-dB (<0.5) resolution in the estimation of longitudinal fiber attenuation points and optical amplifier gain, respectively, using DSP-based monitoring scheme.
- KPI 5.2: Performance improvement achievable with an OSA embedded in the amplifier setup and control identified for different link designs and applications.
- KPI 5.3: OTDR Interrogator for latency / position measurement with 4 ns / < 1 meter accuracy respectively
- KPI 5.4: Applicability of modulation format insensitive OSNR measurement techniques in different scenarios determined, sources of inaccuracy identified, impact of signal distortions worked out.

Driver: Advanced monitoring and control systems for transport networks which are increasingly pressing needs for operators.

Considerations: Telemetry data is a collection of data from many different sources and can be described by means of a number of characteristics [Lan01], known as the 5 V’s, standing the five V for volume, velocity, variety, veracity, and value. In support of the 5 V’s it is possible to specific requirements for the telemetry system, they are not reported here but they will be included in D2.1.

Identified actions and enabling technologies to satisfy the macro requirement (at general level of the Objective, not specific per KPI):

- Intelligent data aggregation as a key component in the monitoring architecture. Techniques to be explored include monitoring data summarization, supervised feature extraction, and compression using auto-encoders [Rui22].
- Use of Digital twin (DT) as another key component for self-managed networking that needs to be continuously fed with monitoring data. A DT should generate, among others, expected signals that can be compared with those obtained from the network by monitoring [Vel23].
- Telemetry as component of the multi-agent system (MAS): telemetry data are consumed at the intelligent control plane, where a MAS controls the infrastructure.

Requirement 8: smart edge nodes for packet/optical integration with computing resources

This requirement is directly connected to project Obj. 6 and includes the following KPIs.

- KPI 6.1: 40% CAPEX reduction by collapsing computing, IP networking, and usage of high-speed intelligent coherent optical transmission in a single element, i.e., DPU, which has not been designed for the Telecom market but for much wider computing markets and verticals (e.g., automotive).
- KPI 6.2: >40% reduction of O/E/O conversions in edge-edge and edge-cloud communications by developing smart edges with high-speed coherent intelligent pluggable and by moving 5G functions closer to the cell sites.
- KPI 6.3: Supporting traffic adaptation/monitoring at µs granularity on innovative HW-accelerated networking SmartNICs/DPUs (including computing, networking, and optical resources) for selected low-latency services.

Driver: simplify (less systems to be hosted, powered and managed) and reduce the cost at the edge.

Considerations: the tendency to decentralize telco functionality at the edge (not just mobile radio ones) together with the opportunity to integrate the computational, packet and optical layers n a single box for the purposes of simplification and CAPEX and energy savings makes the use of integrated smart edge nodes very interesting and potentially convenient.

Identified actions and enabling technologies to satisfy the macro requirement (at general level of the Objective, not specific per KPI):

- Analysis of technology gaps and definition of potential solutions to overcome such limitations during experimental validations.
- Analysis and definition of the underlying working software platform including the operating system and tools for the deployment of containerized applications.

- Analysis of the most relevant acceleration capabilities provided by the SmartNIC/DPU that are of specific interest for the SEASON Project.
- Definition of specific technical activities to provide proof of concept of the proposed packet-optical and computing integrated solution.

2.3.1.2 WP3 related optical and optoelectronic system and subsystem level requirements

The project objective Obj. 3 defines the design and development of novel optical systems and subsystems for multiband over SDM. Optical and optoelectronic systems specified, designed and developed in WP3 will be integrated with the control functionalities developed in WP4 and used in the final demonstrations within WP5. Table 2-6 reports the Obj. 3.

Table 2-6: Optical and optoelectronic systems related project objective.

Objective	Description
Obj. 3	*Design and development of novel optical systems and subsystems for multiband over SDM.*

The specific KPIs of Obj. 3 give origin to the following requirements.

Requirement 9: develop a MBoSDM space-wavelength flexible modular node of Pb/s capacity

This requirement is directly connected to project KPI 3.1 "*Design and implement flexible and modular MBoSDM node prototypes able to switch/add/drop channels in at least 3 different bands (e.g., S, C, L) in an SDM/MCF fiber infrastructure featuring up to 10 fibers/cores, able to cope with switching capacities scalable up to between 2.4-3.6 Pb/s (considering a 4-degree node with 50% local add/drop and depending on the number of used bands and SDM cores/fibers) [SRIA20], by approaching (fractional) space-wavelength flexible architectures"* [Mar15].

Driver: cost-effective prototype node capable of switching bands, accordingly, adding and dropping bands within the node. Fully programmable procedure, allowing for remote MB system operations. A second programmable node prototype offering three different granularities comprising WDM, MB and SDM (lambda, band and core switching).

Considerations: Applicable to core and metro networks with acceptable insertion loss over the operations bands (1460 - 1650 nm), reconfigurable switching according to the telemetry data collected and upon detecting anomalies. For the second prototype WDM operation limited within the C-band (one direction flexi-grid and one direction fixed-grid) also enabling S+C+L band (1460-1650 nm) and core switching (2 per direction).

Identified actions and enabling technologies to satisfy the requirement:

- Use of MB multiplexers/demultiplexers along with an optical matrix responsible for switching the band accordingly.
- For the second prototype, use of MB and SDM multiplexers/demultiplexers and WSS/AWG filters along with an optical matrix for switching the bands, cores and wavelengths accordingly.
- Analysis for controlling the operation of the node via software including the operating system and tools.
- Connection with the MB testbed infrastructure for testing and further analysis.

Requirement 10: develop a MBoSDM transceiver (slice/band/core/fiber) of Tb/s capacity

It follows from KPI 3.2:

- KPI 3.2: MBoSDM transceivers able to increase the capacity of SotA transceivers [Nad22] up to 2× - 4× by exploiting enhanced wavelength/space dimensions while enabling appropriate slice/band/core/fiber selection according to the network path.

Driver: MB(oSDM) sliceable bandwidth/bit rate variable transceiver (S-BVT) prototype consisting of 3 lower capacity transceivers/slices that can operate across different bands. Each slice can be sent to a different spatial channel.

Considerations: Transceiver architecture fully scalable and modular to satisfy/meet the required capacity targets. Programmable within the S+C+L bands by means of SDN control. Extendable to additional spectral bands by suitably integrating key subsystems/devices capable of operating within these bands.

Identified actions and enabling technologies to satisfy the requirement:

- Use of a MB optical aggregator/distributor device to aggregate/distribute the different contributions/slices that can work in different spectral bands.
- SDN integration to enable transceiver programmability and reconfiguration. Different transceiver slices can be enabled/disabled according to the network capacity requirements.
- Integration with a network/testbed infrastructure capable of enabling MBoSDM operation for validation and analysis.

Requirement 11: develop a DSP for metro/core coherent applications at 1.6 Tb/s per port with power consumption compatible with pluggable module.

It follows directly from KPI 3.2:

- KPI 3.3: Optimized DSP for metro/core coherent applications, able to increase 4× data-rate, reaching up to 1.6 Tb/s per port with power consumption suitable for future pluggable modules.

Driver: it is the simplification of the network that could lead to a reduction in cost (both capex and energy consumption) and footprint, by being able, at the extreme, to incorporate this functionality into packet layer switching equipment (router or layer 3 switches).

Considerations: the challenge in achieve this requirement is the reduction of the power consumption of these very high-capacity modules and make them compatible with pluggable modules without losing performance (compared to DSPs implemented in traditional transponders). Another issue is the management of these modules, in particular whether they will be hosted in packet switching equipment. The order of magnitude of power consumption of such pluggable modules, considering the form factors available and their power dissipation limits, is 15 W.

Identified actions and enabling technologies to satisfy the requirement:

- not yet established, the work is in progress.

2.3.1.3 Other requirements

In addition to the general objectives and those specific to optical systems, the project must also achieve the objectives of Table 2-7, which will be addressed in the activity of WP4 and WP5. Like those already analysed, the objectives include specific KPIs that can be translated into requirements on the systems or on their integration.

Table 2-7: Control and orchestration plane (WP4) related project objectives.

Objective	Description
Obj. 7	*Control plane, Monitoring and streaming telemetry*
Obj. 8	*AI/ML Service Orchestration and Self-Management and Secure AI*

2.3.2 Solutions

2.3.2.1 Architectures to reduce OEO devices and power consumption.

Historically, metro networks were built by telephone operators to create connectivity between local exchanges in metropolitan areas. Most phone calls were local and required connectivity only to a different local phone exchange in the same metro area.

The resulting traffic was highly meshed and P2P in nature, and the few long-distance phone calls were routed to a Central Office (CO) to reach the remote destination [Sin94]. Internet Protocol (IP) data traffic is quite different, as end users are connected to Internet Content Provider (ICP)s hosting their services from a small number of Data Center (DC)s [Dwi00].

With the explosion of user data traffic, network patterns have shifted and are now dominated by hub-and-spoke (H&S) traffic, regardless of whether the end user is connected to the Internet through a mobile handset, a cable modem, a Fiber-to-the-Home (FTTH) media converter or an Asymmetric Digital Subscriber Line (ADSL) device.

In the context of H&S traffic patterns, P2P networks are not ideal anymore, as the traditional approach relies on higher layers like OTN (Optical Transport Network) to achieve some level of P2MP functionality, but it is not perfect. In [Wel21], a new architecture with coherent digital subcarrier multiplexing (DSCM) has been introduced, and this has the potential to transform current P2P networks into flexible, scalable, and multi-generational compatible P2MP networks. This is achieved by using individually routed and digitally generated subcarriers [Wel21], which allow for interoperability between different transceivers operating at various speeds. In fact, DSCM could seamlessly interconnect various transceivers – a feature absents in traditional P2P coherent optical networks – by aggregating the digital subcarrier by using passive coupler. By using this technology, a central hub could be equipped with a high-speed pluggable, i.e., 400G, and it could transmit data to multiple destinations (spokes) at varying speeds, all on the same infrastructure. This flexibility is particularly well-suited for metro and access networks characterized by H&S traffic patterns. An equivalent network, realized with traditional P2P pluggable would struggle to efficiently handle traffic patterns where a central hub needs to communicate with multiple endpoints. An example of how the two solutions (P2P and P2MP) realize aggregation in a metro-access network is illustrated in Figure 2-12 from [Wel21].

Figure 2-12(a) shows a simplified metro/access aggregation network architecture. Here, the transceivers of N endpoints (5G antennas, curb aggregation boxes, etc.) are directly connected with those at the electrical aggregation stage. In this configuration, N low data rate transceivers are needed on each side, therefore $N \times 2$ transceivers, plus 2 high-speed ones are necessary to build the network. This solution is optimal for traditional telephony, where the connections were point-to-point, but it becomes sub-optimal in the case of highly asymmetric hub-and-spoke traffic. An alternative approach is reported in Figure 2-12(b). Here, only N low-speed transceivers and 1 high-speed one are required, i.e., 50% less than in the previous figure. In addition, in the P2MP architecture, multiple low-speed transceivers (spokes) are now directly connected to high-speed ones (hubs), thus removing the bookended transceiver paradigm. This approach eliminates the need for intermediate traffic aggregation stages while leveraging larger, more efficient switching devices at centralized sites. The related costs for power consumption, footprint, sparing parts, and grooming equipment are consequently reduced.

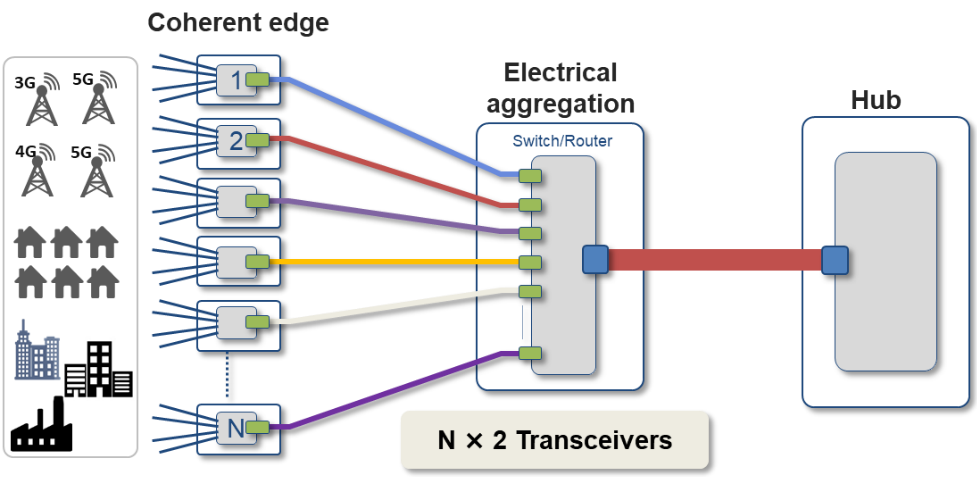

(a)

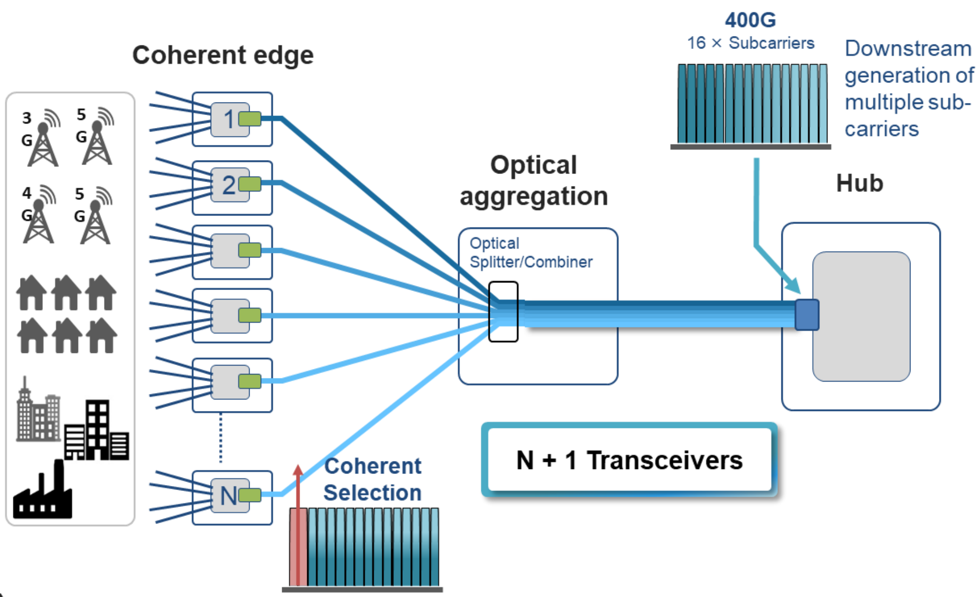

(b)

Figure 2-12 – Single-carrier coherent transceiver (a) vs. multi-carrier transceiver (b) [Wel21].

The coherent P2MP approach is a new concept for the physical layer, but it is already common in higher network layers. For example, in Optical Transport Networks (OTN), the different data streams are multiplexed for different destinations within a single unit. Similarly, routers can divide a high-speed signal into multiple lower-speed signals for shorter distances. To successfully implement P2MP transmission in this context, the system needs an efficient mechanism to map incoming data traffic onto the designated digital subcarrier for its specific recipient. This ensures the data reaches the correct destination within the network.

The same solution can be considered at the edge of the network, as will be reported in section 4.3.5. Here, thanks to the digital subcarrier approach, the optical layer can be significantly simplified by removing the gateway. In SEASON, we will investigate the feasibility of this solution with experimental evaluation.

2.3.2.2 Efficient and flexible devices

To address the network requirements in terms of energy efficiency and adaptability, flexible innovative transmission and switching solutions (detailed in section 4.2 and 4.3, respectively) are investigated and proposed in SEASON. These approaches include the adoption of different key technology such as super-channel (or multicarrier) transmission, P2MP operation, the use of pluggable transceivers and amplifiers (within the access/metro segment) while adopting a disaggregated approach. On the one hand, super-channel (or multicarrier) transmission will enhance overall network flexibility and efficiency by the exploitation of adaptive modulation (implementation of bit and power loading algorithms) and spectrum saving optimization techniques. Since traffic in most aggregation networks shows a hub and spoke pattern, P2MP solutions are attractive as they eliminate the need for redundant equipment and infrastructure at multiple destinations and can provide efficient and flexible use of the different network resources. P2MP devices enable centralizing the transmission, also reducing the number of active components and, consequently, energy consumption and equipment costs while providing dynamic bandwidth allocation. The strategic use of pluggables in the access and metro segments of the network will provide a high level of scalability and adaptability to varying traffic demands allowing for seamless network adjustments and expansions without necessitating extensive hardware overhauls. Moreover, using P2MP solutions allows aligning CapEX with actual bandwidth requirements while keeping the ability to adapt to changing bandwidth requirements and traffic patterns. This approach optimizes the network's flexibility while reducing long-term operational costs, footprint, and power consumption. Indeed, high capacity P2MP devices enable maximizing router efficiency, density, and simplicity by replacing large numbers of low-speed ports with far fewer high-speed ports, and with the ability to use these same high-speed ports as both aggregation and network interfaces. Moreover, open, and disaggregated approaches will lead to more granular and modular solutions which will enable individual optimization and upgrades of the different components providing a more efficient use of the power and bandwidth resources. In summary, SEASON’s cutting-edge technologies and innovative efficient and flexible solutions/devices are holistically designed to enhance overall network efficiency, flexibility, adaptability, and cost-effectiveness.

2.3.2.3 SDM PON spatial aggregation

SEASON addresses the challenge of dynamic resource allocation in PONs by focusing on spatial division multiplexing (SDM) and aims at a sustainable capacity scaling in the optical access segment by implementing dynamic allocation mechanisms that are not confined to traditional time or wavelength divisions but extend to spatial dimensions. This approach is particularly relevant for supporting mobile networks through front/mid/back-hauling, where the integration of optical (via NETCONF) and radio (via O-RAN) networks can yield enhanced efficiency and cost savings. The fluctuating nature of user traffic in PONs and Radio Access Networks (RANs) is a key consideration in this architecture. This allows us to adjust the number of active and power consuming elements based on fluctuating traffic, leading to inefficiencies. SEASON's proposed architecture introduces the concept of spatial aggregation in PONs. By dynamically managing spatial channels, the architecture allows for the consolidation or expansion of network capacity based on real-time traffic conditions. This is achieved through sophisticated control mechanisms, likely involving software-defined networking (SDN), enabling more efficient use of network resources.

This means that in conditions of low traffic, it's possible to aggregate multiple optical distribution networks (ODNs) over fewer spatial channels. This reduces the number of active transceivers and line cards required at the Optical Line Terminal (OLT), leading to significant energy savings. Conversely, during periods of high demand, the network can activate additional spatial channels to accommodate the increased traffic load. The architecture's flexibility extends to its applicability across various PON technologies, including next-generation and pluggable PON solutions. This adaptability allows for dynamic bandwidth allocation tailored to the specific needs of different network types, further enhancing the potential for energy efficiency and cost-effectiveness.

2.3.2.4 Energy efficient network

Typically, transceivers (and transponders) utilize power-hungry digital-to-analog and analog-to-digital converters (DAC and ADC), and electronic application-specific integrated circuits (ASICs) to perform digital signal processing (DSP). Traditionally, DSP has been designed to meet transmission requirements rather than to optimize energy consumption. In addition, the power consumption of these devices increases with the symbol rate, which must grow to accommodate higher-speed traffic. Moreover, we must consider that where different domains are connected (e.g., at the edge of metro/access segments), traffic is aggregated at the electronic domain (e.g., at the IP layer), thus relying on power-hungry electronic interfaces and processing. As an example, the work in [Her20] assumes several traffic aggregation scenarios at the edge: e.g., (A) 2×100G, where half of the traffic is related to the access (as several flows at 10G) and the other half to the data center inter-connections, all aggregated at Layer 3; B) a similar scenario of (A) with the aggregation carried out by 2× Layer2/Layer3 switches; the related power consumption values can reach 2000 W for the former scenario and 400 W for the latter. Thus, traffic aggregation and, in general, edge nodes are very important functionality / network point impacting the overall network power consumption.

Within the framework of the SEASON project, an energy-efficient solution for the edge node has been proposed [Sam23] based on digital sub-carrier multiplexing (DSCM) and P2MP. DSCM adds an extra layer of multiplexing over Wavelength Division Multiplexing (WDM) by allowing several digital sub-carriers to be multiplexed over a wavelength channel. Moreover, the digital sub-carriers can be all-optically multiplexed. This optical aggregation can replace electronic traffic aggregation typically used at the metro edge, reducing the use of power-intensive interfaces in favor of passive optical devices that consume negligible power.

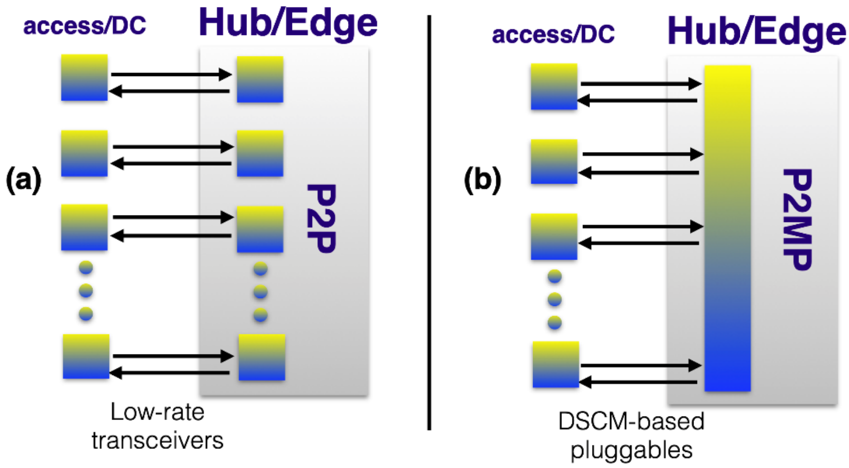

Figure 2-13 – (a) P2P; (b) P2MP.

Figure 2-13(a) shows a traditional edge node architecture, in which point-to-point (P2P) low-rate connectivities (e.g., at 10 Gb/s) serve metro and accesses or data centers (DCs); at the edge, an interface is needed for each connection, moreover, traffic is electronically aggregated flowing in the metro segment.

Figure 2-13(b) shows a P2MP architecture where, at the edge, a single interface can serve several interfaces at the access. Indeed, thanks to DSCM, each connection can be served through a digital sub-carrier. Energy saving is thus achieved by saving several transceivers at the edge. Moreover, we can also think of removing that interface and aggregate sub-carriers all-optically through a splitter/coupler.

The P2MP architecture is compared against the P2P over the network topology shown in [Sam23]. Traffic projections are considered for the short-, medium-, and long-terms. First, the number of interfaces (i.e., transceivers) is evaluated considering P2MP and P2P. Several interfaces (or transceivers) are considered: 100Gb/s, 200Gb/s, and, in the case of P2MP, also XR pluggables that support a maximum rate of 400 Gb/s. With P2MP, all interfaces support DSCM. Results are reported in Figure 2-14. P2MP strongly reduces the number of interfaces for any projection in the short-, medium-, and long-term. For example, at the short-term, P2MP requires 20 interfaces in the considered scenario, while P2P requires 36 interfaces; at the long term P2MP requires around 24 interfaces, while P2P, around 36.

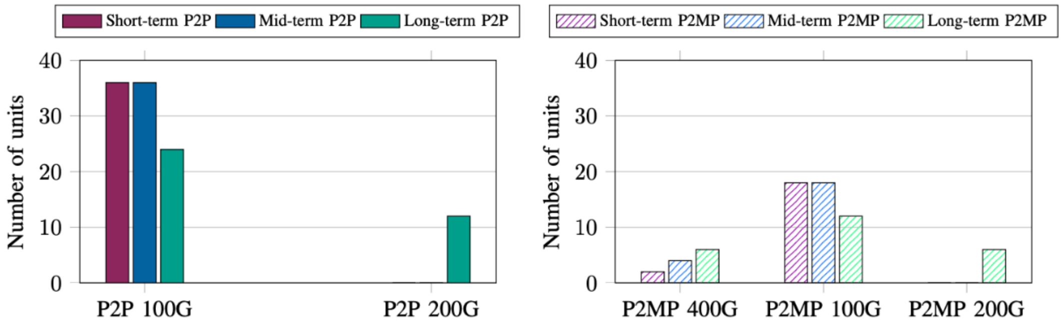

Figure 2-14 – Number of required interfaces vs. traffic projections for electronic P2P aggregation (left) and P2MP aggregation (right).

The reduction of interfaces with P2MP translates to power savings. To analyse the power savings, the following two power consumption scenarios are considered: S1 the power consumption of 100G is 28 W, 45 W for 200G, and 75 W for 400G (computed as interpolation of the previous ones); S2 all transceivers are assumed to be comparable in terms of power consumption to the 400G ZR+ consuming 15 W. The two S1 and S2 scenarios aim to emulate two conditions: when power consumption increases with bit rate and when power consumption at the different bit rate values is comparable.

Table 2-8: Power consumption at the edges.

	Short term		Medium term		Long term	
	S1	**S2**	**S1**	**S2**	**S1**	**S2**
P2P	1008	540	1008	540	1212	540
P2MP	654	300	804	330	1056	360

The power consumption in the two scenarios is shown in

Table 2-8 and has been computed considering the number of 100G, 200G, and coherent P2MP DSCM-based interfaces in the three traffic projections conditions. Given that overall P2MP reduces the number of transceiver interfaces, relevant energy savings can be achieved with P2MP with respect to traditional network architecture where, in the edge node, opto-electronic conversion is performed. As an example, in the short term, in scenario S1 (where power consumption increases with bit-rate interfaces), P2MP reduces power by 35%, while in scenario S2 (where power consumption does not strongly depend on the bit rate) by 44%. In the long term, in scenario S1, P2MP reduces power by 13%, while in scenario S2 by 33%. Note that these numbers only account for transceiver interfaces, while electronic traffic aggregation in the traditional case is not reported. As an example, the power consumption of an IP router can be in the order of thousands of Watts, with the potential for P2MP to further reduce power consumption.

2.3.2.5 Enabling high-capacity transmission

The enabling of high-capacity transmission, considering that the further increase in spectral efficiency (SE) has rather limited margins, can be based on MboSDM systems or through their synergy.

MBT has a high potential to enable the cost-effective upgrade of optical networks since it maximizes the usage of the existing infrastructure, potentially postponing new fiber roll-out and maximizing the return-on-investment. This is the fundamental advantage of MBT when compared with the remaining SDM approaches. Particularly, MBT aims at expanding the transmission spectrum beyond the currently utilized C-band only, by considering the complete low-loss bandwidth of single-mode fibers (SMF). Therefore, MBT has the potential to increase the bandwidth offered by a factor exceeding 10x.

An early form of MBT is already a reality, since commercial systems exploiting C+L-band for data transmission have become available and have been deployed in live networks. A significant number of contributions have been recently published in the major journal and conferences of the area, covering MBT systems exploiting different combinations of the O-, E-, S-, C-, L- and U-bands [Sad22]. A key aspect to consider with MBT is the difference in performance that may be expected across the different bands. For instance, O-band shows quite poor optical performance when compared to the remaining bands.

The use of multiple spatial light-paths is an effective approach to scaling available bandwidth and capacity of fiber-optic systems, and its most straightforward implementation is the one based on parallel single-mode fibers (SMF) and systems. However, a major limitation of this solution is that the increase in system capacity comes with the same cost per bit of the individual single-mode systems operated in parallel.

Cost-per-bit reduction can be enabled by system-resource integration, in which case the use of multiple spatial light-paths is referred to as Space-Division Multiplexing (SDM)

An SDM system is a system in which some of the end-to-end (e2e) components are shared among the spatial light-paths used for transmission. However, the cost effectiveness of an SDM system using multi-core fiber, compared to the cost of a multi-fiber system using traditional fiber of the same capacity, will need to be evaluated on a case-by-case basis and it will depend on the maturity and cost of the two alternative technologies at the time of the deployment.

A special flavor of spatial multiplexing is the one based on the use of novel fibers, where multiple spatial light-paths are integrated into a single fiber, which we refer to as SDM fibers. In particular, two main types of SDM fibers can be identified: Multi-Core Fibers and Few-Mode Fibers (FMFs). These fiber technologies can provide a considerable increase in cable spatial-channel density, compared to single-mode fiber cables that are available today.

The spatial density of transmission channels can be increased not only by using special fibers like MCFs and FMFs/MMFs mentioned above, but also by increasing the number of single-mode fibers in a cable. This approach is based on extreme packing engineering of many fibers inside a classic fiber cable, and it entails a paradigm shift from increasing spectral efficiency to increasing spatial efficiency.

An extended discussion on MBT on the SDM is provided in section 3, hereafter an approximate evaluation on how the capacity can be increased by a factor of 120 compared to the current capacity of C-band only systems (we consider systems for use in the meter segment and backbone) is proposed.

Thinking about the use of multiple bands on the same fibre, while remaining cautious to prevent deleterious effects due to the interaction of signals on different bands, we can think that the band usable with the MBT could be 3 times the standard C band (5 THz) exploited in the systems today. If we then assume that the spectral efficiency (SE) can increase, compared to that of today's systems, but considering the rather limited margin in this improvement, we can think of a 35% growth in capacity due to SE improvement. Thus, the combination of multiband and spectral efficiency allows an increase in capacity of the order of a ×4 factor. To reach the ×120 capacity of Requirement 1 (KPI 3.1), it will therefore be necessary to obtain from the SDM a multiplication factor of the order of ×30, i.e. multi-core fibers with 30 cores (in alternative, two multicore fibers with 15 cores in parallel, or 3 fibers with 10 cores) or, in alternative, systems with 30 standard single core fibers in parallel.

3 PHYSICAL LAYER MODELLING

This section shortly introduces the transmission models that will be used within SEASON, including MB and SDM transmission. The Gaussian noise model is introduced considering its generalization for wideband optical systems as well as the ones to model multi-core and multi-mode fibers.

3.1 MULTI-BAND TRANSMISSION

MB transmission solutions are designed to optimize the utilization of existing infrastructure, thereby postponing the necessity for new fiber deployments. The widely utilized ITU-T G.652D fiber provides a transmission spectrum with low loss, spanning about 54 THz from the O- to the L-band, as illustrated in Figure 3-1. This signifies a more than tenfold expansion in available bandwidth compared to C-band-only systems (4.8 THz). However, it's important to note that optical performance in other transmission bands is not as efficient as in the C-band. Consequently, the increase in bandwidth does not directly result in a tenfold enhancement in network capacity. In practical terms, ultra-broadband systems can achieve a capacity increase of approximately up to five times, as extensively discussed in [Win17].

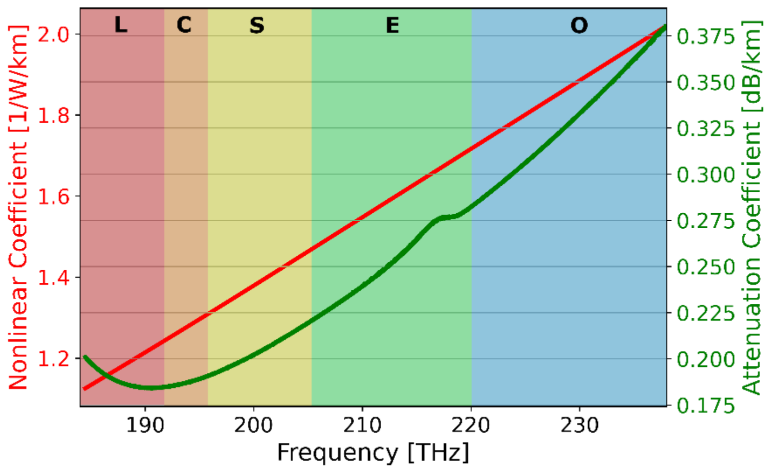

Figure 3-1 – Frequency evolution of the attenuation and nonlinear coefficients of a G.652D fiber.

Developing fast yet sufficiently accurate models for estimating the Quality of Transmission (QoT) is crucial for efficient network optimization within a reasonable timeframe. This task poses a challenge in wideband systems. In coherent multilevel-modulated dispersion uncompensated wavelength division multiplexed (WDM) optical transmission systems, the QoT of a lightpath can be reasonably accurately estimated using the generalized signal-to-noise ratio (GSNR), as discussed in [Fer20]. The GSNR considers the impact of additive Gaussian disturbances introduced by optical amplifiers, such as amplified spontaneous emission (ASE) noise, and the nonlinear interference (NLI) caused by self- and cross-channel nonlinear crosstalk during optical fiber propagation. In this case, the GSNR of channel i after is given by Eq. 1.

$$GSNR_i = \frac{P_i}{P_i^{ASE} + P_i^{NLI}} \qquad \text{Eq. 1}$$

Where P_i is the signal power, P_i^{ASE} and P_i^{NLI} are the power of accumulated ASE noise and nonlinear effects of channel i , respectively.

The introduction of coherent detection, coupled with digital signal processing, and the subsequent widespread adoption of dispersion uncompensated optical systems, has facilitated the creation of numerous perturbative models for estimating NLI [Pog17]. These models have become essential for effective system design and network optimization at the physical layer. For example, various studies have validated the accuracy of the conventional Gaussian Noise (GN) model in both point-to-point and network scenarios, particularly in the context of C-band-only transmission. These studies utilized the GN model for network design and to determine the optimal operational conditions for the system [Pog14, Fer20, Lop20].

In wideband transmissions, certain simplifications commonly employed in modelling single-band transmissions lose their applicability. Notably, considerations for the frequency dependency of dispersion, attenuation, and nonlinear coefficients become imperative. For illustration, Figure 3-1 depicts the nonlinear and attenuation coefficients within the bandwidth of interest for a G.652D fiber. In the context of C-band-only transmission, these parameters exhibit a maximum variation of 6% across the bandwidth. In contrast, within the entire low-loss bandwidth, the values of these parameters in the O-band are nearly double their lowest values. The frequency variation of the dispersion parameter is typically addressed by its value at a specific wavelength and its slope. A typical G.652D fiber, for instance, features a dispersion parameter of 16.8 ps/nm/km at 1550 nm and a dispersion slope of 0.058 ps/nm^2/km.

Another crucial factor in modelling wideband transmissions is the stimulated Raman scattering (SRS), a nonlinear effect that induces the transfer of optical power from higher to lower frequencies, described by a set of ordinary differential equations (ODE). Figure 3-2 illustrates the Raman gain coefficient of a G.652D fiber as a function of the frequency separation between interfering frequencies. While SRS always influences signal propagation in optical fibers, it remains a relatively weak effect in C-band-only transmissions (typically spanning 4 to 4.8 THz). However, SRS becomes a dominant transmission effect in wideband systems, where the transmission band may extend and even surpass 13 THz of continuous spectral occupation. Consequently, more sophisticated models [Can18, Sem18, Rob17], such as the well-established Generalized Gaussian Noise (GGN) model [Can17], are necessary for assessing the physical layer in such cases.

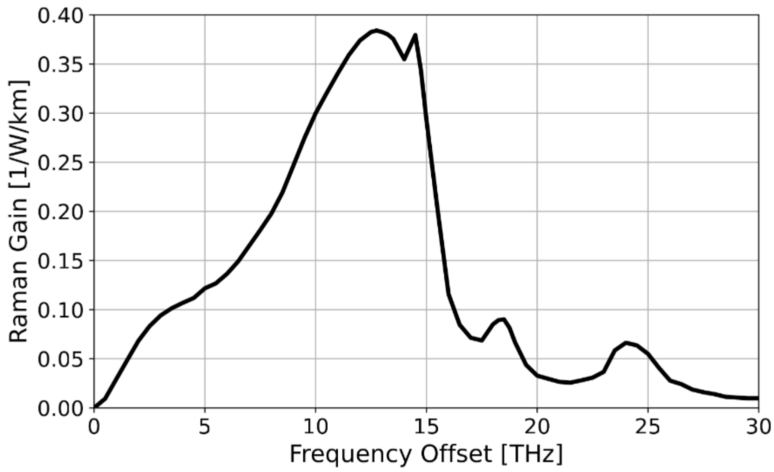

Figure 3-2 – G.652D fiber measured Raman gain profile.

Consequently, several extensions of the GN model that simplify the estimation of the NLI power, while aiming to assess it with reasonable accuracy when exploiting MB transmission systems, have been proposed in the literature. Each model makes different assumptions, shortlisted in Table 3-1, that lead to different trade-offs between accuracy and computational complexity.

Table 3-1: NLI power estimation methods' main assumptions. Adapted from [Sou23].

Method	Approach	Assumptions					
		Modulation Format Effects	Impact of SRS on NLI	Raman Gain Profile	SPM Accumulation	XPM Accumulation	Uniform Launch Power
GGN	Integral [Can17]	NO	YES	Real	Incoherent	Incoherent	NO
	Semi-analytical [Ami22]	NO	YES	Real	Incoherent	Incoherent	NO
ISRS-GN	Integral [Sem18]	YES	YES	Linear	Coherent	Incoherent	YES
	Closed form [Sem19]	YES	YES	Linear	Coherent	Incoherent	YES
eFWM	Closed form [Sou23]	YES	YES	Real	Coherent	Coherent in link, Incoherent between links	YES
GN	Closed form [Pog17]	NO	NO	---	Incoherent	Incoherent	NO
Enhanced GN-ISRS	Closed form [Rob17]	YES	NO	----	Coherent	Incoherent	YES

The models may be classified as requiring numerical integration (such as the integral forms of the GGN [Can17] and ISRS-GN [Sem18] models), semi-analytical (semi-analytical approximation of the GGN [Ami22]) and fully analytical (closed-form ISRS-GN [Semrau:2019], eFWM [Sou23], GN [Pog17] and Enhanced GN-ISRS [Ian:17]). The analytical models are the fastest ones but require more approximations, which may lead to worse accuracy. Moreover, some models do not consider the modulation format's impact on the NLI, leading to a worst-case scenario by considering signals that statistically behave as stationary Gaussian noise (“signal-Gaussianity” assumption). This Gaussianity assumption causes inaccuracies in the NLI estimation on the first spans. However, it was found that the reach predictions are pretty good for practical system configurations [Pog12]. Regarding the SRS effect on the NLI power, a few models ignore it entirely (e.g. enhanced GN-ISRS), leading to estimation errors on wideband transmissions. However, it has been shown that the error in margin prediction is smaller than 0.3 dB for a long-haul transmission on a fully loaded C+L-band system [Ian:17]. Additionally, some models consider approximations of the accurate (i.e., real) Raman gain profile. The self-phase modulation (SPM) accumulation along the different fiber spans of a lightpath may be assumed as coherent or incoherent. In contrast, the accumulation of cross-phase modulation (XPM) should be kept incoherent, at least between the fiber links of the lightpath for practical reasons. When entirely neglecting the coherency of the NLI accumulation, the launch power can be optimized on a span-by-span basis, which significantly simplifies the power optimization process. Quite accurate reach predictions are usually achieved when following this approach. However, it fails to provide a detailed picture of the NLI accumulation along a link [Pog12]. On the other hand, when assuming the coherent accumulation of the NLI (by assuming that the SPM accumulates coherently along the lightpath and the XPM accumulates coherently in each fibre link), the launch power has to be optimized for all the spans of the lightpath simultaneously, leading to a much more complex optimization problem, predominantly if the lightpath is composed of a high number of network elements. To mitigate this limitation, closed-form models that consider the coherent accumulation of the NLI (such as the ISRS-GN and the FWM model) assume identical spans in the lightpath. This limitation hinders their application to real optical network scenarios (with non-homogeneous fiber links). Moreover, some models also assume a uniform launch power in the entire transmission band (rectangular power spectrum) to derive analytical solutions to calculate the impact of the SRS effect. Despite this limitation, these models may still be used to obtain a rough estimate of the optical performance.

We are especially interested in NLI estimation accuracy in the following scenarios:

- C-band-only (4.8 THz),
- SuperC-band (6 THz),
- C+L-band (10 THz),

SuperC+SuperL-band (12 THz),

- C+L+S1-band (15 THz),
- C+L+S-band (20 THz), and
- Any of the previous scenarios + O-band.

According to [Sou23], the simple GN model is fast and sufficiently accurate for the C-band-only scenario. For bandwidths wider than 4.8 THz and up to 15 THz (Super-C, C+L and

SuperC + SuperL), the best trade-off solution is the closed-form inter-channel stimulated Raman scattering (ISRS)-GN model. For wider bands, it is better to use the not so fast but very accurate GGN model. For the scenario that uses the O-band, we suggest using the previous models to estimate the performance of the transmission bands other than the O-band and ignoring the presence of the O-band. To estimate the performance of the channels on the O-band, single-band split step Fourier Method (SSFM) simulations will be used since the bandwidth is not very large and the simulation would not take very long. This strategy is accurate if there is more than 14 THz spacing between the O-band and the other transmission bands, making the SRS power transfers from/to the O-band negligible [Sam22] and therefore the performance of the two groups of bands is independent.

Beyond the NLI, estimating the ASE noise power and the power evolution of channels during fiber transmission are simpler. The power of the ASE noise added by amplification is estimated by Eq. 2.

$$P_i^{ASE} = hG_iB_if_iNF_i \qquad \text{Eq. 2}$$

Where h is Planck's constant, B_i and f_i are the channel's bandwidth and central frequency, NF_i is the amplifier noise figure and G_i is the amplifier gain. The gain of the amplifier is normally set to perfectly compensate for the loss experienced by each channel, and therefore requires a precise estimation of the signal power at the output of the fiber. This is done by solving the system of SRS ordinary differential equations.

3.2 SDM TRANSMISSION:

3.2.1 Multi-core fibers

Multi-core fibers for space-division multiplexed transmission are of two types:

- Uncoupled-core multi-core fibers (UC-MCFs).
- Coupled-core fibers (CC-MCFs).

Uncoupled-core MCFs are designed with the goal of suppressing the crosstalk between signals transmitted in different cores, so that the individual signals can be received with independent single-mode receivers. Inter-core crosstalk is fundamental, and its presence is dictated by coupled-mode theory already in ideal multi-core fibers, where it takes the form of periodic or quasi-periodic power-exchange between cores [Hay11]. In the presence of perturbations to the ideal fiber structure, that are always present in practice, it becomes random in nature and its statistics are dominated by scalar effects, like fiber bending and twist [Kos12], as well as by polarization effects, primarily polarization-mode coupling and polarization-mode dispersion [Ant20-1]. A popular model that was introduced for the study of scalar effects is the one known as the "*phase-matching points model*" [Hay11]. Crosstalk suppression to levels of the order of –

40 dB/km is pursued by properly spacing the cores as well as by using a trench in the refractive-index profile or by introducing small inhomogeneity between cores [Hay11]. The number of uncoupled cores that can be accommodated in a standard 125-μm cladding ranges between four, in terrestrial and trans-oceanic links in the O-L bands, and eight, in data-center interconnects in the O-band [Mat22]. Inter-core crosstalk may substantially affect the effectiveness of digital back-propagation for nonlinearity compensation [Els18].

Coupled-core MCFs are designed with the goal of increasing spatial mode density. To this aim the fiber cores are arranged more closely to each other than in UC-MCFs, thereby producing substantial inter-core coupling. In this regime of operation, the signals transmitted in the individual cores are extracted by means of multiple-input-multiple-output (MIMO) techniques in combination with coherent reception of the fields propagating in the fiber cores. The MIMO complexity depends primarily on the phenomenon of modal dispersion, whose magnitude depends on the coupling regime. When this is random in nature, modal dispersion accumulates proportionally to the square-root of propagation distance [Ho11-1, Ant12]. Random inter-core coupling is achieved by properly spacing the fiber cores [Hay22]: if these are too close, modal dispersion accumulates proportionally to propagation distance, which requires much greater MIMO complexity [Ari13, Ina12]. Models that allow to estimate the growth rate of modal dispersion because of the fiber design and perturbation statistics [Ant15] are key to minimize the complexity of the MIMO receiver. A practical way of estimating the modal dispersion of a CC-MCF is by measuring the duration of its intensity impulse response [Ryf12], which has a Gaussian profile, as expected from the modelling of this fiber type [Mec15]. The record-low value of modal dispersion reported in the literature is 2.5 ps/$\sqrt{km}$.

Modal dispersion is a unitary propagation effect, and therefore does not affect the SDM system capacity, but only the receiver complexity. In contrast, mode-dependent loss (MDL) is a non-unitary, yet still linear effect that causes different propagation modes to experience unequal gain and loss values. Mode-dependent loss is responsible for a fundamental loss of capacity [Win11]. Its modeling must account for the presence of modal dispersion, which is responsible for averaging the effect of MDL across the propagating signal spectrum [Ho11-2, Ant20-2].

Coupled-core MCFs offer enhanced tolerance to nonlinear distortions, compared to single-mode fibers with the same core characteristics [Ryf17]. This follows from the multi-component Manakov equation that describes nonlinear propagation in fibers with strongly coupled modes, where the nonlinearity coefficient is seen to be inversely to the number of strongly coupled cores [Ant16]. The tolerance to nonlinear distortions can be further reduced by modal dispersion, and for relevant system settings a minimum in the nonlinear distortion is observed for modal dispersion values of approximately 8 ps/$\sqrt{km}$ [Ser22]. The so-far largest number of coupled cores in a standard 125- μm cladding diameter is 19 [Rad23].

3.2.2 Multi-mode fibers

Multi-mode fibers are characterized by non-degenerate mode groups, where modes in the same group have similar propagation constants and therefore couple strongly during propagation, whereas modes in different groups propagate with little coupling. Of course, the degree of inter-group mode coupling depends on propagation distance [Ant13], and therefore two regimes of operation are possible [Sil22].

1) The regime of weak coupling, where inter-group coupling is small to the extent that it can be treated as additional noise. In this regime different mode groups can be received independently, and MIMO processing is only necessary within each mode group. In this case the key challenge in the fiber design is to suppress inter-group coupling, and a step-index refractive index profile is typically the solution of choice.
2) The regime of full coupling, where all the modes are received jointly with MIMO techniques, like in systems using coupled-core multi-core fibers. In this regime, the key challenge in the fiber design is to suppress modal dispersion, which is the key factor in setting the receiver complexity. For this purpose, the graded-index refractive index profile is typically the solution of choice.

The two regimes of operation are sometimes referred to as *partial MIMO* [Som17, Gat23] and *full MIMO* [Sil22], and they are appropriate for short-reach and long-reach transmission, respectively. In the first case the MIMO complexity depends on intra-group modal dispersion, which accumulates proportionally to the square-root of propagation distance. Conversely, in the second case, modal dispersion is dominated by the difference in group velocities between non-degenerate modes, and it accumulates linearly until substantial inter-group coupling is achieved, then it continues accumulating proportionally to the square-root of propagation distance [Fer17]. The intensity impulse response of these fibers can vary quite significantly if inter-group coupling is incomplete [Maz23], while it approaches the typical Gaussian shape in the regime of full mode mixing [Fer17]. The suppression of modal dispersion is pursued primarily through the optimization of the refractive index profile [Fer14, Sil22]. More recently, however, periodic mode permutation has been investigated as an effective approach to speed up inter-group coupling and reduce the difference in transmission delay between different spatial modes [Shi20, Dis23]. While in recirculating-loop experiments mode permutation is implemented by extracting the individual modes at each amplification stage, more practical schemes based on periodically inscribing gratings in the multi-mode fiber can be considered [Ari16]. Mode permutation is also effective in suppressing mode-dependent loss, by reducing its accumulation from a linear law to a square-root law. This technique has enabled demonstrating transmission of 270 Tb/s over 100 km of 15-Mode multi-mode fiber [Van23].

Nonlinear effects in multi-mode fibers are more diverse than in coupled-core multi-core fibers, as non-degenerate modes can also interfere nonlinearly with resonances [Ess13]. Nonlinear propagation in multi-mode fibers obeys coupled multi-component Manakov equations [Ant16]. The characterization of the nonlinear distortions in terms of nonlinear interference noise is more involved than in the case of coupled-core multi-core fibers. The only regime in which analytical results are available is the one where the coupling between non-degenerate mode groups is negligible, while numerical studies show the existence of a maximum in the nonlinear penalty in the regime of partial coupling between mode groups [Fer19]. On the other hand, intra-group modal dispersion has been seen to have a beneficial effect in reducing the magnitude of the nonlinear interference noise [Las23].

4 DATA-PLANE TECHNOLOGIES

This section introduces and summarizes the main SEASON data plane technologies highlighting the innovative aspects of the proposed solutions in relation to the state of the art. Mainly, flexi-grid, MB and SDM technologies are pointed out as promising technology options to cost-efficiently scale network capacity and meet the increasing traffic demand while fulfilling stringent 5G and 6G requirements. Hence, innovative, and flexible transceiver, switching and monitoring solutions are presented, also dealing with energy and power efficiency aspects.

4.1 STATE OF THE ART AND INNOVATIVE ASPECTS OF THE CONSIDERED DEVICES

Emerging network technologies like 5G, B5G and 6G specify stringent requirements regarding capacity, latency, reliability, and connectivity. Operators can leverage these advantages to offer a wide range of new services to customers, all using the same physical network. Through network slicing, operators can establish multiple virtual networks, or network “slices”, which can be used for different applications with specific requirements. Therefore, it is crucial for operators to prioritize the development of innovative and flexible data plane technologies. These advancements allow them to offer customers entire virtual topologies instead of traditional end-to-end connections, all while cost-effectively scaling to meet the increasing demand for traffic growth.

One approach is the efficient use of the optical spectrum in the transport network, and consequently, research is now focusing on flexi-grid or elastic optical networks (EONs). One key element of an EON is the flexible transponder. These transponders have a range of functions, including support of multiple bitrates (e.g., from 10 Gb/s to 1 Tb/s) and dynamically setting modulation formats and symbol rates. This flexibility enables the operator to optimize network capacity by configuring the transponder with the bitrate that best fits the required distance. This flexibility is achieved through the aggregation of individual capacities provided by transceivers known as bandwidth/bit rate variable transponder (BVT). Each BVT is a versatile and programmable transceiver that supports multi-rate transmissions. New BVTs are capable of supporting data rates of 400 Gb/s, 300 Gb/s and 200 Gb/s, with 60 GBd dual-polarization 16QAM, 8QAM, or QPSK modulations, respectively. Each BVT offers up to 0 dBm of output power transmission, i.e., it provides 10 dB higher output power transmission and improved reception sensitivity compared to traditional single-rate transceivers. The transmission can reach distances of over 600 km at a 400 Gb/s bitrate, with extended reach capabilities at lower data rates.

However, to address the anticipated demand for 600 Tb/s capacity in future optical fiber systems, it is crucial to integrate innovative techniques, in addition to wavelength-division multiplexing (WDM), high-order modulation formats and polarization division, to boost optical fiber capacity while maintaining cost-effectiveness. Commercial optical transport commonly employs coherent optical technologies with dual polarization, covering the entire C-band across a spectral range of 4.8 THz. This enables a transmission throughput of approximately 38.4 Tb/s per fiber when utilizing dual polarization and 16QAM modulation. To enhance transmission throughput, SEASON explores innovative techniques such as Multi-Band (MB) transmission and spatial-division multiplexing (SDM) to exploit the spatial dimension of the fiber. SDM can be implemented utilizing multicore (MCF), multimode (MMF), or multi-parallel (MPF) fibers. Among SDM-based options, only MPF is commercially available. It relies on the utilization of existing dark fibers or the installation of new ones. However, the remaining SDM alternatives, such as MCF and MMF, hold significant potential for increasing transmission capacity. However, their implementation requires a comprehensive overhaul of the optical transport ecosystem, including the installation of new fibers and equipment.

Nevertheless, additional flexibility is currently under extensive research to design transponders capable of generating multiple optical flows, which can be routed to different destinations using optical switches and filters. Hence, a comprehensive transponder architecture supports super-channels (i.e., optical connections composed of several adjacent subcarriers) and sliceability (i.e., subcarriers grouped into several independent super-channels with different destinations). A single transponder equipped with these capabilities is known as a sliceable bandwidth/bit rate variable transponder (S-BVT). The aggregation/distribution of the multiple flows is performed by using data plane elements, generally referred to as multi-flow aggregators/distributors, such as bandwidth-variable (BV) wavelength selective switches (WSSs) or other reconfigurable photonic processors, which can be considered part of either the transceiver or the network. The S-BVT can be programmable (SDN-enabled), and its modular design enables it to be scalable to the capacity upgrade, spanning multiple bands and multiple spatial dimensions.

4.2 TRANSMISSION

4.2.1 The MB (oSDM) S-BVT

Within SEASON project, innovative programmable, scalable and modular multi band over spatial division multiplexing, MB(oSDM), sliceable bandwidth/bit rate variable transceiver (S-BVT) solutions are designed and investigated to provide suitable capacity scaling in a cost-effective manner as highlighted in the previous section. The proposed transceiver architecture is composed of multiple BVTs which can create multiple slices at different transmission bands, covering for example C-, S-, L-, E, O or even U-bands, as depicted in Figure 4-1. Moreover, each slice can be transmitted to different spatial channels (such as cores of a multi core fiber, MCF) in order to further increase the overall system's capacity. The proposed scheme follows a pay-as you grow approach, where the different slices can be enabled or disabled according to the traffic demand. Each BVT can be based on different technologies, such as direct or external modulation (at the transmitter) and coherent or direct detection (at the receiver), trading off cost and performance. Adaptive modulation based on orthogonal frequency division multiplexing (OFDM) is implemented at the digital signal processing (DSP) level suitably adapting the modulation format and power value per subcarrier to the network condition achieving variable data rate/reach and performance, as seen in the inset of Figure 4-1.

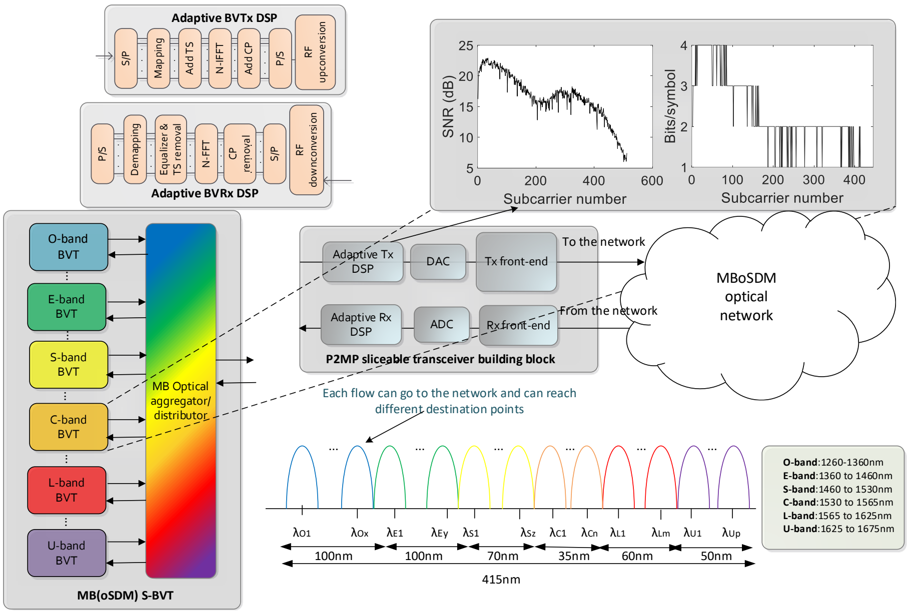

Figure 4-1 – MB(oSDM) S-BVT architecture.

The different slices are aggregated/distributed with a MB optical aggregator/distributor, which can be based on different technology (i.e., band pass filters (BPFs), wavelength selective switches (WSSs)) to create a high-capacity flow to be transmitted over the network. Finally, the proposed solution enables both point-to-point (P2P) and point-to-multi point (P2MP) operations, being able to serve different network destinations/end-points, with different path/connections requirements in terms of length/data rate, with a single S-BVT. The proposed MB(oSDM) S-BVT architecture, proposed within SEASON, will scale the capacity of the SoA transceivers by exploiting enhanced wavelength/space dimensions while enabling appropriate slice/band/core/fiber selection according to the network path. This solution will be particularly relevant in the metro/aggregation segment of the network, enabling flexible bandwidth allocation and efficient management of the network resources. In the mid-term (≈ in 5 years) a partial exploitation of the proposed transceiver can be envisioned, which can consist of enabling only MB operation and in particular a limited set of bands which can include C+L, and eventually an additional one (i.e., C+L+S). Furthermore, the adoption of a software-defined networking (SDN) control plane along with the corresponding SDN agents will provide successful adaptation and configuration of the proposed transceiver solution [Nad23].

MCF transmission is a promising SDM technology offering increased capacity, efficient space utilization, high scalability, simplified network architecture, redundancy, reliability, and energy efficiency. However, crosstalk (XT) can occur when signals in one core interfere with adjacent cores, degrading signal quality and network performance. Proper fiber design and signal isolation techniques are necessary to mitigate this frequency/wavelength-dependent issue. Employing a refractive index trench in the fiber design is an effective technique to reduce XT levels in MCFs. This modification creates a barrier between cores, preventing light leakage and enhancing signal quality and reliability. On this regard, a preliminary analysis on the XT impact on transmission over different spans of a trench-assisted 19-cores MCF of 25.4 km has been performed in [Nad23b]. The mean XT value of a core has been approximated through evaluating a straightforward analytical formula depending on the core pitch, mode linear coupling coefficient between two neighboring cores, the bending radius, fiber length and propagation constant [Nad23].

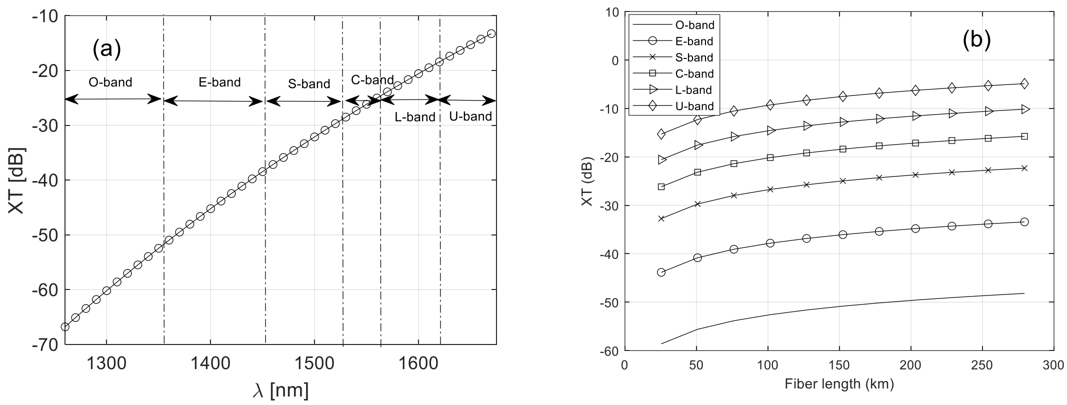

Figure 4-2 – (a) Estimated XT versus wavelength in trench assisted 19-cores MCF of 25.4 km. (b) XT analysis over different MCF lengths and considering MB transmission.

The considered wavelength range spans from 1260 nm to 1675 nm, encompassing the O-, E-, S-, C-, L-, and U-bands. Figure 4-2(a) illustrates that the O-band experiences the least XT impact, with values below -50 dB. In the C-band, XT ranges between -30 dB and -25 dB, with a specific value of -26.1 dB at 1550.12 nm matching the MCF specifications. The U-band exhibits higher XT degradation, exceeding -20 dB. Figure 4-2(b) evaluates the XT across various MCF lengths, up to 279.4 km (11 spans of 25.4 km each). Central wavelengths for analysis include 1310 nm (O-band), 1410 nm (E-band), 1495 nm (S-band), 1550 nm (C-band), 1600 nm (L-band), and 1650 nm (U-band). Results indicate increased XT with longer MCF lengths, with the U-band showing values from -15 dB (after 25.4 km) to -5 dB (after 279.4 km). After the maximum length, XT values are measured at -48 dB (O-band), -33.4 dB (E-band), -22.3 dB (S-band), -15.7 dB (C-band), and -10.1 dB (L-band).

A first proof-of concept assessment of the MB(oSDM) S-BVT solution considering S+C+L transmission over a 19-cores MCF of 25.4 km has been performed as depicted in Figure 4-3.

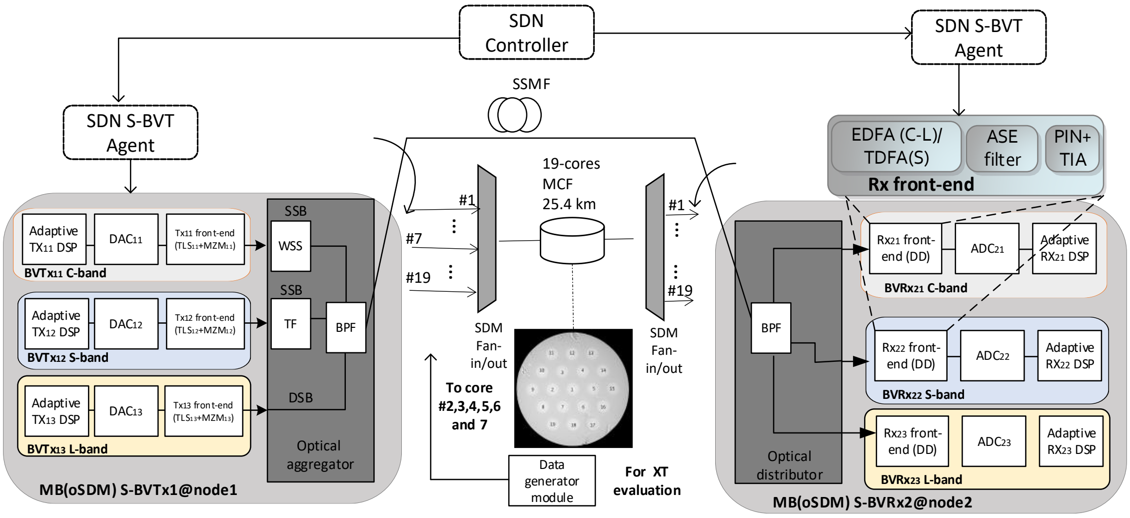

Figure 4-3 – Experimental setup.

A high-speed DAC at 64 GSa/s is utilized to generate an OFDM electrical signal with 512 subcarriers and a 20 GHz bandwidth. The transceiver front-end, employing external modulation, consists of a laser array configurable within the S-, C-, and L-bands, along with quadrature-point-operating Mach-Zehnder modulator (MZMs). Specifically, an electro-absorption modulated laser (EML) set to 1500 nm is employed for the S-band and 2 TLSes at 1550.12 nm and 1600 nm are used for the C- and L-band, respectively. An optical aggregator creates a high-capacity flow in the MB, incorporating single sideband (SSB) filters and a BPF. SSB modulation is implemented in the C- and S-band slices, utilizing a WSS with a 25 GHz bandwidth and a tunable filter (TF) with a 30 GHz bandwidth, respectively. This enhances resilience against chromatic dispersion (CD), improving overall performance. However, due to laboratory/setup constraints, the L-band contribution remains unfiltered, and a double sideband (DSB) signal is aggregated by means of a BPF with the other contributions. The receiver side of the proposed transceiver features an optical distributor with a BPF. Each slice is distributed to bandwidth/bitrate variable receivers (BVRxs), utilizing specific components and technology suitable for the respective bands. For the C-band contribution, an Erbium-Doped Fiber Amplifier (EDFA) and a WSS for ASE noise filtering (centered at 1550.12 nm with a 50 GHz bandwidth) are employed. The S-band slice is amplified using a Thulium-doped Fiber Amplifier (TDFA) and filtered with a static filter. The L-band utilizes an EDFA and a static filter. Photodetection is performed using different PINs, and the signals are ADC converted with an oscilloscope at 100 GSa/s.

In a first use case, MB transmission is experimentally assessed considering transmission over standard single mode fiber (SSMF) up to 75 km. The performance results, illustrated in Figure 4-4, demonstrate the achieved maximum data rate and optical signal-to-noise ratio (OSNR) for varying SSMF lengths. In the back-to-back (B2B) configuration, a total aggregated capacity of 212 Gb/s is obtained at 4.62e-3 target bit error rate (BER). Beyond 25 km SSMF, the aggregated data rate decreases to 134 Gb/s. The implemented adaptive loading schemes based on Levin Campello algorithm ensure consistent performance for all three contributions [Nad23b]. At 50 km and 75 km, the aggregated capacity decreases to 107 Gb/s and 73 Gb/s, respectively. Due to setup constraints, the L-band contributions achieve higher OSNR values. However, DSB transmission is more susceptible to CD. Figure 4-4 indicates that, after transmission over the fiber with lower OSNR values, the C-band contributions outperform the L-band contribution in terms of achieved data rate.

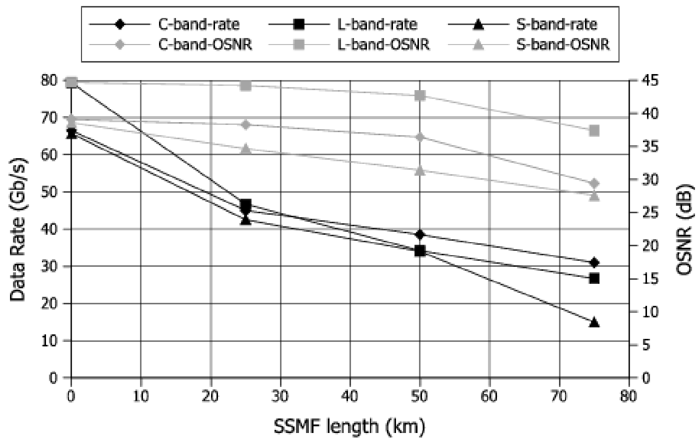

Figure 4-4 – Short Achieved maximum capacity and OSNR per slice considering different SSMF lengths up to 75 km.

Concerning transceiver scalability, the modular architecture of the MB (oS-BVT) S-BVT allows the incorporation of additional slices in different bands for higher capacities. Considering the entire analyzed bands with 25 GHz (S+C) and 50 GHz (L-band) channel bandwidths, a total aggregated capacity of 47 Tb/s is envisioned in the B2B configuration. This corresponds to 23 Tb/s for the S-band (350 channels), 12 Tb/s for the C-band (175 channels), and 12 Tb/s for the L-band (150 channels).

In a second experimental assessment for MBoSDM transmission, a 19-cores MCF of 25.4 km is employed, as depicted in Figure 4-3. The C-band contribution attains the highest data rate of 44 Gb/s at the target BER and 36 dB OSNR. The L-band and S-band achieve capacities of 35.8 Gb/s and 39.3 Gb/s at 37.8 dB OSNR and 31.7 dB OSNR, respectively. Variations in performance across bands are expected due to the wavelength dependence of fiber properties, including effective area, CD, and fiber attenuation/loss. The consideration of the spatial dimension introduces new resources for expanding the overall network capacity. Utilizing a single core from the 19-core MCF across the S+C+L bands would result in data rates of 13.8 Tb/s for the S-band (350 channels), 7.7 Tb/s for the C-band (175 channels), and 5.5 Tb/s for the L-band (150 channels). Consequently, when incorporating the S+C+L bands and all 19 cores of the 25.4 km MCF, the aggregated capacity has the potential to scale up to 500 Tb/s (19x27 Tb/s).

Finally, an assessment of out-band and in-band XT has been performed by utilizing the data generation module shown in Figure 4-3, feeding adjacent cores (#2, 3, 4, 5, 6, and 7) of the MCF. For out-band XT evaluation, the data generation module comprises the S-band amplified contribution after MCF. Varying the current of the S-band amplifier pump laser diode (LD) in steps of 100 mA up to 500 mA assesses the impact of out-band XT within the C-band and L-band. Despite a consistent capacity of approximately 38 Gb/s in all cases due to the OSNR remaining around 34 dB, this results in a 6 Gb/s decrease compared to scenarios not considering XT, where 44 Gb/s was achieved at 35 dB OSNR. In the L-band, a constant data rate of 35.8 Gb/s is achieved at the target BER and 37.8 dB OSNR, regardless of out-band XT, given the 100 nm separation of selected S-band and L-band wavelengths.

Next, in-band XT within the C-band is evaluated using a C-band broadband source (BS) and an EDFA in the data generation module Figure 4-3. The power profile before and after amplification is depicted in Figure 4-5(a). Varying the EDFA output power reveals the impact of in-band XT on the achieved data rate versus OSNR, as shown in Figure 4-5(b). Without in-band XT, a maximum data rate of 44 Gb/s is achieved at 35 dB OSNR and the target BER. However, the data rate of the C-band contribution decreases as in-band XT signal power increases, reaching 22 Gb/s at 23.6 dB OSNR. Despite MCF design efforts to reduce XT levels, high signal power in adjacent cores can lead to XT issues, causing optical interference and unwanted coupling between cores. This interference degrades overall performance, emphasizing the importance of managing signal power levels across different cores to minimize in-band XT for reliable communication.

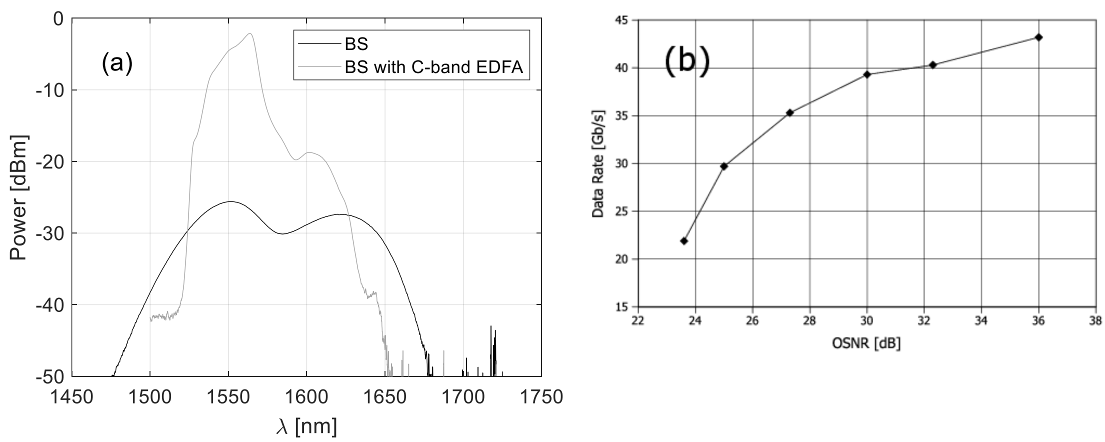

Figure 4-5 – (a) Power profile of the data filled in the neighboring cores of the MCF to evaluate the XT. (b) Maximum achieved data rate for the C-band contribution, considering in-band XT.

4.2.2 Leveraging Raman Amplification to Improve and Equalize the Performance of a 20-THz Multi-band Optical System

Increasing the bandwidth utilization of the currently deployed optical fiber infrastructure by deploying multi-band transmission (MBT) systems is an effective strategy to improve network capacity and postpone costly fiber deployment [Fer20-2]. However, one should perform a careful techno-economic analysis to determine the viability of the additional transmission bands since they typically have higher fiber loss, and key enabling components usually show worse characteristics not only but also due to the use of less mature technologies.

Within the framework of the SEASON project, we numerically compare the network capacity using two strategies to improve the optical performance of MBT systems comprising the C-, L- and S-bands, i.e., a total transmission bandwidth of 20 THz in the Italian backbone network

[Sou23]. The proposed approaches are to deploy Raman amplification on existing sites or to expand the set of in-line amplification sites, i.e., to deploy new optical amplification sites. These approaches are mostly mutually exclusive since Raman amplification is not a viable solution in short spans.

To highlight the potential of Raman amplification to equalize optical performance, Figure 4-6 depicts the channel capacity as a function of the number of traversed 80-km spans when the MBT system is upgraded by increasing the number of in-line amplifier sites (left-hand side) or by deploying four Raman pumps in each existing amplification site (right-hand side). Splitting each span into two effectively doubles the span count, but we neglect this effect in this study to ease the comparison. The analysis of Figure 4-6 shows that, when using Raman amplification, most of the frequencies typically support the same modulation format after transmission along a given distance, e.g., 400 Gb/s signals are still supported in all frequencies after transmission along four spans whereas some of the channels only support 300 Gb/s signals in the case of increasing the number of in-line amplification sites. Nevertheless, increasing the number of amplification sites enables transmitting 400 Gb/s signals up to 9x80km distance (in a few channels), whereas only 7x80km can be traversed by the same 400 Gb/s signals when Raman amplification is used instead. Interestingly, for a lightpath with 6 spans, the MBT system with Raman amplification supports 75% of the channels with 400 Gb/s while the system where the number of amplification sites is increased supports only 50% of channels with 400 Gb/s.

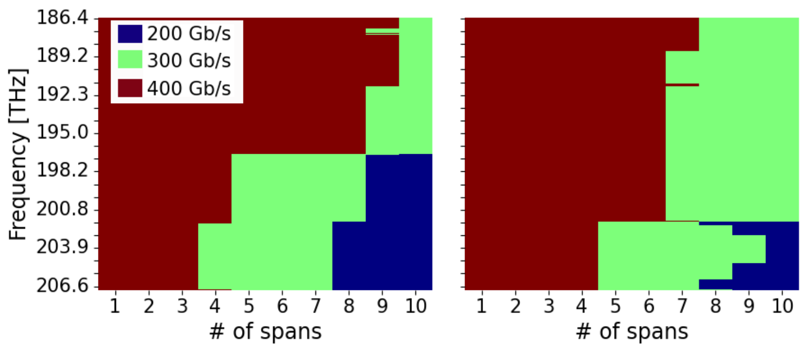

Figure 4-6 – Channel capacity as a function of the number of 80-km spans when increasing the number of in-line amplifier sites.

To better evaluate the benefits of each upgrade solution, Figure 4-7 depicts the total allocated traffic versus blocking probability for the non-upgraded system, the optimized system with four Raman pumps and the case with amplifier site expansion (40 km spans). The analysis of Figure 4-7 shows that deploying Raman amplification is the upgrade solution that leads to the highest capacity improvement. As an example, at a blocking probability of 1%, the total allocated traffic for the network with Raman amplifiers is 374 Tb/s, which is 40% higher than the non-upgraded system (267 Tb/s) and 4% higher than the one that achieved by reducing the span length to half of the original value (359 Tb/s). This result further stresses the potential of Raman amplification for MBT system upgrades.

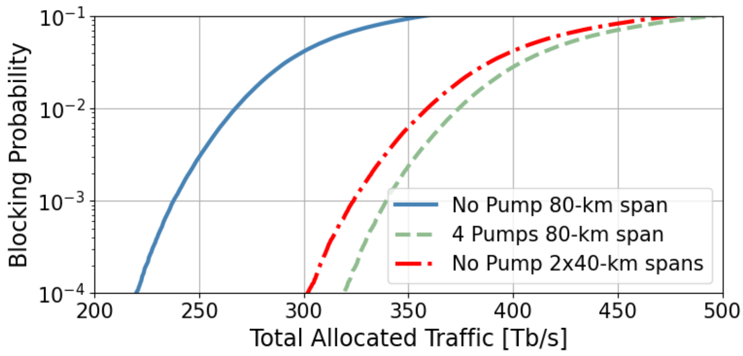

Figure 4-7 – Total allocated traffic for different system upgrades.

4.2.3 Comparative Assessment of S+C+L-band and E+C+L-band Systems with Hybrid Amplification

Contemporary commercial systems already integrate the L-band, resulting in a twofold increase in capacity. The deployment of systems with even more bandwidth is now a subject of increased discussion, with research endeavors dedicated to developing devices compatible with transmission bands beyond the C and L bands, as well as evaluating their techno-economic prospects. Exploiting the S-band, which has fiber characteristics still like those of the C and L bands, is a promising option. Several studies have demonstrated the additional capacity achieved by incorporating the S-band into a C+L-band system [Sem20].

Since introducing the S-band comes with the additional challenge that existing services can be impacted by the power interactions caused by SRS, an alternative proposition is to bypass the S-band and instead utilize the E-band. Particularly, by keeping a guard band of 14 THz between the E-band and the already operational C and L bands, it is possible to avoid power transfer between the newly added and existing bands [Sam22]. However, previous works do not consider the impact of using Raman amplifiers to enhance the performance of the C+L-band.

In this study, we conduct a network performance comparison among four configurations: C+L, S+C+L, Int-S+C+L, and E+C+L bands, all employing hybrid amplification techniques, including fiber-doped lumped amplification and backward-propagating Raman distributed amplification (with up to ten pumps), with each band occupying 6 THz of spectrum (as shown in Figure 4-8). The optimization of channel and pump powers is carried out using a multi-objective genetic algorithm with dual objectives of maximizing system capacity and equalizing the performance across the bands.

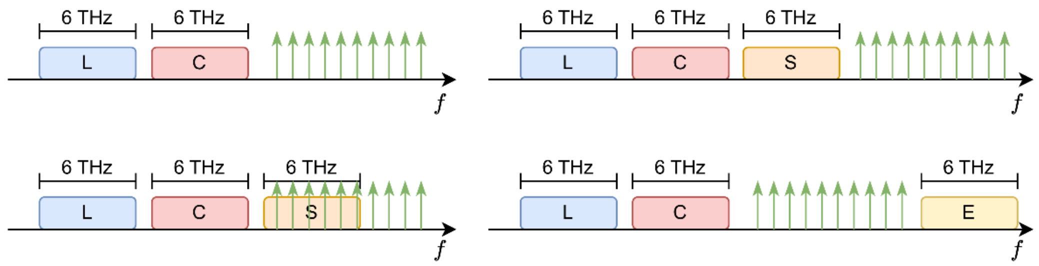

Figure 4-8 – Spectrum of different transmission system configurations. From left to right and top to bottom: C+L, S+C+L, Int-S+C+L, and E+C+L.

The key advantage of employing multi-objective optimization algorithms, as opposed to single-objective ones, lies in their ability to generate a range of solutions, each of which satisfies the specified objectives to an acceptable degree without being dominated by any other solution. In the context of this study, these solutions represent the trade-off between maximizing capacity and minimizing GSNR variation.

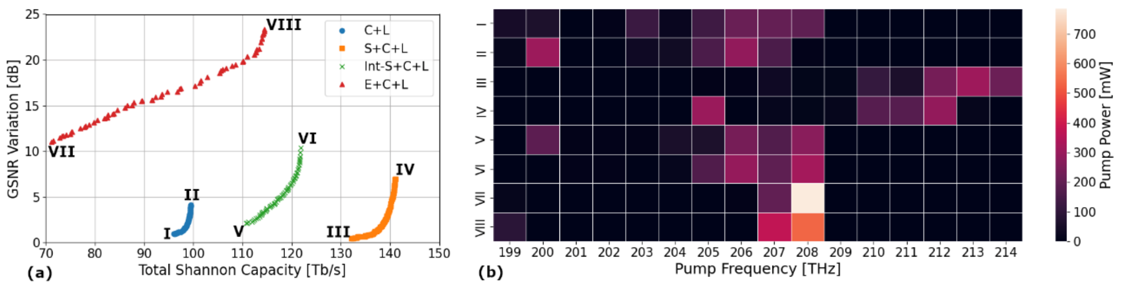

Figure 4-9 – (a) Optimal non-dominated solutions and (b) Raman pump power distribution for selected solutions.

Figure 4-9 a illustrates the non-dominated solutions the optimization algorithm achieves upon convergence for each transmission scenario. Among these solutions, the S+C+L-band system stands out as the top performer. It attains the highest capacity of 141 Tb/s while maintaining a GSNR variation of 7 dB. It is worth noting that the GSNR variation can be reduced to 0.5dB with a 6% reduction in total capacity (down to 132 Tb/s). This upgrade results in an approximately 40% capacity boost for the C+L-band system while preserving the same GSNR variation. Conversely, the E-band upgrade ranks as the least favorable solution. It can provide 15% more capacity than the C+L system at the expense of a high GSNR variation. This is due to the lack of Raman amplification to improve the E-band's performance, as well as the adverse impact of deployed Raman pumps, which, while enhancing the C and L bands, deplete the power of the E-band channels.

Figure 4-9(b) presents the power levels of the Raman pumps for the eight optimized solutions identified in Figure 4-9(a), each representing the best outcome in one of the two objectives for each transmission configuration. Notably, it is evident across all these solutions that some Raman pumps have a negligible effect due to their low power. Only 4 or 5 out of the 10 pumps exhibit power levels exceeding 50 mW, suggesting the potential for simplifying the implementation of these systems. Interestingly, very little power is allocated to pumps operating at the same frequencies as the S-band. Consequently, interleaving channels and Raman pumps on the S-band is not a practical solution. Furthermore, in the E+C+L-band system, the algorithm appears to have avoided using the lower frequency pumps, likely as a strategy to mitigate the power depletion of the E-band. This precaution comes from power transfer via SRS being more pronounced for frequency offsets around 13 THz. Nevertheless, the E-band's performance remains significantly affected by the remaining pumps, resulting in a considerable GSNR variation that the algorithm could not reduce below 10 dB within the prescribed power constraints.

4.2.4 Point-to-point and point-to-multipoint coherent transceivers

As we reported in section 2.3.2, optical aggregation can be realized using P2P and P2MP transceivers [Wel21, Wel23]. In this section, we describe how the two solutions are realized in terms of transceivers and DSP.

Figure 4-10 illustrate the similarities and differences between a P2P (a) and a P2MP transceiver (b). This is a visual comparison between a P2P coherent transceiver (using single-carrier) and a P2P & P2MP one (using multi-carrier approach with DSCM). The two solutions are similar and differentiate mainly in the parallelization of the DSP blocks, which for the case of a DSCM transceivers are parallelized with respect to the digital subcarrier. In fact, by observing Figure 4-10(a) and Figure 4-10(b), we notice that the blocks are essentially the same, but in Figure 4-10(b) they are repeated in a parallel way, to individually post-process the digital subcarriers. As reported in [Sun20], this approach led to a simplification of the electronic compensation of accumulated dispersion.

Consequently, the DSCM approach works at a reduced symbol rate per subcarrier, but the overall spectrum occupation is comparable. The guard-band among the subcarrier is in the order of ~100 MHz. For further details, please refer to [Wel21, Wel23].

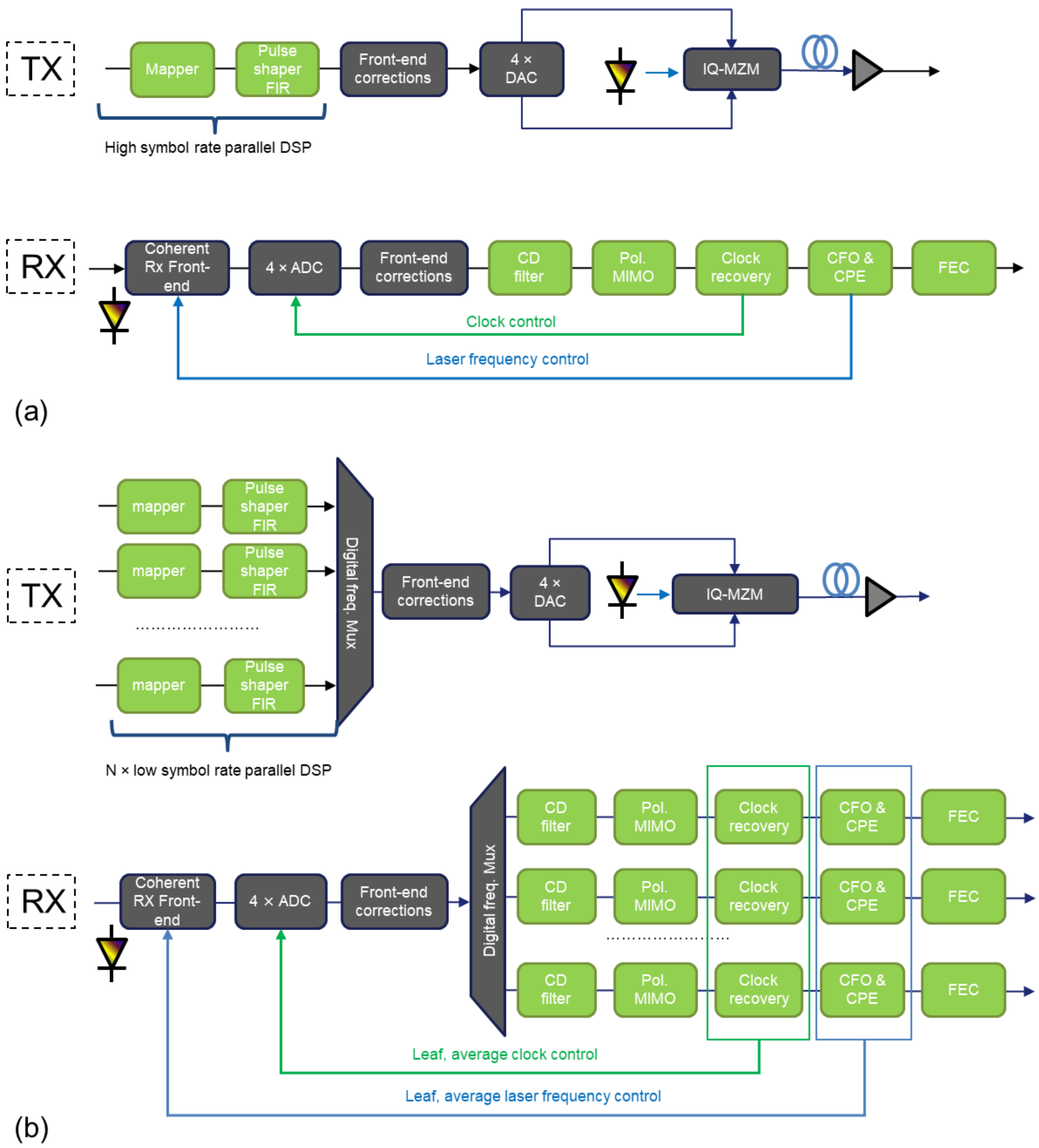

Figure 4-10 – Details of the architecture of single-carrier coherent transceiver (a) vs. multi-carrier transceiver (b).

In the context of SEASON, we are exploiting the functionalities of the coherent P2MP devices to dynamically adapt the bandwidth used by the transceiver to variable traffic. In the context of SEASON, we are exploiting the functionalities of the coherent P2MP devices to

dynamically adapt the bandwidth used by the transceiver to variable traffic. A new tool,

originated by the one reported in [Cas23] in B5G-OPEN, enables to create or upload network topologies and assign dynamic traffic matrix. Such a tool will be used to perform investigations on node clustering such as the one we carried out in [Her23] but when considering physical layer and components impairments. Furthermore, the different allocation of the digital sub carriers will provide an optimized spectral distribution, a reduce energy consumption, and the possibility of assessing the optical performance for new services that could be created at different times of the day as envisioned in [Her23]. The first results of this analysis will be submitted to ECOC 2023.

4.2.5 Super-channel transmission in elastic optical networks

Super-channel Spectrum Saving Optimization Procedure has been designed and implemented within the SEASON project to improve the spectral efficiency in EONs. Super-channel (or multicarrier) transmission, supported by EONs, has been identified as a suitable solution for accommodating the high line rates necessary to satisfy continuous traffic growth. However, super-channel optimization is particularly challenging due to the subcarrier XT and filtering effects on the side subcarriers, resulting in degradation of the overall QoT. However, the network costs could be greatly reduced by lowering the margins, thus increasing network efficiency. Therefore, by reducing margins and thus moving closer to the minimum performance threshold [e.g., the pre-forward error correction (FEC)–bit error rate (BER) threshold], EONs can be operated even more dynamically, connections can support higher bit rates, and cost in terms of spectrum can be saved by adjusting existing connections to meet varying traffic. NETCONF, along with YANG models, has been recognized as a software defined networking (SDN) configuration and management protocol enabling control in a vendor-neutral way. Moreover, the OpenConfig YANG model defines vendor-specific transmission parameters, such as modulation format and bit rate, within operational modes, enabling the model to remain stable while maximizing performance. A journal paper “Super-channel Spectrum Saving Optimization Procedure in Elastic Optical Networks”, published in Journal of Optical Communication and Networking (JOCN) in January 2023, within the SEASON project, investigates the trade-off between super-channel quality of transmission (QoT) and spectrum saving by allowing slight subcarrier to overlap and tight filtering, hence reducing system margins [Rad23-1]. The proposed automatic spectrum-efficient super-channel optimization procedure is experimentally demonstrated using a 600 Gbit/s transponder supporting OpenConfig OP modes in an SDN-controlled EON, by considering super-channels composed of the same OP mode (*homogeneous super-channels*) and super-channels composed of sub-carriers of different OP modes (*hybrid super-channels*). The automatic procedure performs the adaptation of filter bandwidth and subcarrier spacing as shown in Figure 4-11.

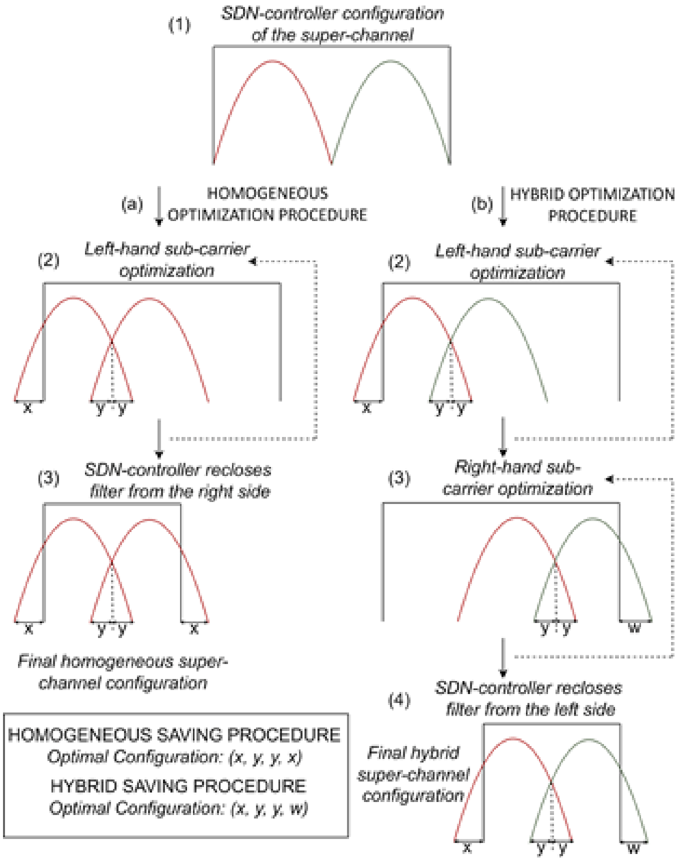

Figure 4-11 – Short Spectrum saving optimization procedure of (a) homogeneous and (b) hybrid super-channels.

The latter is effectively operated by transponder NETCONF agents, without involving the SDN controller. Therefore, the data plane devices can reconfigure themselves, as instructed by the optimization procedure, without querying the SDN controller to perform the subcarrier spacing optimization. Fig. 48 (a) describes the control messages for the initial provisioning, the connection monitoring and the reconfiguration during the optimization procedure. The experiments are carried out in the context of the optical testbed reported in bottom of Fig. 48 (b), considering the optical reach of 80, 160, 240, and 320 km, respectively. It has been observed that, in the considered testbed, crosstalk due to the slight subcarrier overlap has a greater impact on the pre-FEC-BER degradation than tight filtering. Furthermore, it has been recognized that the system imposes higher margins for subcarriers of OP modes with higher bit rates. Finally, the proposed optimization procedure provides more flexibility to dynamically meet the varying traffic requirements and allows for spectrum reduction of up to 25%.

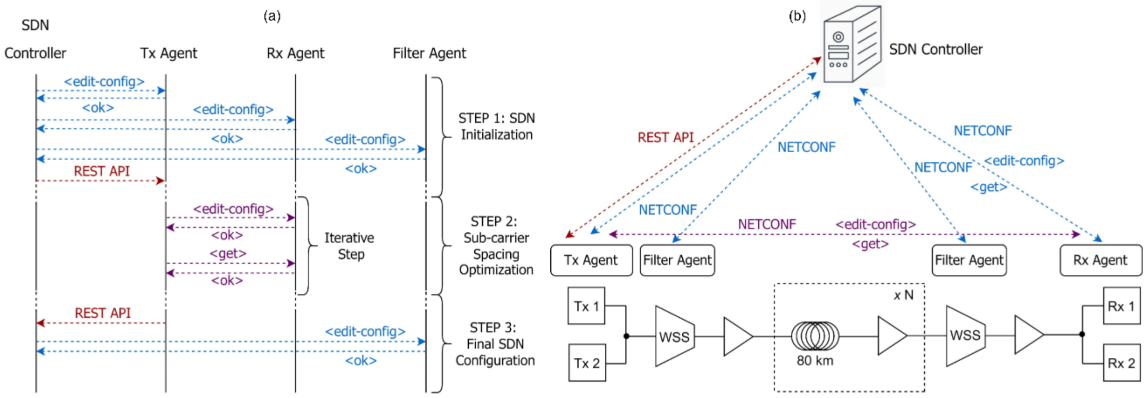

Figure 4-12 – (a) NETCONF messages exchange for provisioning, monitoring and reconfiguration, (b) Network reference scenario.

Furthermore, power-aware super-channel optimization is experimentally demonstrated using a 600 Gbit/s transponder in the SDN-controlled EON. The optimization of super-channel parameters for spectrum-efficient transmission might be challenging due to the linear XT, reduced spacing among sub-carrier central frequencies, and narrow optical filtering resulting in the QoT degradation, as reported in [Rad23-1]. On the other hand, power consumption has never been deeply considered in the optimization of super-channel transmission, such as trading off between energy and spectral efficiency and margin reduction. In this work, the trade-off between power consumption and spectrum efficiency is investigated by operating super-channels at nominal and low-margin conditions. Power consumption is monitored and reported relying on NETCONF protocol considering the aforementioned super-channel spectrum occupancy (Fig. 49). The procedure considers homogeneous super-channels, i.e., super-channels composed of sub-carriers with the same OP mode, and hybrid super-channels that are composed of sub-carriers with different OP modes. The latter allows for higher flexibility in meeting the actual traffic requirements (i.e., requested line rate) while satisfying proper QoT. Optimization is experimentally demonstrated by utilizing an OpenConfig-enabled transponder capable of different bit rates (i.e., 200 - 600 Gbit/s) and OP modes in an SDN-controlled EON testbed. Then, experiments are conducted considering 800 Gbit/s super-channels in two scenarios: with an optical reach of 40 km and 320 km, respectively. Results show that physical layer and operational modes impact power consumption regardless of the spectrum efficiency. However, the spectrum-efficient super-channels lead to higher power consumption compared to super-channels operating in nominal condition. Results identified a trade-off between spectrum efficiency and power consumption. In particular, a power saving of 7% can be achieved if spectrum resources are kept at nominal values. This work was presented at the Optical Network Design and Modelling (ONDM) Conference in May 2023 [Rad23-2].

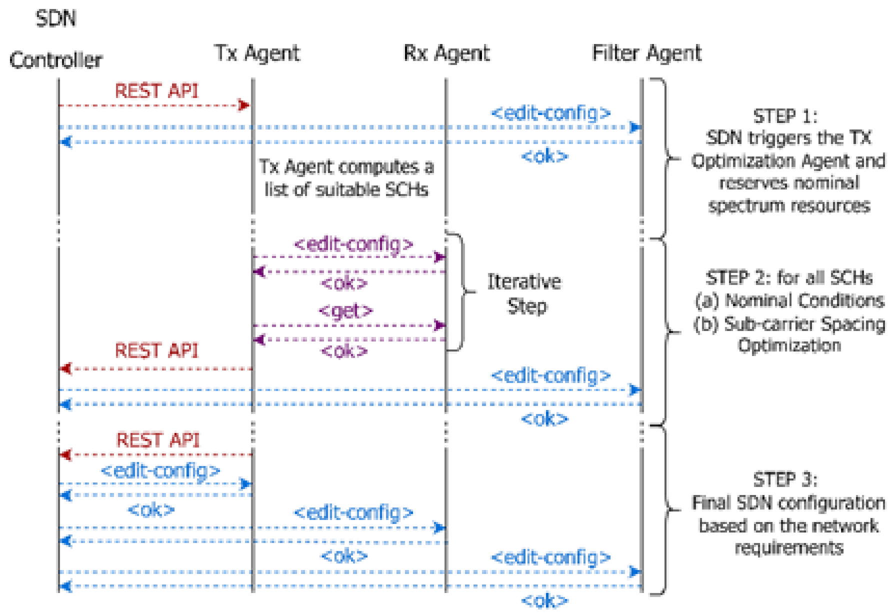

Figure 4-13 – NETCONF messages exchange for provisioning, monitoring and reconfiguration in power-aware super-channel optimization.

4.3 SWITCHING AND NODE

4.3.1 Multi-core & multi-band nodes

Multi-granular modular and flexible switching architectures with advanced functionalities, capable to exploit MB and SDM technologies, are investigated within the SEASON project to serve the expected increasing traffic demand and stringent targets/requirements of next generation optical networks. The proposed node architectures will be able to dynamically route and add/drop traffic while potentially increasing the switching capacity in a flexible manner. Different switching approaches are envisioned to adaptively exploit multiple granularities (i.e., spectral, in terms of wavelengths and bands, and spatial granularities) according to the network segment of interest and application scenario/use case. In this regard, a three-layer approach (WDM, MB and SDM) adopting key technology at each granularity level can include different technology options such as contentionless MB wavelength selective switches, WSSs, of N input/output ports (for WDM), band pass filters, BPFs, (for MB), fan-in and fan-out (for SDM when considering MCFs) or simpler solutions based on a bundle of fibers (also for SDM). This approach can be seen as a long-term solution to be adopted for example at the backbone network segment, as explained in section 4.6.2 of D2.1, where enhanced and stringent node capabilities in terms of bandwidth/capacity are expected. Specifically, each layer can include different technology options, such as contentionless MB WSSs of N input/output ports (for WDM), BPFs (for MB) and multiplexers (for SDM). However, the most straightforward design of a node capable of switching SDM-DWDM signals spanning multiple spectral bands would be an evolution of current ROADM nodes relying on 1xN WSS (which could be MB or operate within a given band), such as the one depicted in Figure 4-14. It represents a highly flexible colorless-directionless (CD) route-and-select (R&S) ROADM architecture for a multiband, multi-fiber optical network node following the conventional ROADM architecture widely deployed today. For a CDC architecture, the A/D module, comprising two dual WSS placed back-to-back, can be replaced with a multi-cast switch (MCS) or a contentionless MxN WSS. It assumes separate fiber amplifiers and WSS per band, although multiband implementations for the WSS and the use of Raman amplification could also be considered, which would simplify the node design to some extent. In the Figure we also assumed dummy light (DL) to fill the gaps between channels, thus preventing uncontrolled power transfer between bands when new channels are provisioned.

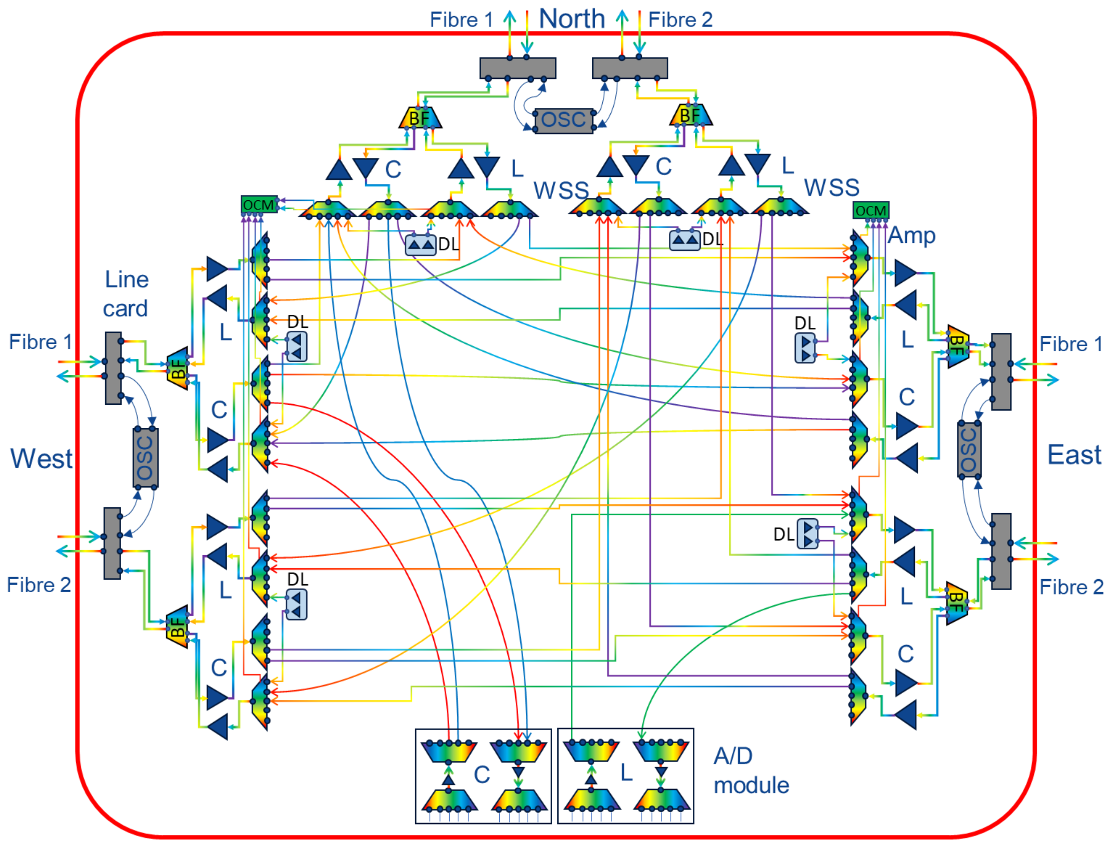

Figure 4-14 – Illustration of a high-capacity conventional CD R&S ROADM node design with three nodal degrees exploiting two spectral bands (C, L) and two spatial dimensions (Fiber pairs 1 and 2). We show the simplest architecture, with just one A/D module per band, but two or more A/D modules could be considered for redundancy. BF: Band Filter; OSC: Optical Supervisory Channel; OCM: Optical Channel Monitoring; DL: Dummy Light (to mitigate the SRS effect).

This design, however, has the disadvantage that it does not scale well with the number of spectral and spatial dimensions. Table 4-1 shows the number of WSSs required in a CD R&S ROADM node architecture such as the one presented in Figure 4-14 for different numbers of degrees (D), fibers per degree (F) and spectral bands per fiber (B). It shows that, as the number of any of those dimensions increases slightly, the number of optical components rises very rapidly. Consequently, such design should be avoided in an MBoSDM scenario when F or B is marginally greater than 2, especially in the case of nodes with D > 3.

Table 4-1: Number of WSS required in the conventional CD R&S ROADM node architecture for different numbers of degrees (D), fibers per degree (F) and spectral bands per fiber (B). We assume WSS with 20 ports and one A/D module per band.

F	B	D	WSS (line)	WSS (CD A/D)	Dual WSS Total
1	1	2	2	2	4
2	2	3	12	4	16
3	3	3	27	6	33
3	3	5	45	6	51
5	3	5	75	12	87
10	6	8	486	48	534

In SEASON we have been investigating more simplified designs for the MBoSDM node. One such design is depicted in Figure 4-15. It is composed of band filters at the ingress and egress of the node to separate out the different portions of the spectrum within an amplification band, an M×N spatial optical crossconnect (S-OXC) to direct each of the filtered bands toward an egress band filter or to a contentionless N×N WSS, and an N×N WSS which processes bands at the channel level whenever a channel needs to be dropped or new channels need to be added to those bands.

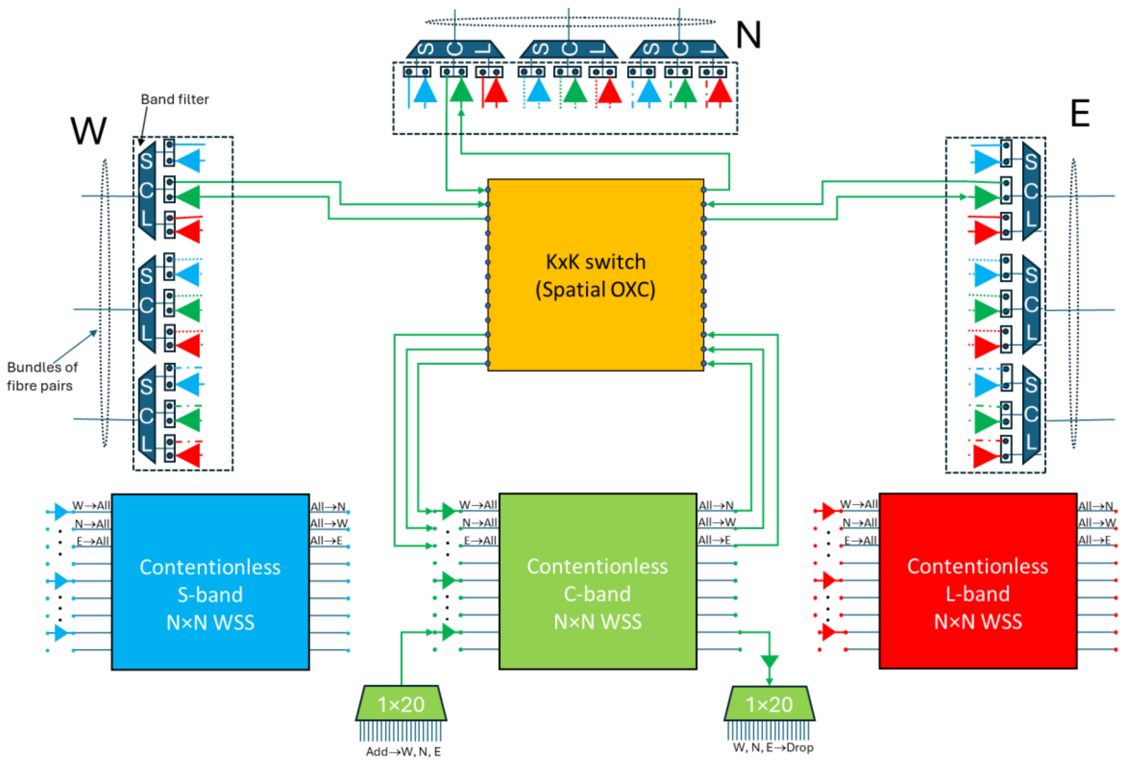

Figure 4-15 – SEASON MBoSDM node design #1. Only the connectivity for the C-band within the first fiber in each degree is shown. The connectivity for the rest of bands and fibers will be done in a similar manner.

Depending on the actual implementation of the N×N WSS, this design can enable switching of bands and channels across fiber dimensions (e.g. the C-band in the first fiber in W could be switched to the second fiber in E by the S-OXC, while the contentionless N×N WSS could mix channels from different fiber dimensions and different degrees and direct them to any egress port of the node). It would also allow the add/drop of full-band channels to/from the S-OXC, with colorless-directionless-contentionless functionality. The architecture shown is colorless-directionless (CD) for individual channels within a band because channels are added/dropped through a 1×20 WSS. If they were added/dropped directly to/from the N×N WSS, the architecture would also be CDC.

The main issue with the design in Figure 4-15 is the existence of a single point of failure in the S-OXC. To circumvent this problem, in Figure 4-16 we present a second design that does not make use of an S-OXC.

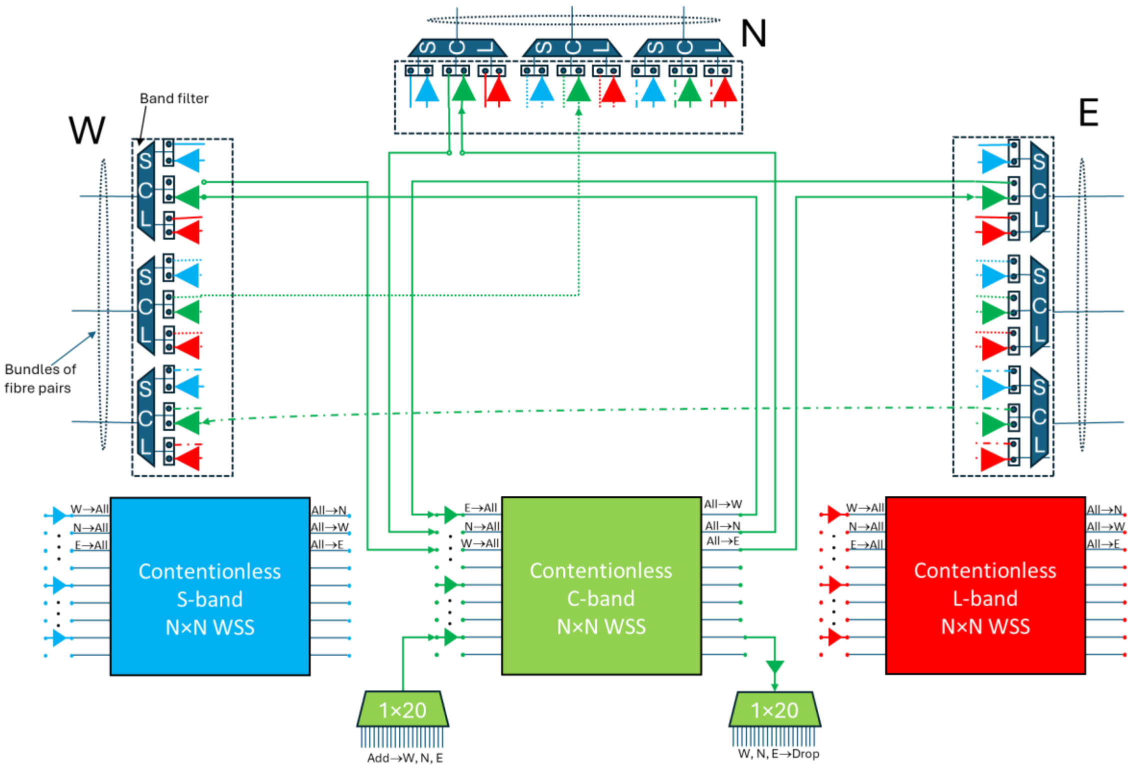

Figure 4-16 – SEASON MBoSDM node design #2. Only the connectivity for the C-band within the first fiber in each degree is shown. The connectivity for the rest of bands and fibers will be done in a similar manner.

This design is simpler but lacks the flexibility that the previous one exhibited. Though cross-connections within a ROADM node are usually static, the programmability offered by the S-OXC allows performing optical restoration of bands that are not processed by the N×N WSS (as is the case of the C-band within the second and third fibers in W, which are directly connected to the band filters in N and E, respectively), as well as automated reconfiguration of the node if new cross-connections are to be created or an existing one needs modifying.

A third, more modular design that provides more flexibility and avoids single points of failure is shown in Figure 4-17 . It is composed of (at least) as many S-OXC as fiber dimensions and one contentionless N×N WSS per band, but the principle of operation is the same as explained above.

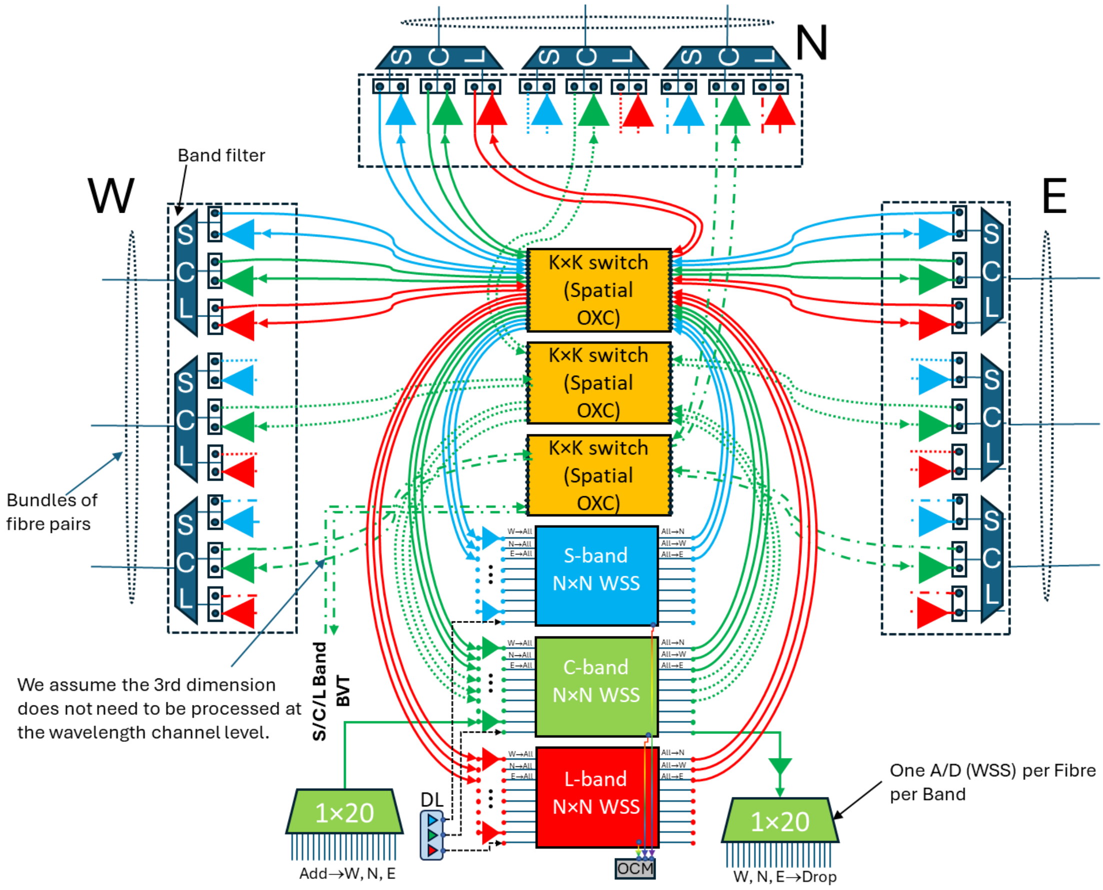

Figure 4-17 – SEASON MBoSDM node design #3.The design also includes the optical channel monitoring (OCM) modules and the dummy light (DL) to improve the performance of multi-band transmission.

For the sake of comparison, the number of components and port count for each of the three designs is presented in Table 4-2.

Table 4-2: Number of components and port count for the three MBoSDM designs presented in Figure 4-15, Figure 4-16 and Figure 4-17. In the calculations, we consider the same number of bands and fibres in all degrees. Port count assumes a simplex fibre optic connector (IN or OUT), not a duplex connector (IN & OUT). (*) Assuming CD architecture with a number "N_AD" of 1 × M WSS per contentionless N × N WSS.

	Design #1	**Design #2**	**Design #3**
Number of degrees	D	D	D
Number of fibres per degree	F	F	F
Number of amplification bands per fibre	B	B	B
Contentionless N × N WSS port count	N	N	N
Number of S-OXC	1	0	F
S-OXC port count	4 × F × B × D	*NA*	4 × B × D
Number of contentionless N × N WSS (*)	B × ⌈(F × D + N_A/D) / N⌉		
Total number of contentionless N × N WSS ports (*)	2 × F × D + N_A/D		

A potential implementation of a contentionless N×N WSS is shown in Figure 4-18 . It consists of two contentionless M×N WSS, such as the TrueFlex Contentioness Twin 8x24 WSS by Lumentum [Lum24], with the connectivity depicted in the figure. This connectivity does not allow mixing channels from different fibers. With the connections shown, only channels belonging to a given spatial dimension, whichever degree they come from, can be mixed and directed to an egress port belonging to the same fiber dimension. Mixing channels across spatial dimensions would require more crossconnections between tributary ports of the WSS.

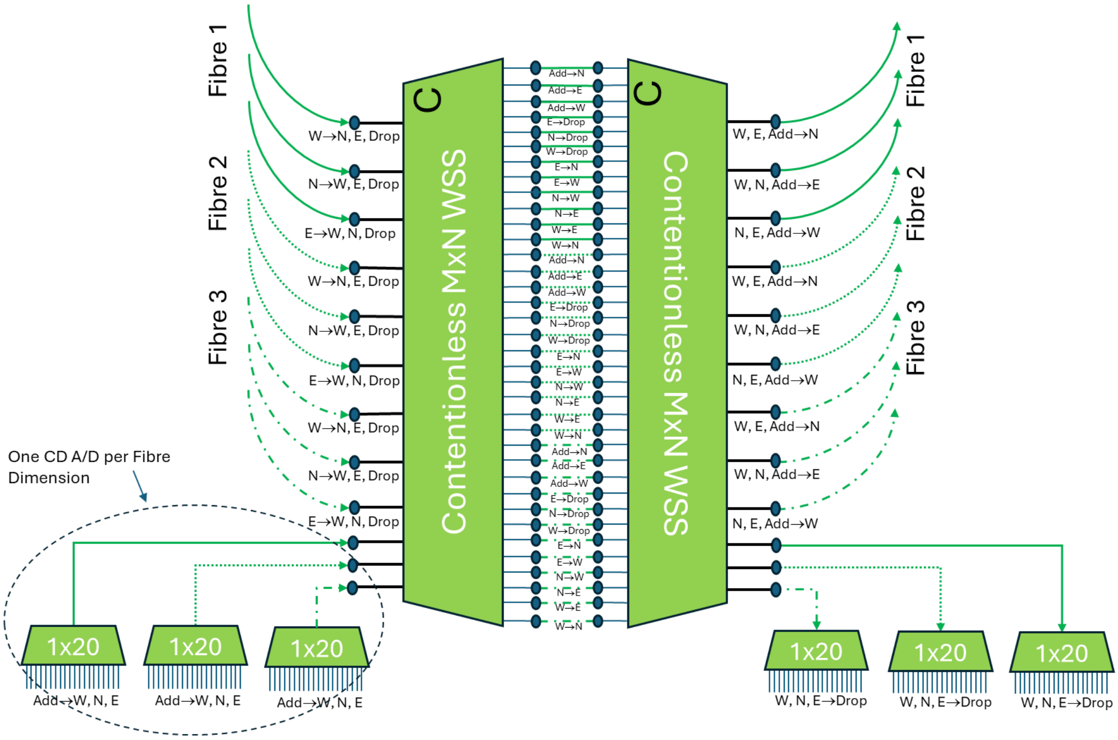

Figure 4-18 – Realization of an N′ × N′ WSS (only for the C-band) employing a contentionless M×N WSS such as the TrueFlex Contentioness Twin 8x24 WSS by Lumentum [Lum24] for a 3-degree, 3-fibre node according to the SEASON MBoSDM node designs #1, #2 or #3. Note that the number of ports N′ = 2 × M.

For the implementation illustrated in Figure 4-18, the calculation of the required number of M×N WSS ports is shown Table 4-3 for two scenarios: a general scenario with N_A/D 1×20 WSS per M×N WSS, and a scenario where we use one 1×20 WSS per fiber dimension.

Table 4-3: Number of ports of a contentionless M×N WSS such as the one available in [Lum24]. We refer to M as the line ports and N as the tributary ports.

	General formula	N_A/D = F
Contentionless M × N WSS Line port count (M)	2 × F × D + N_A/D	F × (2 × D + 1)
Contentionless M × N WSS Tributary port count (N)	2 × D × [F × (D-1) + 2 × N_A/D]	2 × F × D × (D+1)

For comparison of the simplified designs for the MBoSDM node being investigated in SEASON with the evolution of the current architecture depicted in Figure 4-14, for which some data was provided in Table 4-1, in Table 4-4 we show the number of K×K S-OXC, number of S-OXC ports (K) required, and number of contentionless NxN WSS and 1xM WSS (for CD A/D) for the node architecture illustrated in Figure 4-17 with the same numbers of fibers (F), spectral bands (B) and nodal degrees (D) chosen in Table 4-1. We evaluated two scenarios: a worst-case scenario where all spectral bands in all fiber dimensions are processed at the contentionless NxN WSS, and a more practical scenario where only the spectral bands within one of the spatial dimensions (e.g., Fiber 1) are processed at the wavelength level. We observe that, even though the number of band filters and contentionless NxN WSS remain quite small as F, B and D increase in the worst-case scenario, the number of 1xM WSS (for the CD A/D) increases exponentially, therefore showing no benefit when compared with the conventional architecture in Figure 4-14. However, the scenario where only one fiber is processed at the contentionless MxN WSS, succeeds in keeping the number of components at bay, and could be an option to be considered in the networking and techno-economic studies in SEASON.

Table 4-4: Number of KxK S-OXC (and number of ports K), contentionless NxN WSS and 1xM WSS (for CD A/D) in a worst-case scenario where all bands in all fibers are processed by the contentionless NxN WSS and a more practical scenario where only the spectral bands within one of the spatial dimensions (e.g., Fiber 1) are processed by the contentionless NxN WSS for the node architecture presented in Figure 4-14. We assume contentionless NxN WSS with N = 16 (unidirectional) and 1xM WSS with M = 20 (bidirectional) ports.

						N×N WSS, N=	16
			WORST CASE			1×M WSS, M=	20
F	**B**	**D**	**Band Filters**	**K×K S-OXC**	**K**	**N×N WSS**	**1xM WSS (Dual)**
1	1	2	0	0	0	1	1
2	2	3	6	2	12	2	4
3	3	3	9	3	18	3	9
3	3	5	15	3	30	6	18
5	3	5	25	5	30	12	60
10	6	8	80	10	96	90	900

						N×N WSS, N=	16
			Fiber 1 processed			1×M WSS, M=	20
F	**B**	**D**	**Band Filters**	**K×K S-OXC**	**K**	**N×N WSS**	**1xM WSS (Dual)**
1	1	2	0	0	0	1	1
2	2	3	6	2	9	2	4
3	3	3	9	3	12	3	9
3	3	5	15	3	20	3	9
5	3	5	25	5	18	3	15
10	6	8	80	10	53	12	12

Other MBoSDM node implementations using multi-band amplification and, potentially, fiber switching will continue to be investigated in the project and will be reported in the upcoming deliverables D3.2 and D3.3.

Likewise, in other network segments (i.e., metro-access segment) simplified switching architectures/implementations are preferable.

The three-layer switching paradigm approach is ideal for flexibility of networks, however, such a complex architecture does not always scale cost-efficiently with the number of spatial dimensions. Therefore, SEASON proposes two different cost-efficient prototypes as proof of a multi-granular optical switching node, offering a more relaxed flexibility. One approach focuses on fiber and whole-band switching (S-, C- or L-band), aiming to simplify the architecture in specific use-cases and scenarios, whereas the second approach also exploits WDM granularity by means of AWGes and WSSs. This band-specific segregation allows different bands to be explored by distinct applications, especially since there is significant variability in optical performance between these individual transmission bands. As an example, O-band can be explored for single-hop transmission only, thus simplifying the switching architecture. Moreover, simpler optical interfaces can be explored for this application. Additionally, one of the node prototypes also offers wavelength switching within the C-band.

4.3.2 IP over DWDM nodes

4.3.2.1 Pluggable transceivers

For the packet switching network layer, and for the Access-Metro Segment. SEASON is considering the usage of L2/L3 white box switches, equipped now with coherent pluggable optical transceivers at 100 Gb/s and 400 Gb/s and in the future up to 800Gb/s or 1.6-3.2 Tb/s, depending on the target period. This disaggregated paradigm and the proposal of high-performance interoperable standards (for example vendor independent optical and digital specifications in OIF and OpenROADM) seem to indicate that this approach is effective in the Access-Metro for the inherent low cost and power consumption. For Backbone, SEASON assumes that transponder cards will still be employed, since they can be designed with a “no compromise” approach in mind, together with pluggable transceivers on switch/routers.

4.3.2.2 Pluggable amplifiers

The evolution to compact pluggable form factors, started first for client side/grey transceivers and then evolved to line side WDM transceivers, is now approaching the optical layer.

The benefits resulting from the introduction of pluggables for the optical line systems are many-fold:

- CAPEX: reduced cost of the device itself but also pay-as-you grow incremental introduction of new functions

- OPEX: reduced foot-print and improved installation, operations, and maintenance
- FLEXIBILITY: pluggable functions can be combined according to design choices, topologies and network evolution

Some functions are now available in pluggable solutions (EDFAs, OSCs, VOAs, OTDR, Filters), others will soon appear on the market (Switches, WSS, Raman amplifier).

Pluggable Line Systems are particularly suitable for access and metro applications where low - cost, small footprint, and low power consumption are important requisites. Metro-Core/Core network segment will still be better served by system-on-a-blade solutions (e.g., ROADMs) or optical modules to be integrated in proprietary vendors' designs.

In SEASON pluggable optical amplifiers will be used and tested within the Radio Access Network WDM ring architecture and metro aggregation context. Currently, only fixed gain solutions with two options are available:

- Dual EDFA: limited to a limited number of channels (e.g., 8). Two amplifiers within the same pluggable Quad small form-factor pluggable (QSFP). This option has been selected for the RAN use-case to provide a cost-effective amplification for the WDM coherent dual-fiber transport system. The amplifier will compensate for the line loss and the loss of the splitters which provide colorless add/drop functionality.
- Single EDFA: supports the whole C-Band. This option will be analyzed from a system modeling point of view to assess its potential use in aggregation/metro networks.

Pluggable EDFAs integrate transient management and zero-touch configuration. They provide at least +15dBm output power.

4.3.3 Edge-computing node

Edge computing enables stakeholders to maintain IT infrastructures, Artificial Intelligence (AI) processing and service management closer to where data are produced and consumed. To achieve this target, edge computing resources need to support advanced networking capabilities with ultra-high bandwidth connectivity. Data Processing Units (DPUs), also called Smart Network Interface Card (SmartNIC), originally designed for intra-data center operations, are emerging as attractive solutions to provide edge computing infrastructures with powerful and advanced networking capabilities. DPUs have recently been developed at rates of up to 400Gbps and equipped with embedded graphics processing unit (GPU). Furthermore, they have the potential to directly encompass coherent pluggable transceivers. This way, DPUs represent an innovative technology that cost-effectively combines packet, optical, and edge computing resources in a single networking element, opening the way to new use cases and solutions for programmable optical networking.

In the SEASON project, we propose the use of DPU equipped with P2P and P2MP coherent transceivers as an innovative cost-effective *edge* solution providing converged packet, optical and computing resources in a single platform.

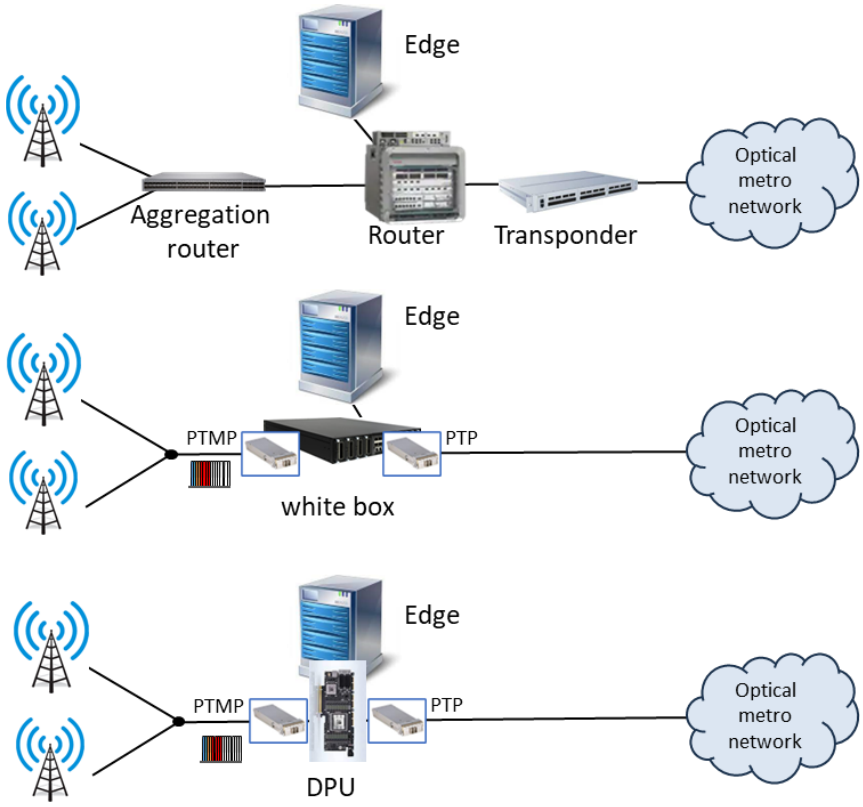

Figure 4-19 – Traditional optical network scenario with aggregation routers and standalone transponders (top); Evolved scenario with white box and coherent transceivers (center); innovative SEASON optical metro network scenario with edge computing nodes and DPUs with coherent transceivers (bottom).

Enabling technology: DPU with embedded GPU and coherent pluggable modules

DPU is a specialized hardware component designed to deliver high-speed data processing. While DPUs are typically utilized in data centers, server setups, and supercomputers, there is growing interest in their potential application in edge networking scenarios. This is because DPUs possess the capability to manage data movement, storage, and processing for large datasets, enabling rapid computations and facilitating real-time analysis and acceleration of data-intensive applications. In contrast to traditional NICs, which mainly focus on low-level protocol acceleration, such as Ethernet, and rely on the server's Central Processing Units (CPUs) for other networking tasks, DPUs offer the advantage of programmability at higher layers. They can directly execute advanced in-network functions, thus freeing up processing resources for tenant and application services. The current generation of DPUs is equipped with up to four interfaces operating at speeds of up to 400 Gb/s, advanced timing and synchronization capabilities, hardware encryption, and embedded security features. Additionally, they feature up to 16 ARM CPUs for handling embedded computing operations. The latest generation also includes embedded GPU resources. DPUs traditionally employ only flat-top connectors (e.g., OSFP, QSFP112/56/28 form-factors) and not yet the QSFP-DD form factor used in packet-optical switches supporting coherent pluggable modules. However, a new generation of coherent transceivers fitting these form factors has been already announced for 100Gbps, while future DPU generations are expected to also support QSFP-DD for rates at 400Gbps and beyond. Once this gap is filled, two main advantages can be achieved in the context of optical metro/edge infrastructures.

The first advantage involves reducing the number of active standalone nodes and the need for intermediate Optical-Electrical-Optical (OEO) conversions. Figure 4-19(top) illustrates the traditional optical network scenario with aggregation routers and standalone transponders. Figure 4-19(center) shows an evolved scenario with white box equipped with coherent transceivers of type P2P and P2MP, which enables the removal of standalone transponders and aggregation routers respectively. Figure 4-19(bottom) shows the innovative SEASON optical metro network scenario with edge computing nodes and DPUs equipped with coherent transceivers. This enables the consolidation of optical, packet, and computational resources on a single platform.

The second benefit revolves around latency reduction. This is achieved by collapsing computing and optical network resources on a single platform, thereby minimizing the use of OEO conversions, which, in turn, leads to a reduction in end-to-end latency.

Additionally, embracing high-speed transceivers directly integrated into DPUs will significantly enhance support for ultra-low latency services for access while capitalizing on hardware-accelerated network functions within DPUs (e.g., encryption). These benefits may lead to performance improvements to both low latency user applications as well as to Telco infrastructural elements.

Use cases exploiting DPUs with embedded GPU and coherent pluggable modules.

The first use case refers to the deployment of 5G functions closer to cell sites. Functions like UPF-DU-CU could be moved closer to the cell site and all co-deployed on powerful edge nodes, relying on (i) hardware-accelerated networking solutions provided by DPUs (e.g., deep packet inspection, cyber security, encryption) and (ii) direct p2p optical connections to cloud services and p2mp connections to multiple RUs. Furthermore, embedded GPU enable effective and fast AI-based predictive/proactive functions.

The second use case refers to monitoring. The availability of DPUs equipped with coherent transceivers enables effective monitoring and correlation features directly at the network card. Received packet and optical data can be processed locally also leveraging powerful GPU resources. For example, in-band telemetry reporting per-packet information on experienced latency performance can be processed by embedded P4/DOCA libraries using AI-based algorithms, i.e., outperforming traditional threshold-based mechanisms which just forward data through telemetry towards remote management systems. Furthermore, the DPU has the capability to locally process optical parameters received by the local transceivers.

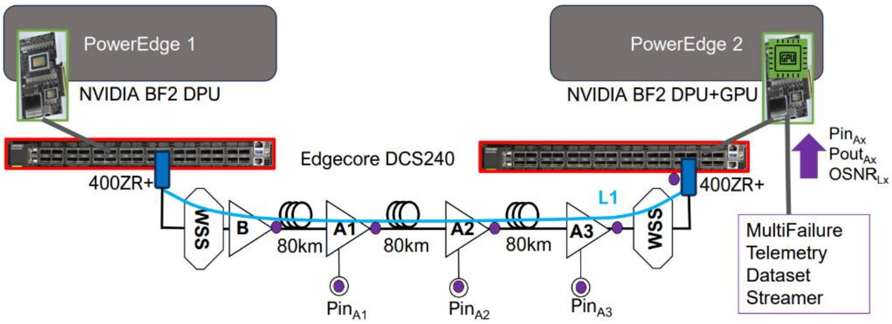

Figure 4-20 – Network scenario for the experimental validation.

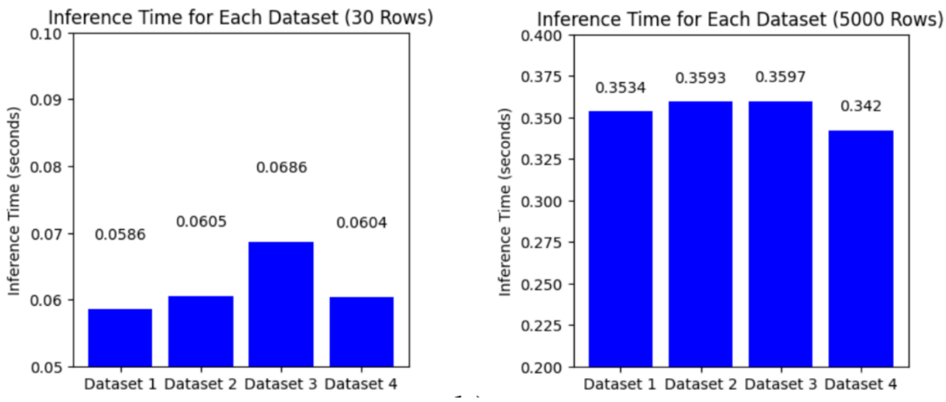

Figure 4-21 – Preliminary measurements of inference time considering different datasets and different amount of simultaneously processed data (30 parameters left, 5000 right).

As a first proof of concept, we describe the experimental validation of an AI-based algorithm originally designed for soft-failure detection operated by a centralized SDN Controller [Sil23], here deployed for local assessments within the DPU. Figure 4-20 shows the considered network testbed. Two DELL PowerEdge Server are equipped with NVIDIA Bluefield2 DPU with embedded GPU. Since these DPUs cannot yet support coherent transceivers, we rely on Edgecore switches equipped with 400ZR+ coherent transceivers. However, the control of the transceivers is performed through Rest interface by the DPU (i.e., not by an SDN Controller), as if the transceivers were installed within the DPU. The pair of transceivers is then interconnected by three optically amplified spans of 80-km each.

Figure 4-21(a) shows the inference time of processing four different sets of data each including N=30 optical parameters extracted from [Sil23], i.e., emulating a single event of received signal. Results show that, depending on the presence of specific anomalies (e.g., soft failures), the inference time varies between 50ms and 70ms.

To assess the scalability performance, we forced the system to simultaneously process N=5000 optical parameters. Figure 4-21(b) shows that in this case inference time always remains below 360ms. Such fast processing opens the ways to radically new decentralized control plane capabilities, where each node may receive telemetry data from multiple data plane nodes without being overwhelmed by scalability issues.

This work has been accepted for publication at the OFC Conference: Piero Castoldi, Rana Abu Bakar, Andrea Sgambelluri, Juan Jose Vegas Olmos, Francesco Paolucci, and Filippo Cugini, "Programmable Packet-Optical Networks using Data Processing Units (DPUs) with Embedded GPU Monitoring devices", OFC Conf. 2024 [Cas24]

4.4 MONITORING FOR NEXT GENERATION OPTICAL NETWORKS

4.4.1 OTDR, Interrogator, and fiber sensing

Fiber sensing utilizing deployed optical network infrastructure has gained much research interest in the telecommunication society in the last five years. The idea is to transform the fiber monitoring system, mainly based on optical time domain reflectometry, into a fiber sensing system and measure strain and temperature fluctuations in the vicinity of the deployed fiber. This provides additional functionality to the operator of telecommunication equipment and opens an additional source of revenue by selling the data to other service providers. In addition, another objective is to make optical networks more resilient to intrusion and malicious attacks by proactively analyzing the information provided by the sensing unit. Furthermore, the data gathered by the sensors can be used for evaluating the life form habitats and their techniques to communicate with each other by measuring the acoustic signals they send out [[1]].

The rapid growth in the market and expected revenue in the last 20 years of versatile fiber sensing technologies is shown in the following diagram Figure 4-22 [[2]]. From that diagram, the revenue increased in Rayleigh scattering-based sensing technologies. This revenue in the market will further increase if telecommunication system manufacturer and operator roll out their developed fiber sensing technologies in the deployed network.

[1] Bouffaut Léa, Taweesintananon Kittinat, Kriesell Hannah J., Rørstadbotnen Robin A., Potter John R., Landrø Martin, Johansen Ståle E., Brenne Jan K., Haukanes Aksel, Schjelderup Olaf, Storvik Frode, "Eavesdropping at the Speed of Light: Distributed Acoustic Sensing of Baleen Whales in the Arctic", Frontiers in Marine Science, 9, 2022, DOI=10.3389/fmars.2022.901348,

[2] InformationGatekeepers 2019 Distributed and Single Point Fiber Optic Sensing Systems Forecast. Available online: http://www.igigroup.com/st/pages/photonic_sensor_report.html (accessed on 07 March 2024).

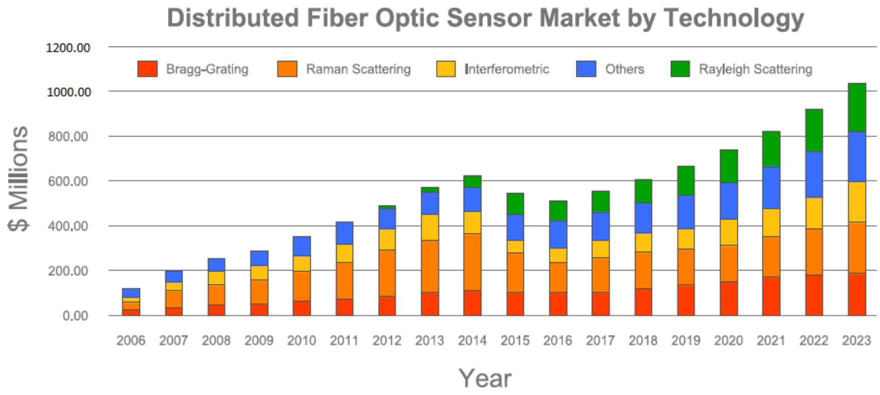

Figure 4-22 Growth of different fiber sensing technologies until 2023 [1].

There are versatile sensing technologies available that can be used for different applications, which is illustrated in Figure 4-23. The intensity-modulated sensors detect physical changes or perturbations in the received light (bend loss, attenuation, evanescent field). Here, the advantages of these sensors are simplicity and lower costs. The wavelength-modulated sensors measure the change in wavelength of the probe light. Here, the fiber Bragg grating (FBG) sensor is the most prominent sensor used in different applications and has the capability for point and multipoint sensing. Phase-modulated sensors based on interferometry principles measure the phase variation in an optical path with high sensitivity, accuracy, and the highest measurement range. The most popular interferometers include Mach-Zehnder, Sagnac, Michelson, and Fabry-Perot interferometers. The disadvantage of these sensors is that the length of the deployed fibers determines the spatial resolution of these sensors. Another group of sensors utilizes different backscattering effects, denoted as reflectometry-based sensing or scattering-based, which can cope with that issue. These technologies exploit either elastic (Rayleigh) or inelastic (Brillouin or Raman) scattering processes, which are sensitive to dynamic and static strain and temperature fluctuations. The main advantage of this technique is that it gives temporal-resolved information about the fluctuations in the fiber environment. In addition, by adapting the setups of these techniques, the amplitude, optical phase, or polarization of the backscattered light can be evaluated. The latter technology is polarization-based sensing using Faraday rotating sensors or coherent transceivers. These sensors exploit the variation of birefringence along the fiber due to lateral strain applied to the fiber. In addition, these sensors can also measure electrical current flow by using the Faraday effect.

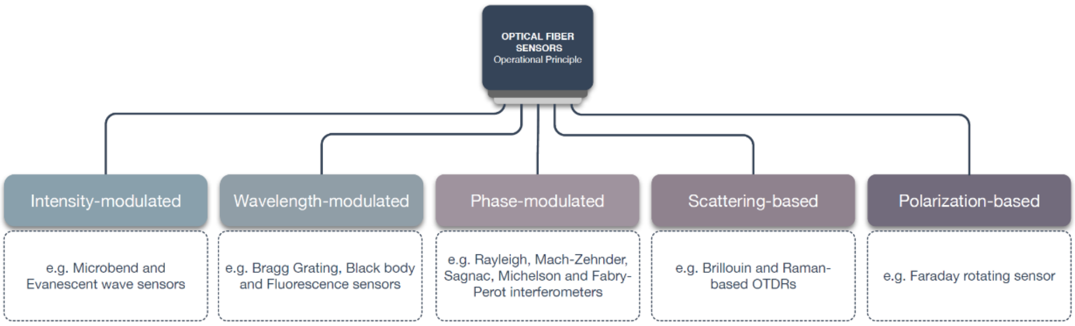

Figure 4-23 Different sensing technologies and their principle of operation[3]*.*

Thanks to the availability of FPGAs with integrated analog components (analog to digital converter), telecommunication manufacturers have started looking into the sensing domain utilizing an adapted OTDR. Here, the time-based reflectometry approach is denoted as distributed acoustic sensing or phase-sensitive OTDR (Phi-OTDR). In both cases, the phase along the fiber is evaluated and not the amplitude or polarization of the optical wave. The advantage of analyzing the phase is the sensitivity of this wave parameter, which immediately changes if the sensor is touched, shaken, or a vibration is applied to it, which changes the length of the sensor and the refractive index. In addition, the approach Adtran investigates is based on a correlation-aided technique by sending a pre-processed probe signal to the sensor instead of sending pulses. The main advantage of this pre-processed probe is that more energy can be sent in the fiber as in a narrow pulse without sacrificing the spatial resolution.

4.4.2 Digital signal processing for monitoring

In the search for self-managed and autonomous networks, monitoring and telemetry platforms become increasingly important to obtain as much data from the network in the best way possible, that is without the need to go through the challenging and the costly task of collecting measurements from multiple nodes across complex networks. This helps as well in the process of secure migration from today's C-band based optical networks to a MB scenario, which heavily relies on monitoring mechanisms that can accurately measure not only wavelength-resolved characteristics of MB optical components (e.g., amplifiers, switches, and transceivers), but also distance-wise properties of optical links across nationwide networks.

In this context, DSP-based optical monitoring techniques are a promising feature that extracts physical layer parameters, such as amplifier gain or chromatic dispersion mapping, without executing direct measurements to the optical device. This is possible thanks to the non-commutative relationship between the chromatic dispersion and the nonlinear interference induced by the channel on itself, i.e., self-phase modulation (SPM). This non-commutativity

[3] Pendão, C.; Silva, I. Optical Fiber Sensors and Sensing Networks: Overview of the Main Principles and Applications. Sensors 2022, 22, 7554. https://doi.org/10.3390/s22197554.

permits those characteristics of the channel to be uniquely determined by applying a reverse-order operation, allowing for estimation of channel properties from digitized samples by using a DSP chain.

The popularity of these DSP-based approaches is due in part to their capability of unveiling multi-span link properties, such as longitudinal power profile [Tan19], [Tan20], frequency response of bandpass filters [Sas20-1], span-wise chromatic dispersion mapping [Sas20-2], PDL [Tak23], optical amplifier gain [Sen22-1, Sen22-2], Raman gain [Sas21] and fault detection [Sen22-1, Sen22-2]. In SEASON, the studies surrounding this technology will focus on improving the spatial and physical resolution of the technique, achieving sub-km and sub-dB resolutions in the estimation of longitudinal fiber attenuation points and optical amplifier gain, respectively, to obtain more precise and reliable measurements for optical networks, such as was studied in [Tan19] and [Kan23].

4.4.3 Processing of monitoring information: model-centric vs. data-centric ML

Failure management has emerged as one of the key use-cases for machine learning (ML) applications in optical networks. However, we must consider that data in simulations and laboratory setups is generated in a controlled environment, so typically the desired amount of failure data can be collected. Failures seldom occur in optical networks under operation and, consequently, the amount of failure data available to train ML models may be scarce. In the case of failure identification, some failures occur more frequently than others, resulting in uneven distribution of samples among different failure types in the training dataset. As a result, datasets collected from real networks for training ML models for failure management are imbalanced, and training ML models on such datasets may result in a bias towards sufficiently well-represented scenarios while negatively impacting performance on less frequent or under-represented scenarios. As an example, this can be seen in the results reported in [tre-23], where field data collected for seven months has been utilized for ML-based failure identification. The imbalance in the resultant dataset biased the performance of employed ML model towards the well-represented failure, resulting in lower F1-scores on under-represented failures. Thus, clearly, the problem of imbalanced datasets for failure management is an open issue and needs investigation.

Within the framework of the SEASON project, we investigated solutions to overcome this problem [Kha23]. We investigated model- and data-centric approaches. The primary objective of model-centric ML is to produce the "best" model for a given training dataset. It accomplishes this by modifying the model to improve its performance on a specific ML task. The data-centric approaches focus on the algorithmic increase in the quantity (e.g., data augmentation) and/or quality of the training dataset for a given ML model. In particular, we investigated focal loss and SMOTE-TOMEK as reference model-centric and data-centric approaches, respectively.

A neural network (NN) was chosen as the ML classifier for this investigation, considering the testbed in [Kha23] and generating the following failures/degradations: narrow filtering, attenuation, narrow filtering + attenuation, narrow filtering + filter shift, filter shift. NN consisted of five layers in total: an input layer with 2 neurons, three hidden layers with 183, 186, and 63 neurons, and an output layer with 5 neurons. *tanh* was used as an activation function in the hidden layers, and *softmax* was used in the output layer. The dropout rate was 0.05456, the learning rate was 0.002574, and the batch size was 8. All these hyperparameters were tuned using Bayesian Optimization. This NN was used as a baseline against which the performance of model-centric and data-centric approaches was compared.

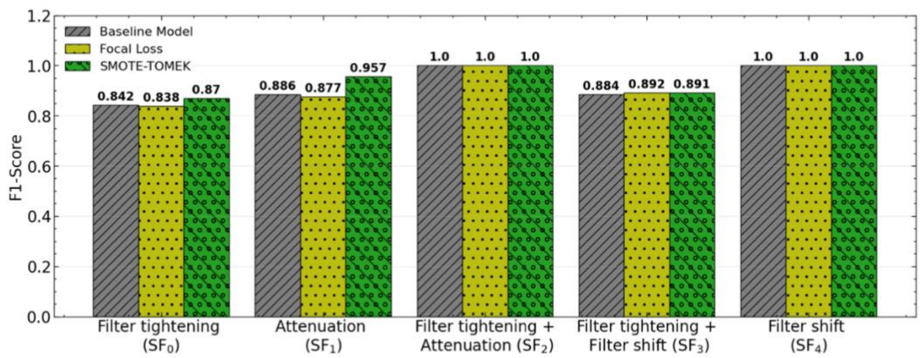

Figure 4-24 – F1-score for classifiers.

Figure 4-24 shows the results on test dataset for each soft-failure in terms of F1-score, which is one of the appropriate evaluation metrics in the case of imbalanced datasets. In our training dataset, SF_0, SF_1, and SF_3 have BER and OSNR values in the same range, making them inseparable, resulting in a comparatively poor performance on these three failure classes.

As it is clear from the figure, a significant performance improvement on these minority classes has been achieved using SMOTE-TOMEK. F1-score improved from 0.842 to 0.87 for SF_0 (2.8% improvement), from 0.886 to 0.957 for SF_1 (7.1% improvement), and from 0.884 to 0.891 for SF_3 (0.7% improvement) with no negative impact on majority classes (SF_2 and SF_4). In contrast, with focal loss, NN failed to improve overall performance on minority failure classes, suggesting that a data-centric approach may outperform model-centric approaches in this scenario. However, this only describes one aspect of the performance. To have a complete comparison, we considered performance in terms of training and computational time as well.

Table 4-5 shows the average training time over 100 training iterations (not epochs) as well as computational time on a Intel(R) Core (TM) i7-12700H @ 2.30 GHz with NVIDIA GeForce RTX 3060 Laptop GPU. It should be noted that computational time is only relevant to the SMOTE-TOMEK where we modified the training datasets. The impact of modifying the loss function is already reflected in the training time, and additional computation is not required. The average training time for baseline NN was 19.62 seconds, which increased slightly with the modification of loss function (i.e., focal loss). However, with the SMOTE-TOMEK approach, we increased both the quality (as indicated by the improved F1-scores) and the quantity (2.53-fold increase in this case) of data by adding synthetic samples. Due to this increase in training dataset size, the longer time was expected as now NN has to deal with many more samples during each training epoch. SMOTE-TOMEK's computational time was around 391 x 10^{-3} seconds, which is insignificant as compared to its training time.

Table 4-5: Computational cost comparison.

	Computational Time (s)	Average Training Time over 100 iterations (s)	Total Time (s)
Baseline Model	N/A	19.62	19.62
Focal Loss	N/A	21.71	21.71
SMOTE-Tomek	391 x 10^{-3}	31.82	31.82

5 SPECIFIC USE CASES IN METRO-ACCESS NETWORKS

5.1 METHODOLOGY OF OVERALL NETWORK DESIGN

In MS2.2, the SEASON architecture identifies several principal aspects and associated technologies that are particularly relevant to the data-plane e2e design. These include:

- "Flat" Access-Metro Segment and Backbone Segment: The architectural vision places a strong emphasis on establishing a "flat" Access-Metro segment that spans a significant distance of 100-400 kilometers, complemented by a distinct and well-defined Backbone segment. This strategic design choice serves as the cornerstone of the network infrastructure, aiming to facilitate efficient data transmission and seamless connectivity across the network. Within this framework, the architecture delineates three distinct categories of COs, each meticulously equipped with a diverse array of equipment including optical, packet, compute, and their hybrid counterparts. This tailored approach ensures that each CO is optimally prepared to handle specific network functions and requirements, thereby contributing to the overall versatility and adaptability of the network architecture.
- Optical Bypass of Intermediate Aggregation Switches/Routers: SEASON advocates for the implementation of optical bypass as a strategic measure to circumvent the traditional segmentation caused by intermediate aggregation switches and routers within the metro network domain. By leveraging optical bypass, the architecture seeks to optimize data flow and streamline the network infrastructure, aiming to eliminate unnecessary bottlenecks and enhance the overall efficiency of data transmission. This innovative approach underscores a commitment to leveraging cutting-edge technologies to achieve optimal network performance and seamless data transfer.
- Transparent Interconnection in the Access-Metro Segment: A pivotal aspect of the architectural framework lies in the seamless and transparent interconnection within the Access-Metro segment. This emphasis on transparent interconnection seeks to ensure that Access Points, which are responsible for generating substantial traffic flows, are seamlessly interconnected with the Service point where Telco and/or Service functions are located within the Access-Metro segment. This seamless interconnection is vital for ensuring the efficient transmission of data within the network, promoting uninterrupted and swift data transfer across the network infrastructure.
- Backbone Segment Optimization: The architecture places a strong focus on optimizing the Backbone segment, aiming to retain the existing network architecture while maximizing traffic capacity and maintaining a high level of flexibility and resilience. This strategic approach ensures that the network infrastructure is well-equipped to handle increasing data demands while remaining adaptable and robust. By prioritizing the optimization of the Backbone segment, the architecture underscores its commitment to

future-proofing the network and ensuring its ability to accommodate evolving data transmission needs.

- Partial Sharing of Access Passive Infrastructure: SEASON introduces a forward-thinking strategy by proposing the partial sharing of access passive infrastructure, particularly with existing or advanced PON technology, to directly interconnect "capacity-hungry" Access Points to Edge COs. This innovative approach aims to optimize resource usage and enhance connectivity within the network, underscoring a commitment to leveraging synergies between different network components to achieve optimal performance and efficiency. By implementing this approach, the architecture seeks to enhance the network's capacity to support high-demand access points while promoting resource efficiency and connectivity enhancement.

Key Technologies Considered in SEASON:

Programmable High Capacity and Performance Transceivers: The architectural framework within SEASON places significant emphasis on the adoption of programmable transceivers capable of multi-band operation. These advanced transceivers are designed to enable efficient and high-capacity data transmission across different frequency ranges, thereby facilitating the seamless transfer of large volumes of data within the network. By leveraging programmable transceivers, the architecture aims to achieve optimal performance and reliability in data transmission, ensuring that the network is well-equipped to handle diverse data transmission requirements across varying frequency bands.

Optical Switches: SEASON underscores the importance of optical switches equipped with advanced optical frequency, sub-band, and fiber/core switching capabilities. These cutting-edge switches are designed to feature many node degrees, enabling them to efficiently route data across the network infrastructure. By incorporating optical switches with sophisticated switching capabilities, the architecture seeks to optimize data routing, minimize latency, and enhance the overall efficiency of data transmission within the network, thereby ensuring seamless connectivity and reliable data transfer.

Flexible Optical Add/Drop and Multi-Band Line Operation: The architectural framework places a strong emphasis on the use of flexible optical Add/Drop technologies and multi-band line operation to enable versatile and efficient management of data traffic within the network. By leveraging these advanced technologies, SEASON aims to facilitate seamless integration and management of data flows, allowing for flexible and dynamic allocation of resources to accommodate varying traffic patterns and data transmission requirements. This strategic emphasis on flexibility and versatility underscores the architecture's commitment to optimizing data traffic management and ensuring efficient utilization of network resources.

Transport Optical Systems: SEASON advocates for the use of transport optical systems that leverage bundles of conventional or multicore fibers to support high-capacity and high-performance data transport. By embracing advanced transport optical systems, the architecture aims to ensure robust and reliable data transport capabilities, capable of supporting the high-performance demands of modern networks. These optical systems are designed to facilitate efficient and high-capacity data transport, ensuring that the network infrastructure can reliably handle the transmission of large volumes of data while maintaining optimal performance and scalability.

In summary, the key technologies considered in SEASON encompass a diverse array of advanced solutions tailored to optimize data transmission, enhance network efficiency, and ensure seamless connectivity. By leveraging programmable transceivers, advanced optical switches, flexible Add/Drop technologies, and robust transport optical systems, the architecture aims to create a high-performance and versatile network infrastructure capable of meeting the evolving demands of modern data transmission and communication.

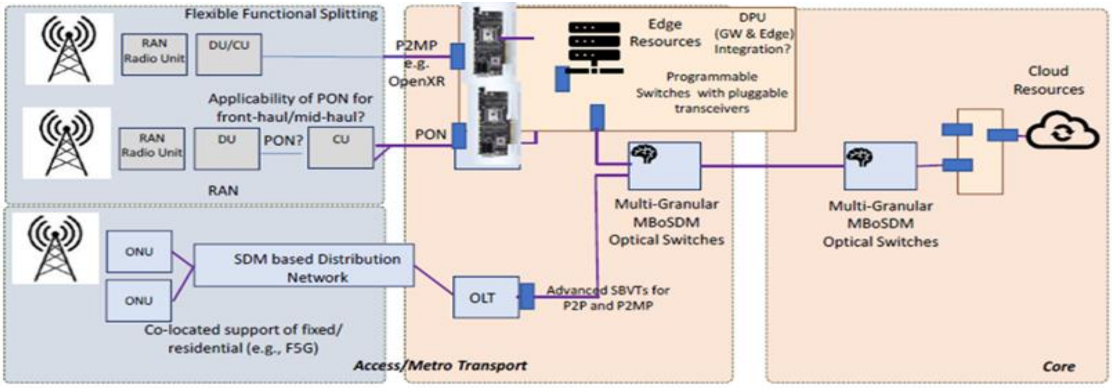

Figure 5-1 – Macroscopic overview of SEASON Control Plane key aspects over the SEASON data plane infrastructure.

Additionally, within the SEASON framework, coherent technology is recognized as the common underlying solution for the data-plane, offering different variations and also including alternative schemes/implementations such as DD tailored to the specific requirements of each network segment and evolutionary phase. This strategic approach acknowledges the need for a nuanced and adaptable deployment of coherent technology, aligning with the diverse needs of the network infrastructure. In this context, SEASON introduces a 'light coherent' solution designed for the access segment, which prioritizes reduced performance cost and energy consumption while ensuring efficient data transmission. This tailored solution addresses the unique demands of the access segment, aiming to optimize performance and cost-effectiveness while facilitating seamless connectivity and data transfer. Conversely, more advanced solutions are earmarked for the metro/core network and inter-domain transparent paths, such as P2MP, reflecting a nuanced deployment strategy that aligns with the specific needs of different network segments and use cases. The diverse e2e data-plane use-cases within the SEASON framework necessitate specific design considerations at the physical layer, encompassing intricate details related to signal propagation, modulation formats, and optical impairments. These considerations are essential for optimizing data transmission and ensuring the efficient utilization of network resources across various network segments. Furthermore, the varied use cases require specific design methodologies tailored to each scenario, ensuring that the network architecture can deliver optimal performance, scalability, and efficiency while accommodating diverse traffic patterns and transmission requirements. By incorporating coherent technology as the foundational solution for the data-plane and tailoring its deployment based on the unique requirements of each network segment, SEASON underscores its commitment to achieving an adaptable, high-performance network infrastructure capable of meeting the evolving demands of modern data transmission and communication. This approach reflects a strategic alignment with the diverse needs of the network while prioritizing performance, efficiency, and adaptability across the entire data-plane, thereby ensuring a robust and versatile network architecture.

Designing optical network links involves understanding the intricate features of each link's unique characteristics, which arise from its designated purpose and range. It is crucial to anticipate challenges, realize the potential physical effects, and provide tailored solutions. Here's a comprehensive breakdown of the design concerns and rules considered in SEASON for the various domains of optical networks:

Optical Access design:

- Distance & Attenuation: Covers shorter distances with concerns about signal attenuation, especially in the PON Spatial Aggregation scenario envisioned in SEASON.
- Energy: Focus on energy-efficient strategies for transmitting optical signals, maintaining optimal performance while minimizing power consumption.
- Bandwidth & Endpoints: Ensures adequate bandwidth for end-users, often shared among various users.
- Protection: Constraints on redundancy due to cost considerations, emphasizing the efficient operation of ONUs at premises and OLTs at the central office.

Optical Metro-Access Design:

- Reach & Dynamics: Spanning from urban centers to broader infrastructure, this segment necessitates considerations like variability in traffic volume and potential need for signal regeneration.
- ROADMs & Flexibility: Utilization of ROADM technology for dynamic bandwidth adjustment, while also emphasizing the need for flexible spectrum use and interoperability with various vendors.
- Protection & Restoration: Importance of quick restoration capabilities and protection schemes.

Optical Metro-Core Design:

- Capacity & Range: The Metro-Core serves as the bridge connecting major urban centers, covering distances usually up to 200 km. Given this range and the aggregated traffic, there's a pronounced need for high-capacity data transport.
- Dispersion & Nonlinear Effects: Addressing dispersion becomes critical due to the long spans and fluctuating traffic volumes. Further, higher power levels in these dense data regions can induce nonlinear effects such as cross-phase modulation and self-phase modulation.
- Amplification & ROADM Utilization: With the increasing demand, the use of Erbium-Doped Fiber Amplifiers (EDFAs) and possibly Raman amplification becomes essential. Furthermore, the deployment of Reconfigurable Optical Add/Drop Multiplexers offers flexibility in routing and channel adjustments.
- Multiband Operations & Resilience: Leveraging various optical bands, notably the C and L bands, is vital for managing capacity effectively. Yet, as dense data traffic increases, sticking to the tried and tested dual bands of C+L is often the most reliable choice, reducing complications and ensuring robustness. Incorporating network redundancy through configurations like rings or meshes ensures resilience. Another important effect that must be considered in the design of multiband systems is inter-channel stimulated Raman scattering, which constitutes the main inter-band effect [https://arxiv.org/abs/2304.11756].

Optical Core Design:

- Long-Haul Transmission & Capacity: The Core network, as the backbone, extends further than the Metro-Core, sometimes spanning thousands of kilometers. Here, issues related to attenuation, dispersion, and non-linear effects become even more dominant. The necessity for Ultra-High Capacity transport is addressed using Dense Wavelength Division Multiplexing (DWDM) with closely spaced channels.
- Amplification, Regeneration & Dispersion: Advanced amplification techniques, possibly including hybrid EDFAs, are essential, with some scenarios demanding 3R regeneration (reshape, retime, re-amplify). Managing chromatic dispersion is crucial, especially given the vast distances involved.
- Multiband Management & Nonlinear Challenges: Efficient utilization of multiple optical bands is crucial. However, with increased power levels, challenges such as self-phase modulation and inter-band interference become significant. Managing these nonlinearities becomes a primary design consideration.
- Security & Physical Layer Concerns: In such a vast network, concerns about potential eavesdropping emerge. Addressing physical layer security and looking into mitigation strategies is pivotal.

In summary, optical link design demands a forward-thinking approach that not only guarantees effective data transport but also ensures the network's resilience, scalability, and adaptability to future technological shifts. Balancing power consumption, cost, and compatibility with new technologies remains a pivotal aspect of the SEASON design.

5.2 USE CASES

5.2.1 Front/Mid-haul and access beyond 5G

The interface known as fronthaul is crucial in Open RAN, particularly in terms of latency and capacity requirements, as it links radio units to the network and significantly impacts air interface performance. Standardization efforts have been led by 3GPP and more recently the O-RAN Alliance, with the latter building upon the foundation laid by the former. An important feature of Open RAN is the ability for multiple vendors to coexist within the RAN domain.

Within the O-RAN architecture, baseband functions are divided into three logical units: O-RAN Centralized Unit (O-CU), O-RAN Distributed Unit (O-DU), and O-RAN Radio Unit (O-RU). The O-CU and O-DU can operate on either Commercial Off-The-Shelf (COTS) hardware or purpose-built hardware, with the former configuration often referred to as Cloud RAN. Meanwhile, the O-RU is typically based on specialized hardware, such as Application Specific Integrated Circuit (ASIC).

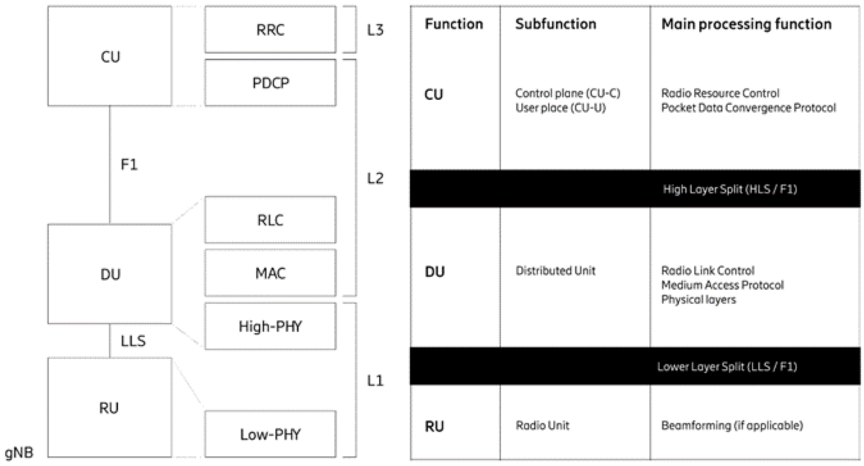

Figure 5-2 – O-RAN split architecture.

The Higher-Level Split (HLS), also known as the mid-haul interface, delineates the responsibilities of the O-CU and O-DU. 3GPP has established a split in which the O-CU manages Layer 3 functions, specifically Radio Resource Control (RRC) and the Packet Data Convergence Protocol (PDCP), while the O-DU handles Layer 2 functions, encompassing Radio Link Control (RLC), Medium Access Control (MAC), and the Layer 1 function known as High-PHY. The F1 interface, which connects the O-CU and the O-DU, as defined by 3GPP, has been integrated into the O-RAN architecture.

On the other hand, the Lower-Layer Split (LLS), also referred to as the fronthaul interface, divides responsibilities between the O-RU and the O-DU. The LLS represents an intra Layer 1 split between the High-PHY in the O-DU and the low-PHY in the O-RU. The precise distribution of functions between High-PHY in the O-DU and Low-PHY in the O-RU significantly impacts the performance achievable over the air interface (spectral efficiency) and is responsible for the most relevant trade-offs related to bandwidth, latency, performance, as well as the cost and complexity of the RU design.

We can distinguish between two radio categories:

Remote radios are utilized in areas with lower traffic demands, such as rural areas. They are linked to antennas with a maximum of eight digital antenna ports. The processing power required in the O-RU is comparatively lower than that of Massive MIMO radios.

Massive MIMO radios are employed in locations with high-capacity needs and support more than eight digital antenna ports. They are more intricate and necessitate greater processing power in the O-RU to manage the intricate beamforming calculations associated with a larger number of digital antenna ports.

The optimal Lower-Layer Split varies for these two radio categories. In the case of Remote Radio, only a limited set of L1 processing functions, in addition to the Digital Front End (DFE), is required, while the O-DU handles most of the L1 processing. This configuration is referred to as the Cat-A split, and it was developed as the standard for these types of radios.

For Massive MIMO radios with a higher number of digital antennas (e.g., 64), increased compute requirements, especially for beamforming, are necessary. Relying on the O-DU, as in the case of Cat-A, would lead to a significant amount of data being transmitted across the fronthaul interface, creating a capacity challenge for the transport network. To address this issue, a new Cat-B split (also known as 7-2x) has been introduced, where RF and low-Phy functions are placed in the O-RU, and the high-Phy, MAC, and RLC functions are handled by the O-DU. The low-PHY is responsible for beamforming. The Cat-B split strikes a balance between the processing capabilities of the O-RU and the capacity of the fronthaul interface, establishing a clear separation of responsibilities to simplify multi-vendor deployments. However, this choice requires high fronthaul capacity in the uplink in Massive MIMO deployments with high interference, load, and User Equipment (UE) mobility.

By implementing channel estimation and equalization in the DU, as stipulated by 7.2x, the transmission of up to 64 digital streams from the RU to the DU would cause the fronthaul bit-rate to soar. To address this, a port reduction function has been introduced, wherein only pertinent streams are transmitted from the RU to the DU. However, this approach leads to some information loss, thereby diminishing interference reduction performance. Additionally, the increased latency between the DU and RU compromises beamforming tracking, particularly in scenarios involving high user density and mobility (such as stadiums and downtown areas). Simulation results have demonstrated a performance degradation of approximately 30% to 40% [Lig23, Eri23].

On the other hand, retaining equalization in the DU would enable joint processing across sites. Considering all these trade-offs from both a performance and a cost/interoperability standpoint, the O-RAN fronthaul standard [3] incorporates the following options:

- Cat-A: Current standard for remote radio units (RRU), (7-2x Cat-A no-BF-RU split)
- Cat-B: Current standard for M-MIMO radios (7-2x Cat-B)
- Cat-B ULPI: New standard for M-MIMO, refers to ULPI improvements on Cat-B
- Cat-B ULPI-A: New standard for M-MIMO, Class A, (7.2x ULPI with DMRS-EQ)
- Cat-B ULPI-B: New standard for M-MIMO, Class B, (7.2x ULPI with DMRS-NEQ)

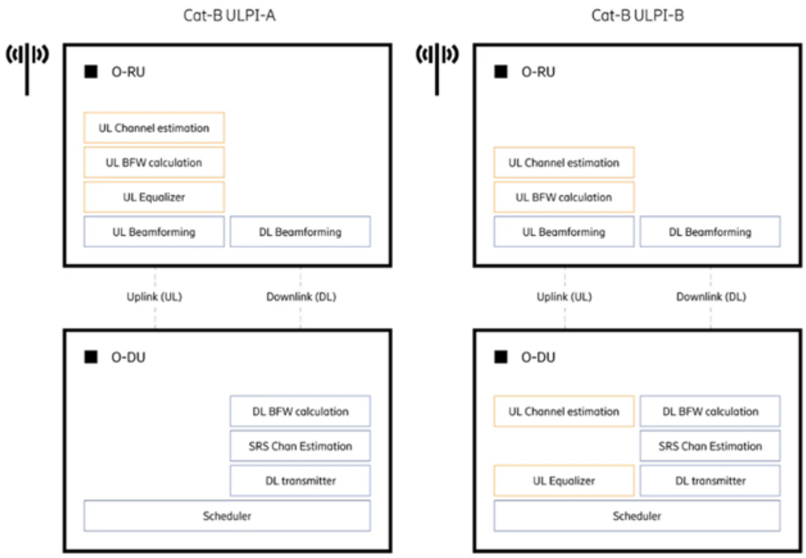

Figure 5-3 – ULPI classes for Cat-B functional split.

The primary distinction between the two ULPI classes lies in the placement of the equalizer function. In Cat-B ULPI-A, the equalizer function is located in the O-RU, while in Cat-B ULPI-B, it is situated in the O-DU. This resolves the original challenge of integrating Massive MIMO Radio into Open RAN with existing fronthaul capacity and facilitates straightforward multi-vendor interoperability due to the clear delineation between O-RU and O-DU. However, a drawback is the potential for a more intricate and costly RU. Manufacturers of RUs have the option to produce either class A or class B kits. On the other hand, DUs are required to support both classes, including equalizers by default, even if not utilized.

Regarding the anticipated capacity expansion in the RAN transport segments, we refer to Ericsson's estimation of the bit-rate requirements over a 10-year period for the radio and baseband processing units (BPUs).

Table 5-4 – RAN Transport Capacity requirements (source: Ericsson).

Interface	2022	2025	2027	2030	2033
eCPRI	2.5-50Gbps/radio	2.5-100Gbps/radio 400Gbps/BPU 50Gbps/port	2.5-200Gbps/radio 600Gbps/BPU 100Gbps/port	2.5-400Gbps/radio ~ 1Tbps/BPU 400Gbps/port?	2.5-400Gbps/radio ~ 2Tbps/BPU 400Gbps/port?
F1 NG/Xn	1-25Gbps/BPU	10-50Gbps/BPU	10-100Gbps/BPU	25-200Gbps/BPU	100-400Gbps/BPU
S1/X2	1-10Gbps/BPU	1-10Gbps/BPU	1-10Gbps/BPU	1-10Gbps/BPU	1-10Gbps/BPU

The fronthaul interface is projected to be the most demanding in terms of capacity, with an anticipated forecast of up to 400Gbps on the radio interface by 2033. This rationale justifies the project's decision to assess coherent 400G interfaces for the fronthaul. These estimates align closely with the projections presented by CTTC at the "Networld Europe: Future Optical Networks" workshop in 2023 for the 6G RAN transport, as detailed below:

Table 5-5 – 6G RAN Transport capacity requirements (source: CTTC).

Functional split option	5G	6G basic	6G advanced
1	DL: 4Gbps UL: 3Gbps	DL: 16Gbps UL: 16Gbps	DL: 100Gbps UL: 80Gbps
2	DL: 4.016Gbps UL: 3.024Gbps	DL: 16.016Gbps UL: 16.024Gbps	DL: 100.02Gbps UL: 80.024Gbps
7-2	DL: 22.204Gbps UL: 21.624Gbps	DL: 86.71Gbps UL: 86.13Gbps	DL: 430.78Gbps UL: 430.20Gbps

In the SEASON architecture, the access segment is meticulously structured around a virtual mesh constructed over a DWDM ring, leveraging filter-less OADM nodes and coherent technology. This innovative design approach is specifically crafted to enable the seamless deployment of P2MP coherent technology within the access segment, catering to the unique requirements and operational demands of this critical network domain. The design and dimensioning of the access segment within the SEASON architecture revolve around the thorough validation of the power budget, which is contingent on a myriad of factors including Coherent transceiver sensitivity, optical pluggable amplifier performances, and splitter loss. Ensuring that the power budget remains within acceptable limits is paramount for the reliable and efficient operation of the access segment, underscoring the meticulous attention to detail and performance optimization within the architecture. The integration of filter-less OADM nodes within the access segment not only facilitates the seamless implementation of P2MP coherent technology but also enhances the flexibility and scalability of the network architecture. This strategic design choice reflects the architecture's commitment to harnessing advanced optical technologies to optimize network performance and adaptability, thereby ensuring that the access segment can efficiently accommodate evolving data transmission requirements. Additionally, the SEASON architecture places a strong emphasis on considering a "light coherent" solution tailored specifically for the access segment, with the DSP meticulously designed to accommodate the maximum ring length. While dispersion compensation is not deemed critical in this context, the deployment of a "light coherent" solution tailored for access is considered highly desirable to optimize the performance and efficiency of the access segment, aligning with the overarching objectives of the architecture. Furthermore, the architecture allows for transparency towards the metro segment, provided that metro-performance coherent transceivers are employed. This emphasis on transparency underscores the architecture's commitment to seamless integration and interoperability between the access and metro segments, contributing to the overall efficiency and performance of the network while promoting a cohesive and unified network infrastructure. As part of the SEASON assessment, the scaling of the DWDM ring in terms of nodes and wavelengths will be rigorously evaluated to determine the optimal configuration for achieving the desired capacity, flexibility, and performance within the access segment. This comprehensive assessment serves as a critical foundation for informing the deployment strategy and technology selection within the access segment, ensuring that it aligns with the strategic objectives and overarching vision of the SEASON architecture.

5.2.2 Multi-core access

We studied the novel PON architecture proposed in SEASON that exploits the spatial dimension for dynamic aggregation and disaggregation of spatial lanes, such as cores in Multi-Core Fibers (MCFs) or fibers in multi-fiber scenarios. This architectural approach enables adaptive activation and deactivation of Optical Line Terminal (OLT) and Optical Network Unit (ONU) components based on traffic conditions, thereby optimizing energy savings without compromising performance. Through an examination of various traffic patterns and PON power consumption scenarios, this architecture underscores the potential for significant energy savings.

The reference architecture illustrated in Figure 5 involves an OLT at the Central Office (CO) site, equipped with several OLT ports. Each port serves an Optical Distribution Network (ODN) through one or more splitting levels using optical splitters, known as Remote Nodes (RNs). The ODN encompasses a primary section extending from the OLT to the primary splitting point and a secondary section from the primary splitter to the ONUs. The primary ODNs are implemented either through traditional single-mode fibers, resulting in a Multi-Fiber system, or through different cores in an MCF.

A notable innovation in this architecture is the addition of a Reconfigurable Spatial Splitter/Combiner at the CO, capable of dynamically aggregating or disaggregating multiple spatial lanes towards single or multiple OLT ports. This mechanism, contingent on traffic load monitoring on each spatial lane, allows for significant energy savings by switching off unutilized OLT ports during low load conditions and activating them during high load conditions.

The proposed architecture not only presents a scalable and energy-efficient solution for next-generation optical access networks but also introduces a versatile platform for seamlessly integrating optical and radio access networks. Through its dynamic spatial aggregation mechanism, it promises immense potential for energy conservation, highlighting the architecture's efficacy and practicality in adapting to diverse traffic patterns and network demands.

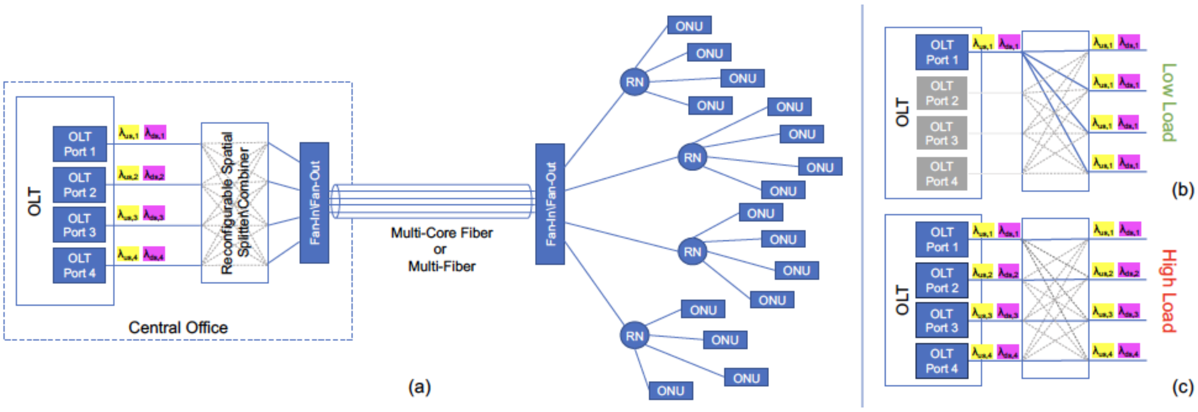

Figure 5-6 – Spatial PON reference architecture.

As shown in Figure 6a, three primary traffic patterns, instrumental to the services supported by the PON infrastructure are considered: Small Office/Home Office (SOHO), Large Business, and Mobile. Each pattern is characterized by its unique diurnal load variations. The SOHO pattern, for instance, displays a notable peak during the traditional working hours, tapering off towards the evening. In contrast, the Mobile traffic exhibits more consistent demand throughout the day, with slight increases aligning with commuting hours. The Large Business load shows a more pronounced usage during business hours, which is expected due to the operational nature of such entities.

The proposed model's performance is critically assessed by the percentage of OLT ports or spatial lanes that can be dynamically deactivated to conserve energy. In Figure 6b, we see the average number of spatial lanes that can be feasibly deactivated, calculated over a 24-hour period, as a function of the total number of spatial lanes, denoted as N. The graph illustrates that with the increase in the number of spatial lanes, there is a proportional rise in the potential for lane deactivation and, consequently, energy savings. The SOHO traffic pattern presents the most substantial potential for deactivation, approximately 40%, underscoring the significant variability in its traffic and the effectiveness of the deactivation mechanism.

It is important to note that there is an increment in potential gains across all three traffic patterns, which reaches a saturation point. As depicted in Figure 6c, the relative increase in the percentage of spatial lanes that can be saved exhibits a steep rise up to the use of 8 spatial lanes. Beyond this point, the relative increase tapers off significantly as the number of spatial lanes grows from 8 to 16. This trend indicates a diminishing return on deactivation potential with the addition of more spatial lanes, suggesting an optimal range for spatial lane deployment in terms of energy efficiency gains.

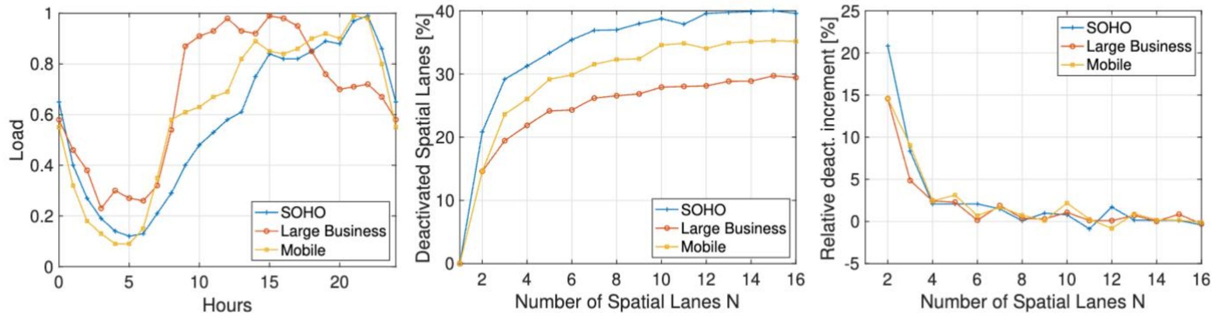

(a) Traffic patterns, data provided by TIM (b) Achievable spatial lanes deactivation (c) Relative increment

Figure 5-7 – Aggregation potential.

5.2.3 Optical bypass

In this section, Telefónica illustrates a practical use case involving optical bypass for P2MP transmission. In the evolving landscape of Beyond 5G, the telecommunications sector anticipates a substantial surge in the volume of devices and the data they generate and consume. Currently, the Telefónica network relies on IP hierarchical levels (HLs) and is constructed using P2P transceivers, along with successive electrical aggregation stages inherent in this architecture. However, the predominant traffic pattern across most network segments resembles a hub-and-spoke configuration.

Optical bypass enables a seamless transition to a network structured around P2MP coherent transceivers, complemented by a hybrid ROADM/filterless line system, collectively better accommodating this type of traffic. This configuration offers the advantage of bypassing certain HL layers, allowing for the optimization of routers, which may not necessarily be removed but can benefit from fewer occupied line ports. This results in reduced switching capacity requirements, with dedicated resources for local termination.

The innovative approach of adopting a P2MP network not only streamlines the bypass of HL routers, consequently decreasing global latency, but also aligns with the vision of establishing a flatter IP architecture, as proposed in SEASON, in accordance with *D2.2 - Section 5.3: SEASON high-level architecture*. This strategic evolution demonstrates a noteworthy reduction in overall costs, as highlighted in [A. Napoli et al., OFC 2022]. This forward-thinking solution not only addresses the impending challenges of increased device connectivity and data demand but also underscores the importance of adapting network infrastructure for optimal efficiency and cost-effectiveness.

Figure 5-8 illustrates the two compared architectures involving routers from HL5 to HL3. The left Figure showcases the P2P solution, while the right Figure displays the P2MP solution. It is evident that the P2MP architecture significantly reduces the number of occupied line ports, switch capacity, and the required transceivers in the bypassed HL4 layer, leading to a notable positive impact on CAPEX.

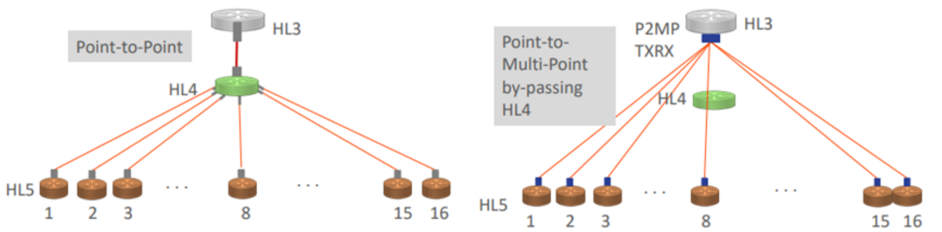

Figure 5-8 – Comparison between the P2P architecture (on the left) and the P2MP architecture (on the right), taking into account IP routers from HL5 to HL3.

Moving on to Figure 5-9, it depicts the detailed testbed that Telefónica will employ to assess the architecture based on P2MP coherent transceivers for transporting data between the HL3 and HL5 layers (and vice versa), bypassing the intermediate IP router in the HL4 layer. Notably, a splitter is utilized to transport data to the HL5 layer, with power transmission divided among the HL5 nodes served by the 400G hub. However, when attending to a substantial number of HL5 nodes, the inclusion of alternative distribution devices with lower power loss, like WSSs, becomes essential. Fortunately, the existing 400G maximum capacity of the hub enables the splitter to efficiently distribute traffic among the considered HL5 nodes. Looking ahead to future networks, as the transceiver hub's capacity grows, the inclusion of WSSs may become imperative.

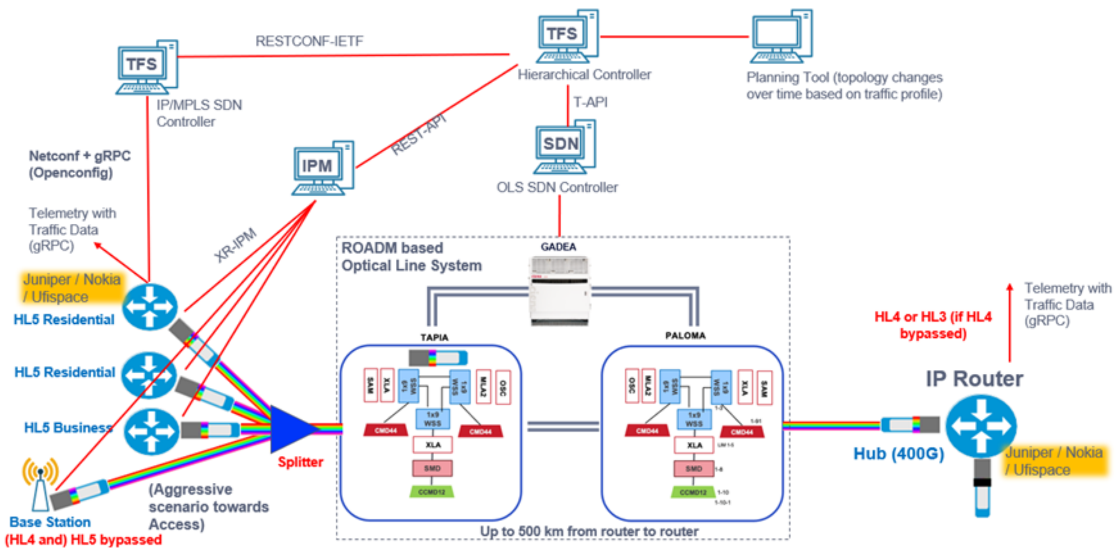

Figure 5-9 – Telefónica's testbed for P2MP transmission between the HL3 and HL5 layers.

5.2.4 Metro – aggregation

Metro-aggregation network segments connect access networks to metro and core networks. In contrast to core networks, the traffic pattern in these networks is still P2MP like that in access networks. The number of networks and nodes is significantly larger than in core networks and needs to be managed appropriately in terms of cost, technology adoption, scalability, and quality of service requirements. In many practical metro-aggregation networks, the need for large capacity demands the use of coherent technology. Tree topologies can provide built-in support for P2MP transmission, but they are not protected against link failure. However, ring or horseshoe topologies not only have built-in support for P2MP but also can be resilient against link and hub failures.

Usually, different access and metro-aggregation segments are operated independently, and O-E-O conversion is needed to serve several purposes including aggregation of different services, protocol adaptation, and regeneration. One way to expand the network and utilize the cost-effectiveness of optical transmission is using an all-optical-network approach. This approach suggests not converting the optical services at the border of a network segment but transmitting it towards the access using appropriate edge optical devices. Another way is to upgrade the reach of metro-aggregation networks by adding branches to the horseshoe topology and accommodating more end-nodes gradually. The combination of this topology and DSCM-based P2MP transceivers can provide dynamic capacity allocation and smooth end-leaf node service deployment.

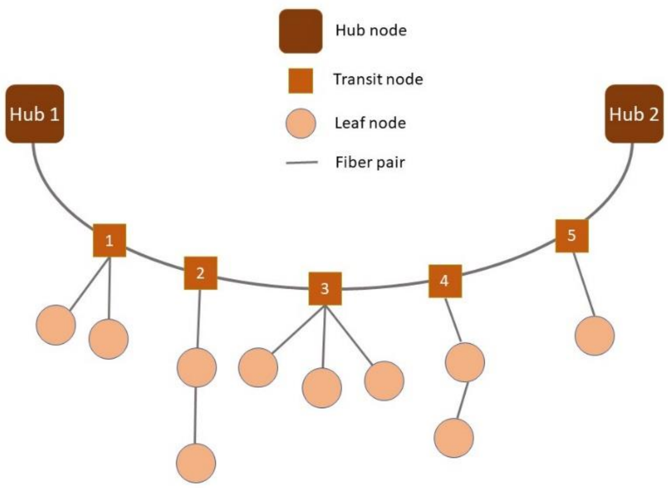

Figure 5-10 – Exemplary of metro - aggregation network.

Figure 5-10 shows a typical considered architecture consisting of two hub nodes, some transit nodes, and several leaf nodes. All nodes can be potentially equipped with passive devices such as splitters and combiners. The goal is to minimize the number of amplifiers while ensuring end-to-end performance and P2MP transmission constraints. There are various design possibilities regarding the nodes' architecture choices, traffic demand, scenario, and specific network requirements. In SEASON, we are assessing this issue, and first results are about to be submitted to JOCN [Hos24].

6 CONCLUSIONS

In this document, we presented the first results obtained within the WP3 of the SEASON project.

The outcomes of the WP2 discussion in terms of network and physical layer requirements were briefly recalled, and we reported on the state-of-the-art and the limitations of current optical systems. Furthermore, we also discuss the SEASON network architecture, which includes a multi-stage approach optimized for the different network scenarios considered, ranging from multi-band to spatial-division-multiplexing, and using P2P and/or P2MP. The final decisions will depend on the operator's needs, particularly in terms of traffic and cost. In this context, two types of network topology are discussed and reported, along with their requirements and the solutions that will be considered within SEASON. We focus on delivering higher capacity through the utilization of multi-band and SDM, and aim to significantly reduce the quantity of network devices and the overall power consumption within the network infrastructure.

Under the discussion of physical layer modelling in terms of literature review and technological advances carried out in SEASON, the most relevant models reported are for single-core, multi-core, and multi-mode, together with the relative improvements and updates proposed within the project.

In terms of transmission, we considered both multi-band and SDM transmission, to target different application scenarios. Several types of sliceable bandwidth variable transceivers for P2P and P2MP, with and without coherent detection were discussed. Concerning components, a particular attention was given to the node architecture, with multi-band and multi-core solutions. Both approaches will be widely investigated in the two remaining years of the project, and a series of studies are ongoing.

In addition to pure data plane topics, we are investigating the capabilities and needs of pluggable transceivers and amplifiers in the context of an IP over DWDM network architecture. Alongside these devices, we also envision a new edge-node architecture. In this context, we plan to exploit the advanced capabilities of data processing units combined with P2P and P2MP transceivers to simplify the overall network architecture at the edge. The optical and digital monitoring of next-generation optical networks is also being assessed.

The main aspects to be considered in the different segments of the telecommunication infrastructure within SEASON are provided in the network design. The main use cases discussed include front-haul and access solutions, and the possibility of significantly extending the capacity by deploying forward-looking multi-core optical fiber in access PON. Furthermore, metro-aggregation and other solutions to simplify the architecture are considered. These can comprise the bypass of network elements or the optimization of component deployment, enabled by flexible transceiver technologies.

7 GLOSSARY

Acronym	Description
ADC	Analog-to-Digital Converter
ADSL	Asymmetric Digital Subscriber Line
AR	Augmented Reality
ASE	Amplified spontaneous emission
ASIC	Application-Specific Integrated Circuit
AWG	Arrayed-Waveguide Grating
b2b	Back-to-back
BNG	Broadband Network Gateway
BVT	Bandwidth/bit rate variable transponder
CC-MCF	Coupled-core fibers
CD	Colorless Directionless
CDC	Colorless Directionless Contentionless
CDN	Content Delivery Network
CO	Central Office
CSG	Cell Site Gateway
DAC	Digital-to-Analog Converter
DC	Data Center
DCM	Dispersion Compensation Modules
DPU	Data processing unit
DSB	Double sideband
DSCM	Digital Supply Chain Management
DSP	Digital Signal Processor/Processing
DWDM	Dense Wavelength Division Multiplexing
E2E	End-to-End
EDFA	Erbium-Doped Fiber Amplifier
EML	Electro-absorption modulated laser
EON	Elastic optical networks
FEC	forward error correction
FMF	Few-Mode Fiber
FOADM	Fixed Filter Optical Add-Drop Multiplexer
FTTH	Fiber-To-The-Home
FTTx	Fiber-to-the-x
GE	Gigabit Ethernet
GGN	Generalized Gaussian noise
GN	Gaussian Noise
GPON	Gigabyte Passive Optical Network
GPU	graphics processing unit
GSNR	Generalized signal-to-noise ratio
HLx	Hierarchical Level x
KPI	Key Performance Indicator
ISP	Internet Service Provider
ISRSGN	Inter-channel stimulated Raman scattering
MAN	Metropolitan Area Network
MB	Multi-band
MBoSDM	Multi-Band over Space Division Multiplexing

MBT	multi-band transmission
MCF	Multi-Core Fiber
MCS	MultiCast Switch
MDL	Mode-dependent loss
MIMO	Multiple-input-multiple-output
MMF	Multimode fiber
MPF	Mult-parallel fiber
MPLS	Multi-Protocol Label Switching
MW	Microwave
MZM	Mach-zehnder modulator
NIC	Network Interface Card
NLI	Nonlinear interference
NN	Neural Network
NOS	Network Operating System
O/E/O	Optical to Electrical to Optical
ODE	Ordinary differential equations
ODN	Optical Distribution Network
OFDM	Orthogonal frequency division multiplexing
OLT	Optical Line Terminal
ONT	Optical Network Terminal
OPC	Optical Packet Core
O-RAN	Optical Radio Access Network
OSC	Optical Supervisory Channel
OSFP	Optical small factor pluggable
OTDR	Optical time domain refloctometer
OTN	Optical Transport Network
P2MP	Point-to-multi-point
P2P	Point-to-point
PGW	Packet Data Network Gateway
PON	Passive Optical Network
QoT	Quality of transmission
QSFP	Quad small factor pluggable
RAN	Radio Access Network
ROADM	Reconfigurable Optical Add-Drop Multiplexer
SE	Spectral Efficiency
SDM	Spatial division multiplexing
S-BVT	Sliceable Bandwidth Variable Transceiver
SMF	Single-Mode Fiber
S-OXC	Spatial optical crossconnect
SoA/SotA	State of the Art
SRS	Stimulated Raman scattering
SSB	single sideband
SSMF	Standard single mode fiber
TDFA	Thulium-Doped Fiber Amplifier
TF	Tunable filter
UC-MCF	Uncoupled-core multi-core fiber
URLLC	Ultra-Reliable and Low-Latency Communications
VPN	Virtual Private Network
VR	Virtual Reality
WDM	Wavelength division multiplexed

WSS	Wavelength Selective Switch
XGS-PON	10Gb Simmetric Passive Optical Network

8 REFERENCES

[Ami22]	A. D'Amico, B. Correia, E. London, E. Virgillito, G. Borraccini, A. Napoli, and V. Curri, "Scalable and disaggregated GGN approximation applied to a C+L+S optical network," J. Light. Technol. 40, 3499–3511 (2022).
[Ant12]	Cristian Antonelli, Antonio Mecozzi, Mark Shtaif, and Peter J. Winzer, "Stokes-space analysis of modal dispersion in fibers with multiple mode transmission," Opt. Express 20, 11718-11733 (2012)
[Ant13]	Cristian Antonelli, Antonio Mecozzi, Mark Shtaif, and Peter J. Winzer, "Random coupling between groups of degenerate fiber modes in mode multiplexed transmission," Opt. Express 21, 9484-9490 (2013)
[Ant15]	Cristian Antonelli, Antonio Mecozzi, and Mark Shtaif, "The delay spread in fibers for SDM transmission: dependence on fiber parameters and perturbations," Opt. Express 23, 2196-2202 (2015)
[Ant16]	C. Antonelli, M. Shtaif and A. Mecozzi, "Modeling of Nonlinear Propagation in Space-Division Multiplexed Fiber-Optic Transmission," in Journal of Lightwave Technology, vol. 34, no. 1, pp. 36-54, 1 Jan.1, 2016, doi: 10.1109/JLT.2015.2510511.
[Ant20-1]	Cristian Antonelli, Gabriele Riccardi, Tetsuya Hayashi, and Antonio Mecozzi, "Role of polarization-mode coupling in the crosstalk between cores of weakly-coupled multi-core fibers," Opt. Express 28, 12847-12861 (2020)
[Ant20-2]	C. Antonelli, A. Mecozzi, M. Shtaif, N. K. Fontaine, H. Chen and R. Ryf, "Stokes-Space Analysis of Modal Dispersion of SDM Fibers With Mode-Dependent Loss: Theory and Experiments," in Journal of Lightwave Technology, vol. 38, no. 7, pp. 1668-1677, 1 April1, 2020, doi: 10.1109/JLT.2019.2959191.
[Ari13]	Sercan Ö. Arık, Daulet Askarov, and Joseph M. Kahn, "Effect of Mode Coupling on Signal Processing Complexity in Mode-Division Multiplexing," J. Lightwave Technol. 31, 423-431 (2013)
[Ari16]	Sercan Ö. Arık, Keang-Po Ho, and Joseph M. Kahn, "Group Delay Management and Multiinput Multioutput Signal Processing in Mode-Division Multiplexing Systems," J. Lightwave Technol. 34, 2867-2880 (2016).
[Can17]	M. Cantono, D. Pilori, A., Ferrari, and V. Curri, "Introducing the generalized GN-model for nonlinear interference generation including space/frequency variations of loss/gain" (2017). arXiv preprint arXiv:1710.02225.
[Can18]	M. Cantono et al., "On the Interplay of Nonlinear Interference Generation With Stimulated Raman Scattering for QoT Estimation," in Journal of Lightwave Technology, vol. 36, no. 15, pp. 3131-3141, 1 Aug.1, 2018, doi: 10.1109/JLT.2018.2814840.
[Cas24]	Piero Castoldi, Rana Abu Bakar, Andrea Sgambelluri, Juan Jose Vegas Olmos, Francesco Paolucci, and Filippo Cugini, "Programmable Packet-Optical Networks using Data Processing Units (DPUs) with Embedded GPU Monitoring devices", OFC Conf. 2024
[Dwi00]	A. Dwivedi and R.Wagner, "Traffic model for USA long-distance optical network," in Proc.Opt. Fiber Commun. Conf.Opt. Soc. Amer., 2000, pp. 1–3.
[Dis23]	G. Di Sciullo et al., " Reduction of Modal Dispersion in a long-haul 15-Mode Fiber link by means of Mode Permutation ", ECOC 2023 (to appear)
[Els18]	D. J. Elson et al., "Nonlinearity Mitigation in the Presence of Intercore-Crosstalk," 2018 European Conference on Optical Communication (ECOC), Rome, Italy, 2018, pp. 1-3, doi: 10.1109/ECOC.2018.8535458.
[Eri23]	Bringing performance at scale to Open RAN, https://www.ericsson.com/en/reports-and-papers/further-insights/driving-open-ran-forward
[Ess13]	R. -J. Essiambre et al., "Experimental Observation of Inter-Modal Cross-Phase Modulation in Few-Mode Fibers," in IEEE Photonics Technology Letters, vol. 25, no. 6, pp. 535-538, March15, 2013, doi: 10.1109/LPT.2013.2242879.
[Fer14]	F. M. Ferreira, D. Fonseca and H. J. A. da Silva, "Design of Few-Mode Fibers With M-modes and Low Differential Mode Delay," in Journal of Lightwave Technology, vol. 32, no. 3, pp. 353-360, Feb.1, 2014, doi: 10.1109/JLT.2013.2293066.

[Fer17]	F. M. Ferreira, C. S. Costa, S. Sygletos and A. D. Ellis, "Semi-Analytical Modelling of Linear Mode Coupling in Few-Mode Fibers," in Journal of Lightwave Technology, vol. 35, no. 18, pp. 4011-4022, 15 Sept.15, 2017, doi: 10.1109/JLT.2017.2727441.
[Fer19]	Filipe Marques Ferreira, Christian S. Costa, Stylianos Sygletos, and Andrew D. Ellis, "Nonlinear Performance of Few-Mode Fiber Links With Intermediate Coupling," J. Lightwave Technol. 37, 989-999 (2019)
[Fer20]	A. Ferrari et al., "Experimental Validation of an Open Source Quality of Transmission Estimator for Open Optical Networks," 2020 Optical Fiber Communications Conference and Exhibition (OFC), San Diego, CA, USA, 2020, pp. 1-3.
[Fer20-2]	A. Ferrari, A. Napoli, J. K. Fischer, et al., “Assessment on the achievable throughput of multi-band ITU-T G.652.D fiber transmission systems”, Journal of Lightwave Technology, vol. 38, no. 16, pp. 4279–4291, 2020.
[Gat23]	A. Gatto et al., "Partial MIMO-based Mode Division Multiplexing Transmission over the First Field-Deployed 15-Mode Fiber in Metro Scenario," 2023 Optical Fiber Communications Conference and Exhibition (OFC), San Diego, CA, USA, 2023, pp. 1-3, doi: 10.1364/OFC.2023.M2B.3.
[Hay11]	Tetsuya Hayashi, Toshiki Taru, Osamu Shimakawa, Takashi Sasaki, and Eisuke Sasaoka, "Design and fabrication of ultra-low crosstalk and low-loss multi-core fiber," Opt. Express 19, 16576-16592 (2011).
[Hay19]	Hayashi, T. (2019). Multi-core Fibers for Space Division Multiplexing. In: Peng, GD. (eds) Handbook of Optical Fibers. Springer, Singapore. https://doi.org/10.1007/978-981-10-7087-7_66
[Hay22]	T. Hayashi et al., "Randomly-Coupled Multi-Core Fiber Technology," in Proceedings of the IEEE, vol. 110, no. 11, pp. 1786-1803, Nov. 2022, doi: 10.1109/JPROC.2022.3182049.
[Her20]	A. Hernandez et al., “Comprehensive model for technoeconomic studies of next-generation central offices for metro networks,” Journal of Optical Communications and Networking, vol. 12, no. 12, pp. 414–427, 2020.
[Her23]	Jose Alberto Hernandez et al. “On clustering coherent optics point-to-multipoint trees for cost-effective bandwidth assignment in MANs”, Journal of Optical Communications and Networking, 2023
[Ho11-1]	K. -P. Ho and J. M. Kahn, "Statistics of Group Delays in Multimode Fiber With Strong Mode Coupling," in Journal of Lightwave Technology, vol. 29, no. 21, pp. 3119-3128, Nov.1, 2011, doi: 10.1109/JLT.2011.2165316.
[Ho11-2]	Keang-Po Ho and Joseph M. Kahn, "Mode-dependent loss and gain: statistics and effect on mode-division multiplexing," Opt. Express 19, 16612-16635 (2011)
[Hos24]	Mohammad M. Hosseini, João Pedro, Nelson Costa, Carlos Castro, and Antonio Napoli, “Optimized Design of Horseshoe-and-Spur Filterless Networks Leveraging Point-to-Multipoint Coherent Pluggable Transceivers “
[Ina12]	Beril Inan, Bernhard Spinnler, Filipe Ferreira, Dirk van den Borne, Adriana Lobato, Susmita Adhikari, Vincent A. J. M. Sleiffer, Maxim Kuschnerov, Norbert Hanik, and Sander L. Jansen, "DSP complexity of mode-division multiplexed receivers," Opt. Express 20, 10859-10869 (2012)
[Kan23]	R. Kaneko, T. Sasai, M. Takahashi, E. Yamazaki and Y. Kisaka, "Experimental Performance Evaluation of Rx DSP-based Fiber-longitudinal Power Profile Estimation," 2023 Opto-Electronics and Communications Conference (OECC), Shanghai, China, 2023, pp. 1-4.
[Kha23]	L. Z. Khan, et al. “Exploring the Potential of Model-Centric and Data-Centric Machine Learning for Soft-Failure Cause Identification in Optical Networks”, ECOC 2023.
[Kos12]	M. Koshiba, K. Saitoh, K. Takenaga and S. Matsuo, "Analytical Expression of Average Power-Coupling Coefficients for Estimating Intercore Crosstalk in Multicore Fibers," in IEEE Photonics Journal, vol. 4, no. 5, pp. 1987-1995, Oct. 2012, doi: 10.1109/JPHOT.2012.2221085.
[Lan01]	D. Laney, “3D Data Management: Controlling Data Volume, Velocity, and Variety,” META Group Technical Report, 2001.
[Las23]	C. Lasagni et al., " Impact of Mode Dispersion on Cross-Phase Modulation in Few-Mode Fiber Transmissions ", ECOC 2023 (to appear)
[Li18]	J. Li, et al, "A Flexible Low-Latency Metro-Access Converged Network Approach Based on Time-Synchronized TWDM-PON," OFC18.

[Lig23]	Open RAN's 5G course correction takes it into choppy waters, https://www.lightreading.com/open-ran/open-ran-s-5g-course-correction-takes-it-into-choppy-waters
[Lop20]	V. Lopez et al., "Optimized Design and Challenges for C&L Band Optical Line Systems," in Journal of Lightwave Technology, vol. 38, no. 5, pp. 1080-1091, 1 March1, 2020, doi: 10.1109/JLT.2020.2968225.
[Lum24]	Lumentum, "TrueFlex Contentionless Twin 8x24 Wavelength Selective Switch (WSS)" [Online] https://www.lumentum.com/en/products/trueflex-contentionless-twin-8x24-wavelength-selective-switch-wss, Retrieved 03/
[Mar15]	D. M. Marom and M. Blau, "Switching solutions for WDM-SDM optical networks," in IEEE Comm. Mag., Feb. 2015.
[Mat22]	T. Matsui, P. L. Pondillo and K. Nakajima, "Weakly Coupled Multicore Fiber Technology, Deployment, and Systems," in Proceedings of the IEEE, vol. 110, no. 11, pp. 1772-1785, Nov. 2022, doi: 10.1109/JPROC.2022.3202812.
[Maz23]	M. Mazur et al., Broadband Characterization of Field-Deployed 15-mode Graded-Index Multi-Mode Fiber Cable, ECOC 2023 (to appear)
[Mec15]	Antonio Mecozzi, Cristian Antonelli, and Mark Shtaif, "Intensity impulse response of SDM links," Opt. Express 23, 5738-5743 (2015)
[Nad22]	L. Nadal et al, "SDN-enabled Multi-band S-BVT within Disaggregated Optical Networks," JLT.2022.
[Nad23]	Nadal, L.; et al., "Capacity Scaling in Metro-Regional Aggregation Networks: The Multiband S-BVT". JOCN 2023, 15, F13–F21.
[Nad23b]	Nadal, L., et al., "The Multiband over Spatial Division Multiplexing Sliceable Transceiver for Future Optical Networks", Future Internet 2023, 15, 381, https://doi.org/10.3390/fi15120381.
[Pog12]	P. Poggiolini, "The GN Model of Non-Linear Propagation in Uncompensated Coherent Optical Systems," in Journal of Lightwave Technology, vol. 30, no. 24, pp. 3857-3879, Dec.15, 2012, doi: 10.1109/JLT.2012.2217729
[Pog14]	P. Poggiolini, G. Bosco, A. Carena, V. Curri, Y. Jiang and F. Forghieri, "The GN-Model of Fiber Non-Linear Propagation and its Applications," in Journal of Lightwave Technology, vol. 32, no. 4, pp. 694-721, Feb.15, 2014, doi: 10.1109/JLT.2013.2295208.
[Pog17]	P. Poggiolini and Y. Jiang, "Recent Advances in the Modeling of the Impact of Nonlinear Fiber Propagation Effects on Uncompensated Coherent Transmission Systems," in Journal of Lightwave Technology, vol. 35, no. 3, pp. 458-480, 1 Feb.1, 2017, doi: 10.1109/JLT.2016.2613893.
[Rad23]	G. Rademacher et al., "Randomly Coupled 19-Core Multi-Core Fiber with Standard Cladding Diameter," in Optical Fiber Communication Conference (OFC) 2023, Technical Digest Series (Optica Publishing Group, 2023), paper Th4A.4.
[Rad23-1]	M. Radovic, A. Sgambelluri, F. Cugini and N. Sambo, "Super-channel spectrum saving optimization procedure in elastic optical networks," in Journal of Optical Communications and Networking, vol. 15, no. 2, pp. 68-77, February 2023, doi: 10.1364/JOCN.475596.
[Rad23-2]	M. Radovic, A. Sgambelluri, F. Cugini and N. Sambo, "Experimental Optimization of Power-Aware Super-Channels in Elastic Optical Networks," 2023 International Conference on Optical Network Design and Modeling (ONDM), Coimbra, Portugal, 2023, pp. 1-3.
[Rob17]	I. Roberts, J. M. Kahn, J. Harley and D. W. Boertjes, "Channel Power Optimization of WDM Systems Following Gaussian Noise Nonlinearity Model in Presence of Stimulated Raman Scattering," in Journal of Lightwave Technology, vol. 35, no. 23, pp. 5237-5249, 1 Dec.1, 2017, doi: 10.1109/JLT.2017.2771719.
[Rui22]	M. Ruiz et al., "Deep Learning -based Real-Time Analysis of Lightpath Optical Constellations," IEEE/OPTICA JOCN, 2022.
[Ryf12]	R. Ryf, R. -. Essiambre, A. H. Gnauck, S. Randel, M. A. Mestre, C. Schmidt, P. J. Winzer, R. Delbue, P. Pupalaikis, A. Sureka, T. Hayashi, T. Taru, and T. Sasaki, "Space-Division Multiplexed Transmission over 4200-km 3-Core Microstructured Fiber," in National Fiber Optic Engineers Conference, OSA Technical Digest (Optica Publishing Group, 2012), paper PDP5C.2.
[Ryf17]	R. Ryf et al., "Long-Haul Transmission over Multi-Core Fibers with Coupled Cores," 2017 European Conference on Optical Communication (ECOC), Gothenburg, Sweden, 2017, pp. 1-3, doi: 10.1109/ECOC.2017.8345874.

[Sad22]	R. Sadeghi et al., “Transparent vs translucent multi-band optical networking: capacity and energy analyses”, in Journal of Lightwave Technology, vol. 40, no. 11, pp. 3489-3498, June 2022, doi: doi.org/10.1109/JLT.2022.3167908.
[Sam22]	N. Sambo, B. Correia, A. Napoli, J. Pedro, L. Kiani, P. Castoldi, and V. Curri, "Network upgrade exploiting multi band: S- or E-band?" J. Opt. Commun. Netw. 14, 749-756 (2022).
[Sam23]	N. Sambo, C. Castro, N. Costa, P. Castoldi and A. Napoli, "Energy Efficiency in Next-generation Optical Networks," 2023 23rd International Conference on Transparent Optical Networks (ICTON), Bucharest, Romania, 2023.
[Sas20-1]	T. Sasai, M. Nakamura, E. Yamazaki, S. Yamamoto, H. Nishizawa and Y. Kisaka, “Digital Backpropagation for Optical Path Monitoring: Loss Profile and Passband Narrowing Estimation,” presented at the European Conference on Optical Communications (ECOC), 2020, pp. 1-4.
[Sas20-2]	T. Sasai et al., “Simultaneous Detection of Anomaly Points and Fiber Types in Multi-Span Transmission Links Only by Receiver-Side Digital Signal Processing,” presented at the Optical Fiber Communications Conference and Exhibition (OFC), 2020, pp. 1-3.
[Sas21]	T. Sasai, M. Nakamura, T. Kobayashi, H. Kawakami, E. Yamazaki and Y. Kisaka, “Revealing Raman-amplified Power Profile and Raman Gain Spectra with Digital Backpropagation,” presented at the Optical Fiber Communications Conference and Exhibition (OFC), 2021, pp. 1-3.
[Sem18]	D. Semrau, R. I. Killey and P. Bayvel, "The Gaussian Noise Model in the Presence of Inter-Channel Stimulated Raman Scattering," in Journal of Lightwave Technology, vol. 36, no. 14, pp. 3046-3055, 15 July15, 2018, doi: 10.1109/JLT.2018.2830973.
[Sem19]	D. Semrau, R. I. Killey, and P. Bayvel, “A closed-form approximation of the Gaussian noise model in the presence of inter-channel stimulated Raman scattering,” J. Light. Technol. 37, 1924–1936 (2019).
[Sem20]	D. Semrau, E. Sillekens, R. I. Killey and P. Bayvel, "The Benefits of Using the S-Band in Optical Fiber Communications and How to Get There," 2020 IEEE Photonics Conference (IPC), Vancouver, BC, Canada, 2020, pp. 1-2
[Sen22-1]	M. Sena et al., "DSP-Based Link Tomography for Amplifier Gain Estimation and Anomaly Detection in C+L-Band Systems," in Journal of Lightwave Technology, vol. 40, no. 11, pp. 3395-3405, 1 June1, 2022.
[Sen22-2]	M. Sena et al., "Advanced DSP-based Monitoring for Spatially resolved and Wavelength-dependent Amplifier Gain Estimation and Fault Location in C+L-band Systems," in Journal of Lightwave Technology, 2022.
[Ser22]	P. Serena, et al., "The Ergodic GN Model for Space-Division Multiplexing With Strong Mode Coupling," in Journal of Lightwave Technology, vol. 40, no. 10, pp. 3263-3276, 15 May15, 2022, doi: 10.1109/JLT.2022.3160207.
[Sga23]	A. Sgambelluri, M. Radovic, F. Cugini, N. Sambo and P. Castoldi, "Self-Autonomous Multi-Carrier Optical Transmissions," 2023 International Conference on Optical Network Design and Modeling (ONDM), Coimbra, Portugal, 2023, pp. 1-3.
[Sha21]	B. Shariati, et al "Demonstration of latency-aware 5G network slicing on optical metro networks," JOCN 2022.
[Shi20]	K. Shibahara, T. Mizuno, H. Ono, et al., “Long- Haul DMD-Unmanaged 6-Mode-Multiplexed Transmission Employing Cyclic Mode-Group Permutation”, in Optical Fiber Communication Conference (OFC) 2020, Optica Publishing Group, 2020, Th3H.3.
[Sil22]	P. Sillard et al., "Few-Mode Fiber Technology, Deployments, and Systems," in Proceedings of the IEEE, vol. 110, no. 11, pp. 1804-1820, Nov. 2022, doi: 10.1109/JPROC.2022.3207012.
[Sil23]	F. Silva et al., “Confidentiality-preserving machine learning algorithms for soft-failure detection in optical communication networks,” J. Opt. Commun. Netw. 15, C212–C222 (2023).
[Sin94]	M. Sinclair, “Improved model for European international telephony traffic,” Electron. Lett., vol. 30, no. 18, pp. 1468–1470, 1994.
[Som17]	D. Soma, Y. Wakayama, K. Igarashi, and T. Tsuritani, "Partial MIMO-based 10-Mode-Multiplexed Transmission over 81km Weakly-coupled Few-mode Fiber," in Optical Fiber Communication Conference, OSA Technical Digest (online) (Optica Publishing Group, 2017), paper M2D.4.

[Sou23]	A. Souza, N. Costa, J. Pedro and J. Pires, "Comparison of fast quality of transmission estimation methods for C + L + S optical systems," in Journal of Optical Communications and Networking, vol. 15, no. 11, pp. F1-F12, November 2023, doi: 10.1364/JOCN.486898.
[SRIA20]	Strategic Research and Innovation Agenda 2021-27, European Technology Platform NetWorld2020 "Smart Networks in the context of NGI" https://bscw.5g-ppp.eu/pub/bscw.cgi/d367342/Networld2020%20SRIA%202020%20Final%20Version%202.2%20.pdf
[Sun20]	Sun, Han, et al. "800G DSP ASIC design using probabilistic shaping and digital sub-carrier multiplexing." Journal of lightwave technology 38.17 (2020): 4744-4756.
[Tak23]	M. Takahashi, T. Sasai, E. Yamazaki and Y. Kisaka, "DSP-based PDL Estimation and Localization in Multi-Span Optical Link Using Least Squares-based Longitudinal Power Monitoring," 2023 Opto-Electronics and Communications Conference (OECC), Shanghai, China, 2023, pp. 1-6.
[Tan19]	T. Tanimura, K. Tajima, S. Yoshida, S. Oda and T. Hoshida, "Experimental demonstration of a coherent receiver that visualizes longitudinal signal power profile over multiple spans out of its incoming signal," presented at the European Conference on Optical Communications (ECOC), 2019, pp. 1-4.
[Tan20]	T. Tanimura, S. Yoshida, K. Tajima, S. Oda, and T. Hoshida, "Fiber-Longitudinal Anomaly Position Identification Over Multi-Span Transmission Link Out of Receiver-end Signals," in IEEE/OPTICA Journal of Lightwave Technology, vol. 38, no, 9, pp. 2726-2733, 2020.
[tre-23]	C. Tremblay, et al. , "Detection and root cause analysis of performance degradation in optical networks using machine learning," ECOC 2023.
[Van23]	M. van den Hout et al., "273.6 Tb/s Transmission Over 1001 km of 15-Mode Fiber Using 16-QAM C-Band Signals," in Optical Fiber Communication Conference (OFC) 2023, Technical Digest Series (Optica Publishing Group, 2023), paper Th4B.5.
[Vel23]	L. Velasco, M. Devigili, and M. Ruiz, "Applications of Digital Twin for Autonomous Zero-Touch Optical Networking [Invited]," invited to the International Conference on Optical Network Design and Modeling (ONDM), 2023.
[Wel21]	Dave Welch, Antonio Napoli, Johan Bäck, Warren Sande, João Pedro, Fady Masoud, Chris Fludger et al., "Point-to-Multipoint Optical Networks Using Coherent Digital Subcarriers", IEEE / OPTICA, JLT; 2021
[Wel23]	Dave Welch, Antonio Napoli, Johan Bäck, Sanketh Buggaveeti, Carlos Castro, Aaron Chase, Xi Chen, Vince Dominic, Thomas Duthel, et al. "Digital subcarrier multiplexing: Enabling software-configurable optical networks", IEEE / OPTICA, JLT; 2021
[Win11]	Peter J. Winzer and Gerard J. Foschini, "MIMO capacities and outage probabilities in spatially multiplexed optical transport systems," Opt. Express 19, 16680-16696 (2011)
[Win17]	P. J. Winzer and D. T. Neilson, "From Scaling Disparities to Integrated Parallelism: A Decathlon for a Decade," in Journal of Lightwave Technology, vol. 35, no. 5, pp. 1099-1115, 1 March1, 2017, doi: 10.1109/JLT.2017.2662082.